

350
11-3-81
EW

(2)

De 50

DOE/ET/12056-27
(DE81030336)

MASTER

**THE EFFECTS OF CONFINING PRESSURE, PORE PRESSURE
AND TEMPERATURE ON ABSOLUTE PERMEABILITY**

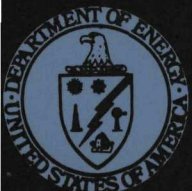
By
Brian D. Gobran
Henry J. Ramey, Jr.
W. E. Brigham

October 1981
Date Published

Work Performed Under Contract No. AC03-76ET12056

Stanford University Petroleum Research Institute
Stanford, California

**F
O
S
S
I
L
E
N
E
R
G
Y**



U. S. DEPARTMENT OF ENERGY

DISCLAIMER

"This report was prepared as an account of work sponsored by an agency of the United States Government. Neither the United States Government nor any agency thereof, nor any of their employees, makes any warranty, express or implied, or assumes any legal liability or responsibility for the accuracy, completeness, or usefulness of any information, apparatus, product, or process disclosed, or represents that its use would not infringe privately owned rights. Reference herein to any specific commercial product, process, or service by trade name, trademark, manufacturer, or otherwise, does not necessarily constitute or imply its endorsement, recommendation, or favoring by the United States Government or any agency thereof. The views and opinions of authors expressed herein do not necessarily state or reflect those of the United States Government or any agency thereof."

This report has been reproduced directly from the best available copy.

Available from the National Technical Information Service, U. S. Department of Commerce, Springfield, Virginia 22161.

Price: Printed Copy A06
Microfiche A01

Codes are used for pricing all publications. The code is determined by the number of pages in the publication. Information pertaining to the pricing codes can be found in the current issues of the following publications, which are generally available in most libraries: *Energy Research Abstracts, (ERA)*; *Government Reports Announcements and Index (GRA and I)*; *Scientific and Technical Abstract Reports (STAR)*; and publication, NTIS-PR-360 available from (NTIS) at the above address.

DISCLAIMER

This report was prepared as an account of work sponsored by an agency of the United States Government. Neither the United States Government nor any agency Thereof, nor any of their employees, makes any warranty, express or implied, or assumes any legal liability or responsibility for the accuracy, completeness, or usefulness of any information, apparatus, product, or process disclosed, or represents that its use would not infringe privately owned rights. Reference herein to any specific commercial product, process, or service by trade name, trademark, manufacturer, or otherwise does not necessarily constitute or imply its endorsement, recommendation, or favoring by the United States Government or any agency thereof. The views and opinions of authors expressed herein do not necessarily state or reflect those of the United States Government or any agency thereof.

DISCLAIMER

Portions of this document may be illegible in electronic image products. Images are produced from the best available original document.

**THE EFFECTS OF CONFINING PRESSURE, PORE PRESSURE
AND TEMPERATURE ON ABSOLUTE PERMEABILITY**

SUPRI TR-27

By

Brian D. Gobran
Henry J. Ramey, Jr.
and

W. E. Brigham, *Principal Investigator*
Stanford University Petroleum Research Institute
Stanford, California 94305
415/497-0691

H. J. Lechtenberg, *Technical Project Officer*
San Francisco Operations Office
Fossil Energy Division
1333 Broadway
Oakland, California 94612
415/273-7951

Work Performed for the Department of Energy
Under Contract No. DE-AC03-76ET12056

Date Published—October 1981

TABLE OF CONTENTS

	<u>Page</u>
ABSTRACT	vi
ACKNOWLEDGEMENT	vii
1. INTRODUCTION	1
2. LITERATURE REVIEW	3
3. THEORY	11
4. EXPERIMENTAL APPARATUS	15
4.1 FLUID FLOW SYSTEM	15
4.2 CONFINING PRESSURE SYSTEM	25
4.3 DIFFERENTIAL PRESSURE MEASUREMENT	27
4.4 PRESSURE TRANSDUCER CALIBRATION	29
5. EXPERIMENTAL PROCEDURE	31
6. RESULTS	34
6.1 UNCONSOLIDATED OTTAWA SAND	34
6.2 CONSOLIDATED SANDSTONE	53
7. DISCUSSION	64
7.1 UNCONSOLIDATED OTTAWA SAND	64
7.2 CONSOLIDATED SANDSTONE	66
8. CONCLUSIONS	69
9. SUGGESTED ADDITIONAL WORK	71
NOMENCLATURE	72
REFERENCES	73

	<u>Page</u>
APPENDIX A CONVERGENT FLOW	78
APPENDIX B HASSLER SLEEVE MATERIALS	81
APPENDIX C CAPILLARY TUBE VISCOMETER	88
APPENDIX D ERROR ANALYSIS	95
APPENDIX E CALCULATION OF PERMEABILITY	98
APPENDIX F EQUIPMENT, MANUFACTURERS AND SUPPLIERS	103

LIST OF TABLES

<u>Table</u>	<u>Page</u>
1 LITERATURE REVIEW SUMMARY	10
2 PUMP FLOW RATES	18
3 EFFLUENT WATER SURFACE TENSION WITH VITON SLEEVE	22
B-1 WATER SURFACE TENSION IN PRESENCE OF EPDM	82
B-2 EFFLUENT WATER SURFACE TENSION WITH FLUOREL SLEEVE	82
C-1 WATER PROPERTIES AT VARIOUS TEMPERATURES	89
C-2 CAPILLARY TUBE CALIBRATION AT 80°F	89
C-3 COILED CAPILLARY TUBE DATA	93

LIST OF FIGURES

<u>Figure</u>		<u>Page</u>
1	Schematic Diagram of the Fluid Flow System	16
2	Schematic Diagram of the Core Holder	20
3	Surface Tension vs Temperature for Effluent Water With Viton Sleeve	23
4	Schematic Diagram of the Fluid Flow and Confining Pressure Systems	26
5	Schematic Diagram of the Fluid Flow, Confining Pressure and Differential Pressure Measurement Systems	28
6	Schematic Diagram of the Entire Experimental Apparatus	30
7	Permeability vs Throughput for Run 11-22-80	36
8	Permeability vs Throughput for Run 4-10-81	37
9	Permeability vs Flow Rate for Run 2-5-81	38
10	Permeability vs Flow Rate for Run 2-5-81	39
11	Permeability vs Temperature for Run 11-22-80	41
12	Permeability vs Temperature for Run 2-5-81	42
13	Permeability vs Temperature for Run 10-10-80	43
14	Permeability vs Confining Pressure for Run 4-8-81	45
15	Permeability vs Pore Pressure for Run 2-5-81	46
16	Permeability vs Pore Pressure for Run 2-5-81	47
17	Permeability vs Pore Pressure for Run 4-8-81	48
18	Permeability vs Confining Pressure for Run 4-10-81	50
19	Permeability vs Confining Minus Pore Pressure for Run 4-10-81	51
20	Permeability vs Confining Pressure for Run 4-10-81	52

<u>Figure</u>	<u>Page</u>
21 Permeability vs Throughput for Run 4-16-81	54
22 Permeability vs Flow Rate for Run 4-16-81	55
23 Permeability vs Flow Rate for Run 4-16-81	56
24 Permeability vs Temperature for Run 12-24-80	57
25 Permeability vs Confining Pressure for Run 4-16-81	58
26 Permeability vs Pore Pressure for Run 4-16-81	59
27 Permeability vs Confining Pressure for Run 4-16-81	61
28 Permeability vs Temperature for Run 4-16-81	63
29 Permeability vs Overburden Pressure from Fatt ⁸	68
B-1 Surface Tension vs Temperature of Water in Presence of EPDM	83
B-2 Surface Tension vs Temperature for Effluent Water With Fluorel Sleeve	84
B-3 Permeability vs Temperature for Run 4-26-81 With Steel Sleeve	86
C-1 Flow Rate-Viscosity Product vs Differential Pressure for Capillary Tube at 80°F	90
C-2 Friction Factor Ratio vs Dean Number for Coiled Capillary Tubes	94

ABSTRACT

This study investigates absolute permeability of consolidated sandstone and unconsolidated sand cores to distilled water as a function of the confining pressure on the core, the pore pressure of the flowing fluid and the temperature of the system. Since permeability measurements are usually made in the laboratory under conditions very different from those in the reservoir, it is important to know the effect of various parameters on the measured value of permeability. While this topic has been investigated extensively for several decades, no complete study has been made where all these parameters were varied to find the effect of each separately and in combination.

All studies on the effect of confining pressure on absolute permeability have found that when the confining pressure is increased, the permeability is reduced.

The studies on the effect of temperature have shown much less consistency. Work at Stanford University and other laboratories has shown that an increase in temperature causes reduced permeability when water is the flowing fluid and sandstone or unconsolidated sand is the porous medium. Most other porous media/fluid combinations have shown no temperature effect.

This work contradicts the past Stanford studies by finding no effect of temperature on the absolute permeability of unconsolidated sand or sandstones to distilled water. The probable causes of the past errors are discussed. It has been found that inaccurate measurement of temperature at ambient conditions and non-equilibrium of temperature in the core can lead to a fictitious permeability reduction with temperature increase.

The results of this study on the effect of confining pressure and pore pressure support the theory that as confining pressure is increased or pore pressure decreased, the permeability is reduced. The effects of confining pressure and pore pressure changes on absolute permeability are given explicitly so that measurements made under one set of confining pressure/ pore pressure conditions in the laboratory can be extrapolated to conditions more representative of the reservoir.

ACKNOWLEDGEMENT

This work was funded by the Department of Energy through contract DE-AC03-76ET12056. The financial support is greatly appreciated.

1. INTRODUCTION

The permeability of a porous medium is its ability to transmit fluids. The unit of permeability is the Darcy. A porous medium having one Darcy permeability will allow one cubic centimeter per second of one centipoise viscosity fluid to flow through one square centimeter cross-sectional area when the pressure gradient is one atmosphere per centimeter. Absolute permeability is the permeability of a porous medium when one fluid fully saturates the rock.

Absolute permeability is an important reservoir parameter occurring in a great many reservoir engineering calculations ranging from pressure transient analysis to water influx. In fact, any equation involving fluid flow includes permeability as a variable. Clearly, absolute permeability is an important reservoir property that needs to be determined accurately so that other reservoir engineering calculations may be correct.

Petroleum reservoirs usually exist at elevated temperatures and are generally produced under approximately isothermal conditions. However, during some operations such as recovery of high viscosity crude oils, the temperature of the reservoir may be increased up to 1500°F. Two methods are used to increase the temperature of high viscosity crude oils thereby lowering their viscosity and allowing them to flow more easily: steam injection (either cyclic or drive) and in situ combustion.

During steam injection, wet steam is injected into the reservoir at temperatures on the order of 400 to 500°F. During in situ combustion, the temperature of the combustion front can reach temperatures as high as 1500°F. Because permeability measurements of reservoir rocks are normally made at ambient conditions, it is important to know whether temperature is a

parameter affecting absolute permeability. Other examples of reservoir temperature changes are the injection of hot water for energy storage, reinjection of spent geothermal water and injection of surface water into warmer subsurface formations. Again, the temperature effect on permeability is important in these projects.

Most of the United States reserves of heavy or high viscosity crude oils are found in California in poorly consolidated or unconsolidated sand reservoirs. Most of the previous investigators who found a permeability change with temperature used sand as the porous medium and water as the flowing fluid. So, sand and water are the porous medium and fluid combination of the most interest in studying absolute permeability as a function of temperature.

Oil and gas are being produced from deeper and tighter (less permeable) reservoirs as shallower reservoirs become depleted. Often these deeper reservoirs are overpressured or geopressured. Under these conditions, the effects of overburden and pore pressure are critical in predicting the behavior of the reservoir during production. Therefore, the effects of pore pressure and confining pressure on absolute permeability are also important and require investigation.

This study investigated absolute permeability of sand and sandstone cores to water as a function of temperature, confining pressure and pore pressure with the intent of correlating results with past research and with measurements made at ambient conditions.

2. LITERATURE REVIEW

The first experimental study of fluid flow through porous media is accredited to Darcy¹, who studied the filtration of water flowing vertically downward through sand beds in 1856. He determined that the velocity of the water was proportional to the head loss of the fluid through the sand beds. He expressed this mathematically as

$$v = - C \frac{dp}{dx} \quad (1)$$

Further study and modification of this equation has yielded the form that is now termed Darcy's law²:

$$v = \frac{q}{A} = - \frac{k}{\mu} \frac{dp}{dx} \quad (2)$$

where k is a proportionality constant, the permeability of the porous medium, and μ is the viscosity of the flowing fluid. This equation has been determined to be valid for a single-phase flowing fluid fully saturating the pores when there is no rock-fluid interaction (clay swelling, etc.) and there is no turbulence.

Perhaps the first ideas that permeability is really an absolute number came from Muskat who wrote in 1937 and again in 1949 that permeability is "... independent of the nature of the fluid and is determined solely by the structure of the porous media."^{3,4}

Despite what Muskat wrote, researchers were still interested in finding out if anything did affect permeability. One of the first studies on the

effect of temperature on permeability was that of Grunberg and Nissan⁵. Using a Jena glass filter, they found a linear decrease in permeability with temperature increase which they attributed to liquid adsorption similar to gas adsorption. The results were also described using an equation involving the surface tension of the fluid which they said came from a "surface energy" effect.

Calhoun and Yuster⁶ attempted to verify the work of Grunberg and Nissan. Using sintered Pyrex glass and silica membranes, they found no temperature, electrokinetic, surface tension or adsorption effects on permeability. They did, however, observe that pH and NaCl concentration in the flowing fluid did affect the permeability measured.

During the 1950's the emphasis of study on permeability turned from the flowing fluids to the porous media and the effect of various types of confining pressure on permeability. At this point the various types of stress applied to cores in experiments need to be defined. The first type of stress is hydrostatic, which is representative of a reservoir having no residual tectonic stresses. Hydrostatic stress, the type experienced by a body submersed in a liquid, is obtained by having the same pressure on all surfaces of the body. The next type of stress loading is triaxial, where there is both a radial confining pressure and an axial one which differ. Here the axial load may differ due to endplug design and thus the axial load is not independently variable; or else there may be a way of independently fixing both the axial and radial forces. The third type of loading is termed radial. While this is actually a subset of the triaxial case, it will be considered separately. With radial loading, there is a radial confining pressure but no axial force.

Fatt⁷ was one of the first to investigate confining pressure and its relation to permeability. Using sandstone cores and measuring gas permeabilities, he found in 1952 a permeability reduction of 11 to 41% when the confining pressure was increased to 3000 psi⁷. In 1953, he also published results⁸ showing permeability reductions of 7 to 27% at 5000 psi overburden pressure for four sandstone cores.

Wyble⁹ used a radial stress configuration with up to 5000 psi and found permeability reductions equal to or greater than 50%. Permeability measurements were made with air as the flowing fluid.

Shaly sandstones were studied by McLatchie et al.¹⁰ in 1958. They hydrostatically loaded the cores and measured oil permeabilities. At 5000 psi they found reductions in permeability from 7 to 70%. An observation they made that has been repeated several times by others is that the lower the initial permeability, the greater the percentage reduction in permeability.

Waldorf¹¹ studied the effect of water on reservoir cores containing water-sensitive clays. In an interesting study, he found that the permeability of these cores was the same when either air or super-heated steam was the flowing fluid. However, a significant reduction in permeability occurred in the cores containing montmorillonite when water was flowed through the cores. The permeability could be restored by evaporating this water using super-heated steam injection.

Knutson and Bohor¹² attempted in vain to correlate the data in the literature on confining pressure versus permeability reduction. In their experimental work they found plugging when the Reynolds number exceeded 0.001 .

Dobrynin¹³ used cores saturated with 3 N. NaCl and confined them hydrostatically at 5000 psi. He found a reduction in permeability of 7 to 30%. The data was fit to a function involving an empirical constant, γ , which was determined from five scattered points. The constant, γ , was expected to be a function of pore size distribution and pore compressibility.

Gray et al.¹⁴ attempted to more closely simulate reservoir stress conditions by applying pressure at a Poisson ratio of 0.33. This stress configuration was developed by first hydrostatically and then axially loading the core. It was found that a greater reduction in permeability occurred during the hydrostatic portion of the loading cycle. The permeability reductions ranged from 7% for Berea to 60% for Grubb sandstones at 5000 psi confining pressure. Air was the fluid used to measure permeability.

Somerton and Selim¹⁵ in 1961 presented the first of several papers from the University of California on the effect of temperature on sandstone properties. They investigated the linear and volumetric expansion of sandstones at temperatures up to 1000°C. They found permanent damage and also found that at certain temperatures extra heat was required to raise the rock temperature due to reactions such as decomposition of carbonate minerals.

Somerton and Gupta¹⁶ studied the effect of deposited salt by adding aqueous solutions to cores prior to heating. Twelve cores were used from three different sandstones. One core from each sandstone was saturated with KCl, NaCl and CaCl₂ prior to heating. They found an increase in permeability in all the KCl and NaCl saturated cores and in one CaCl₂ saturated core. They suggested that their results were due to reactions of salts with clay minerals. The permeabilities were measured after cooling

with air as the flowing fluid. Their findings were similar to McLatchie et al.¹⁰ in that they observed that the lower the initial permeability the greater the percentage change in permeability.

Somerton et al.¹⁷ studied the effect of temperature on confined and unconfined cores. The cores were heated to various temperatures up to 850°C, cooled to ambient conditions and then flowed with air to measure permeability. In all cases the permeability was constant until 400°C above which the permeability increased. This increase in permeability was attributed to differential expansion of the rock components leading to microfractures. As above, the lower the initial permeability the greater the percentage change in permeability.

An interesting study was reported by Paaswell¹⁸. He studied the volume change and the volume rate of change in a saturated, hydrostatically stressed unconsolidated soil sample caused by boundary temperature changes. He found that the volume change and the volume rate of change were higher when the stress or the temperature changes or the speed of the temperature changes were greater.

Wilhelmi and Somerton¹⁹ subjected cores to hydrostatic loading and then increased and decreased the axial load four times. This was determined to be sufficient to stabilize the strain behavior. A reduction of up to 65% was found in permeability when the confining pressure was 4000 psi. As Gray et al.¹⁴ found, the greater portion of the permeability reduction occurred during the hydrostatic portion of the loading cycle.

The effect of increasing temperature of artificially constructed porous media (silica and alumina grains cemented with phenolic resin) was studied by Greenberg et al.²⁰ They found a decrease from 0 to 0.54% per °C over the temperature range 20 to 60°C. Water was the flowing fluid.

Permeability was measured by the pressure-time response to a pressure pulse by Brace et al.²¹ The porous medium that they used was granite confined hydrostatically at 250 to 4440 bars. Water and argon were the two saturating fluids used. As the confining pressure increased, the permeability was reduced from 350 to 4 nanodarcies. An exponential relationship was used to correlate permeability with electrical resistivity.

Vairogs et al.²² studied the effect of confining pressure on clean and shaly sandstones which were hydrostatically loaded. With nitrogen flowing, they found a general decrease in permeability as confining pressure increased. They noted a greater percentage decrease in permeability in cores containing shale or microfractures and in those having lower initial permeability values. Most of the reductions occurred at confining pressures less than 4000 psi.

One of the first works on the combined effect of temperature and pressure was that of Afinogenov²³. He used reservoir cores and transmission oil as the flowing fluid. His results showed a 95% reduction in absolute permeability with temperature increase from ambient to 95°C. His results seem doubtful since no other study has found reductions of such magnitude. He suggested a reaction between the flowing oil and the mineral components of the porous rock.

The absolute permeability studies at Stanford University began with the absolute permeability measurements made by Weinbrandt²⁴ in his relative permeability research. He found a scatter of data showing an average 57% reduction in absolute permeability to water as the temperature was increased from ambient to 175°F. The porous media were Boise sandstone cores.

Casse²⁵ followed up the initial findings of Weinbrandt²⁴ by studying the effect of pressure and temperature on consolidated sandstone cores.

A permeability decrease was found with water flow but none with oil flow when the temperature was increased. He seemed to find a minimum threshold stress (confining pressure-temperature combination) that had to be overcome before any changes in permeability occurred. References 26 and 27 give other published results of Casse and Weinbrandt.

Aruna extended the work of Casse²⁵ to unconsolidated sand²⁸ and limestone²⁹ cores. He found that the combination of sand and water was the only one yielding a permeability reduction with temperature increase. With limestone cores and either oil or water flowing, and sandstone cores with oil flowing, there was no effect of temperature on absolute permeability.

Danesh et al.³⁰ investigated the permeability-temperature relationship for oil and water flow through stainless steel powders. A permeability reduction was found with water flow but not oil flow. This paper contains an excellent boundary layer theory section discussing possible surface layer interactions causing permeability reductions.

Measurement of permeability as a function of temperature under stress was the goal of Aktan and Farouq Ali³¹, but due to failure of the apparatus, their measurements could not be made under stress. They found permeability increased with temperature increase for Berea and Boise sandstone with either air or brine as the flowing fluid.

Zoback and Byerlee³² measured permeability under hydrostatic stress as a function of the confining pressure, pore pressure and effective stress. With oil flowing the pore pressure seemed to be more dominant than confining pressure in affecting permeability in Berea sandstone cores.

Table 1 summarizes the results of the work mentioned above giving the fluids used, porous media, type of stress loading and the variable of interest.

Table 1

LITERATURE REVIEW SUMMARY

AUTHOR	REFERENCE	FLUID	CORE MATERIAL	STRESS	VARIABLE
Afinogenov	23	Oil	Reservoir cores	Hydrostatic	Temperature
Aktan and Farouq Ali	31	Air, Brine	Berea, Boise, California, Tennessee	Triaxial	Temperature
Aruna	28,29	Oil, Water	Massillon, Ottawa, Limestone	Triaxial	Temperature, Pressure
Brace <u>et al.</u>	21	Argon, Water	Westerly Granite	Hydrostatic	Pressure
Calhoun and Yuster	6	Water	Pyrex Glass and Silica Membranes	None	Many
Casse	25,27	Oil, Water	Bandera, Berea, Boise	Triaxial	Temperature, Pressure
Danesh <u>et al.</u>	30	Oil, Water	Stainless Steel	Triaxial	Temperature, Pressure
Dobrynin	13	Brine	Medina, Torpedo	Hydrostatic	Pressure
Fatt	8	Gas, Oil	California, Coastal California, Tuscaloosa	Hydrostatic	Pressure
Fatt and Davis	7	Nitrogen	Arizona, California, Colorado	Hydrostatic	Pressure
Gray <u>et al.</u>	14	Air	Berea, Boise, Grubb	Triaxial	Pressure
Greenberg <u>et al.</u>	20	Water	Artificial	Axial	Temperature
Grunberg and Nissan	5	Air, Water, Amyl Alcohol	Jena Glass Filter	Axial	Temperature
Knutson and Bohor	12	Oil	Bandera, Berea, Boise, Delaware, Grub, Queens, etc.	Hydrostatic	Pressure
McLatchie <u>et al.</u>	10	Oil	Reservoir	Hydrostatic, Triaxial	Pressure
Paaswell	18	Water	Soil	Hydrostatic	Temperature
Somerton and Gupta	16	Air, Water	Bandera, Berea, Boise	None	Temperature, Fluid
Somerton <u>et al.</u>	17	Air	Bandera, Boise, St. Peters	Hydrostatic	Temperature
Somerton and Salim	15	None	Bandera, Berea, Boise	None	Temperature (Expansion)
Vairogs <u>et al.</u>	22	Nitrogen	Chanute, Frio, San Andres, Springer	Hydrostatic	Pressure
Waldorf	11	Air, Steam	Reservoir cores with clay	None	Fluid
Weinbrandt <u>et al.</u>	26	Oil, Water	Berea, Boise	Triaxial	Temperature
Wilhelmi and Somerton	19	Air	Bandera, Berea, Boise	Triaxial	Pressure
Wyble	9	Air	Bradford, Kirkwood, Weir	Radial	Pressure
Zoback and Byerlee	32	Air	Berea	Hydrostatic	Pressure

3. THEORY

As discussed in the previous section, there were several studies which found an effect of temperature on absolute permeability. There were also several attempts to explain the observed results, and it is important to discuss these proposed explanations for the temperature effect on absolute permeability.

First it is useful to summarize the results of the authors finding a permeability change with temperature increase, so that the theories and their contradictions can be put into perspective. Casse²⁵ found that consolidated sandstone cores showed a reduction in permeability with temperature increase when water was the flowing fluid but not with oil or gas flowing. Aruna²⁸ found a permeability reduction with both consolidated sandstone and unconsolidated sand cores with water flowing but not with oil, gas or 2-octanol flowing. A later study by Aruna et al.²⁹ found no effect with oil or water flowing through unconsolidated limestone cores. Danesh et al.³⁰ found a reduction in permeability with temperature increase with water flowing through stainless steel powder cores and water flowing through unconsolidated sand cores. However, when oil was the flowing fluid, there was no permeability change with temperature.

In summary, the majority of authors finding a permeability change with temperature found a decrease in absolute permeability when the temperature was increased with water as the flowing fluid and silica (consolidated or unconsolidated cores) or stainless steel powders as the porous medium.

Various explanations were attempted, but none fully reconciled the results summarized above. In his dissertation, Casse²⁵ mentioned clay

swelling as a possible cause of the reduction in permeability. This might explain the results he found but could not explain the results of Danesh et al.³⁰ with the stainless steel powder cores. Aruna's essentially clay-free unconsolidated cores are another example which is contrary to Casse's suggestion.

Another idea often suggested is that the combination of thermal and mechanical stresses on the core may cause a reduction in the pore sizes and thus reduce permeability²⁶. While this may seem quite reasonable, it does not fully explain why the permeability reduction found by the same author is fluid dependent. This hypothesis would imply that the reduction is purely porous medium dependent.

Sanyal et al.³³ presented a comprehensive study on the effect of temperature on various rock properties. The works of Weinbrandt²⁴ and Casse²⁵ were combined with the capillary pressure studies of Sinnokrot³⁴ and Sanyal³⁵ as well as the works of a great many other authors to yield a rock-fluid model. They concluded that wettability changes were overemphasized in previous explanations and that rock matrix and fluid viscosity changes were probably the main causes of the observed phenomenon.

Aruna²⁸ and Aruna et al.²⁹ discounted the clay-swelling proposal of Casse²⁵ and suggested some sort of silica-water interaction such as chemisorption. He suggested that molecular layers of water bound to the crystal surfaces may reduce the effective size of the pore paths and thus reduce permeability. This bound layer would then have to be temperature dependent to explain his results. To extrapolate this to the results of Danesh et al.³⁰, one would have to assume that stainless steel and silica bind water in a similar manner.

A recent work by Sydansk³⁶ demonstrates that some of the permeability reduction observed is caused by migration of clay or fine particles at ambient temperatures. This has also been discussed recently by Davidson³⁷ as well as Gruesbeck and Collins³⁸. Although the effect of migration cannot be determined for previous studies, it has been investigated in this work.

Danesh et al.³⁰ extended the proposals of Aruna et al.²⁹ concerning boundary layer theory. They discuss results showing the surface layer of water having properties different from the bulk, and work finding water with a high viscosity in quartz capillaries. This last idea is the subject of a great deal of study and deserves more discussion.

From the early 1960's through the middle 1970's, a great deal of research was carried on investigating "Polywater"³⁹. This was the term coined to describe water condensed in very fine quartz capillaries that had anomalous properties such as high viscosity, which were found to be on the order of ten to fifteen times that of ordinary water. A computer literature survey found 64 studies on anomalous water carried out in 14 countries and results published in 10 languages between 1972 and 1976. To the best of its ability, each group verified that there was no contaminants in the water. Finally in 1973, Derjaguin, the man who popularized polywater in 1970⁴⁰, conceded that the results were due to trace amounts of contaminants, which were identified by neutron activation⁴¹.

While the idea of a polymeric form of water has been discounted, work on contaminated condensed water in quartz capillaries has continued⁴². Although this is not representative of the systems studied by those finding a reduction in permeability (there was no condensing flow in their experiments), this is exactly what occurs during steam injection into sand reservoirs and should be considered if some time dependence of permeability

is found in such systems.

From this and the previous section it can be concluded that a great deal of work is needed to first define the permeability-temperature relationship for sand-water systems and then develop some theory to explain the results.

4. EXPERIMENTAL APPARATUS

This section will describe the experimental apparatus designed, built and operated to measure the absolute permeability of unconsolidated and consolidated porous media as a function of temperature, confining pressure and pore pressure. The equipment will be divided into four main component systems with each discussed separately.

4.1 FLUID FLOW SYSTEM

Figure 1 shows a schematic diagram of the fluid flow system. The flow is from right to left beginning at the pump and ending in the graduated cylinder.

In these experiments demineralized, distilled water is the flowing fluid. Tap water is first passed through a demineralizer composed of an organic filter and a high capacity filter. The resistance of the effluent is measured continuously and is kept above one megohm. This water is then introduced into an automatic distillation system. Finally it is stored in Pyrex bottles to help reduce glass dissolution in the water⁴³. In most cases the water is used within three days of distillation.

During early experiments⁴⁴, hydrazine was added to the water in a concentration of 130 ppm as an oxygen scavenger. It was subsequently determined that hydrazine, even in this low concentration, reacted with the Viton sleeve of the core holder (to be discussed later) at temperatures exceeding 300°F. For all of the experiments discussed here, hydrazine was not used.

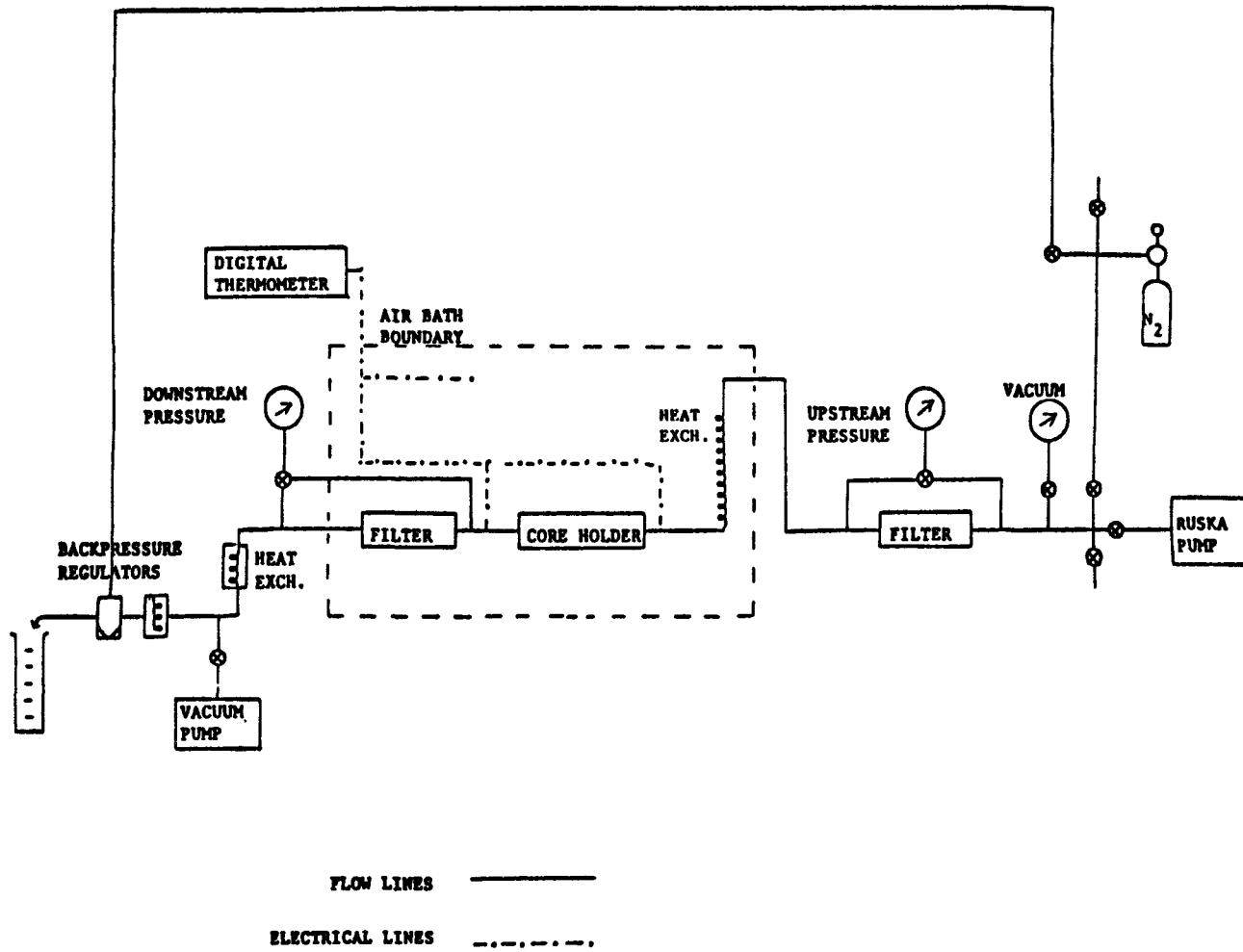


Fig. 1. Schematic Diagram of the Fluid Flow System.

Water flow begins at the Ruska constant rate pump. This model is a dual proportioning pump with two 500 cc cylinders. It is designed for one cylinder to displace fluid while the other recharges. The cylinders switch directions automatically at the end of each cycle and the flow continues. There are 28 flowrate settings ranging from 5 to 1120 cc/hr. While these rates are constant, they are not equal to those stated by Ruska. Table 2 shows the pump settings, the stated rates and those actually measured. The measurements were taken at a line pressure of 200 psi. Although the compressibility of the water needs to be considered in these measurements, it is nowhere near enough to allow for this discrepancy.

This pump is designed for flow against a maximum backpressure of 4000 psi. For safety purposes, the maximum backpressure used was 3600 psi. This gives the highest pore pressure that can be obtained for these experiments.

Two stainless steel filters are used in the flow lines. The first is a 15 micron filter immediately downstream of the pump used to filter the water before entering the core holder. This keeps deposits from collecting either at the core inlet face or on the endplug screen which might give an extra pressure drop and thus the appearance of an artificially low permeability. The second filter is a 7 micron one located downstream of the core. It is used to prevent particulates from reaching and blocking the backpressure regulator. Pressure taps are connected on either side of these filters leading to three-way valves and pressure gauges. This allows monitoring of the pressure differential at any time across the filters to determine if they are significantly plugged.

After the first filter, the water flows into the air bath. This contains about 10.5 cu ft of working space. There is an externally adjustable fan used to circulate air. For energy conservation the air flow rate should be kept

Table 2

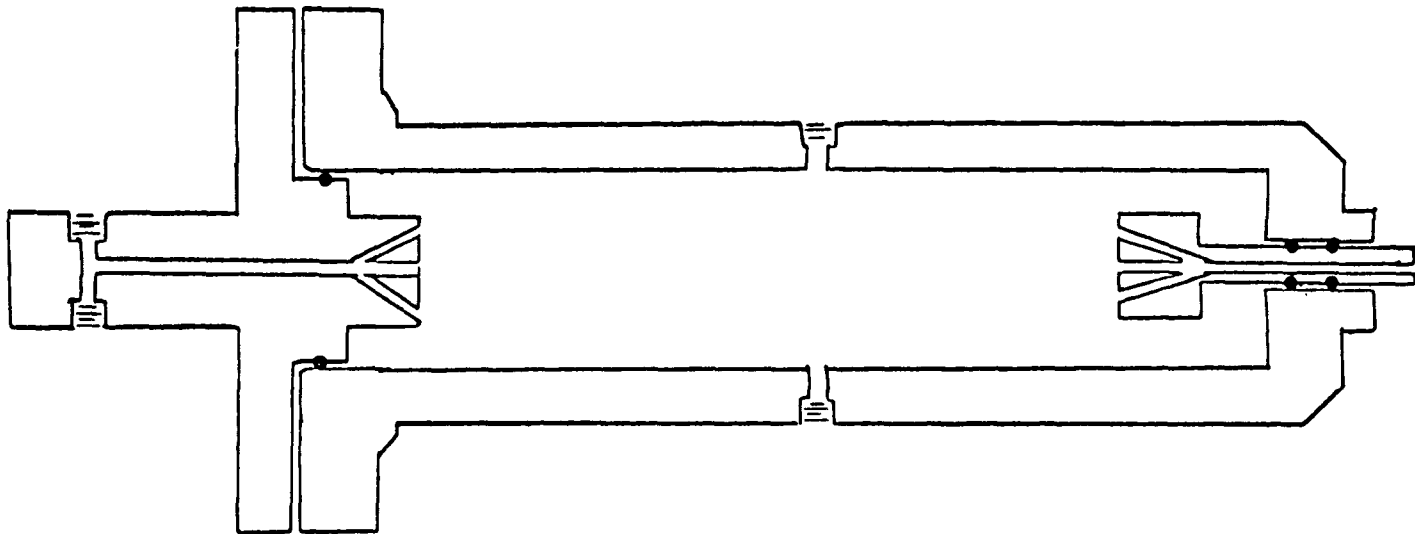
PUMP FLOW RATES

<u>Setting</u>	<u>Stated by Ruska (cc/hr)</u>	<u>Measured at 70°F (gm/hr)</u>
D7	1120	1151
D6	960	981
D5	800	821
D4	640	655
D3	480	492
D2	400	408
D1	320	328
C7	280	286
C6	240	246
C5	200	204
C4	160	164
C3	120	123
C2	100	103
C1	80	82
B7	70	72
B6	60	61
B5	50	51
B4	40	42
B3	30	31

high during heating and cooling cycles and low once equilibrium has been reached. However, for convenience, the rate was kept high at all times. The air bath can maintain a constant temperature in the air within $\pm 2^{\circ}\text{F}$ at settings ranging from 100 to 600°F .

Three thermocouples are used to measure temperature. The first is located in the top of the air bath hanging freely above the core holder. This one is used to adjust the thermostat on the air bath. The second thermocouple is inserted in the flow line immediately upstream of the core holder. This one is used to insure that the water has reached the air bath temperature before entering the core. This was done in response to errors in temperature measurements and non-isothermal flow in early experiments⁴⁴. The third thermocouple is also in the flow line, located downstream of the core holder. This one reaches equilibrium last due to the slower rate of heat transfer inside the core. Flow measurements are not taken until the temperature difference between the two flowline thermocouples is less than 1°F . All three thermocouples lead to a multichannel digital thermometer allowing this difference to be read easily. A chart recorder previously used by others could not be read with greater than $\pm 2^{\circ}\text{F}$ accuracy.

The body of the core holder is shown schematically in Fig. 2. The components will be described here while the loading procedure will be discussed in the Procedure section. This core holder is an improvement on the one used by previous investigators²⁴⁻²⁹. Both this and the previous core holder are triaxially loaded although the previous one was termed "approximately hydrostatic"²⁴⁻²⁹. This difference will be important when discussing results of constant effective stress experiments (section 6.1). A 270-mesh screen is fitted over each endplug to prevent sand flow with either consolidated or unconsolidated cores. A Viton sleeve is used to separate



2 in.

Fig. 2. Schematic Diagram of the Core Holder.

the core from the confining fluid and yet transmit the confining pressure radially to the core. A perforated aluminum sleeve is used around the Viton to prevent deformation of the core. The sliding downstream endplug allows the pressure to be transmitted axially and allows for some variation in core length. The typical lengths range from 18.0 to 18.8 cm. All cores are 1.00 in. diameter. Holes were drilled and both radial and radiating grooves cut in the endplugs to allow flow to diverge as it enters or exits from the core. The previous core holder had only one entrance and exit hole. A study of the flow generated by such a configuration is presented in Appendix A. This core holder was built out of solid 316 stainless steel and was designed to operate at confining pressures of 10,000 psi.

When the effluent water surface tension was measured as a function of the air bath temperature, the results shown in Table 3 and graphed in Fig. 3 were obtained. Although du Pont⁴⁵ stated that Viton, a fluorocarbon elastomer, was indefinitely stable at 400°F, the plasticizer may be dissolving into the water and lowering the surface tension when the temperature exceeds 300°F. This implies that 300°F is a maximum temperature limit on the experiments made with this apparatus. In Appendix B other possible sleeve materials are discussed.

Initially a capillary tube viscometer was installed in the flow line downstream of the second filter. This was used to determine the flow rate-viscosity product of the core effluent. If something happened in the core to change the viscosity of the water (see Theory section), it could be measured directly rather than assuming the fluid to have the tabulated viscosity of pure water. Appendix C discusses the calibration of the coiled capillary tube viscometer. Its use was discontinued when different pore pressures were being used for which the capillary tube was not calibrated.

Table 3

EFFLUENT WATER SURFACE TENSION WITH VITON SLEEVE

<u>Temperature (°F)</u>	<u>Surface Tension (dynes/cm)</u>
70	64.1
250	64.1
300	59.1
350	43.4
400	41.1

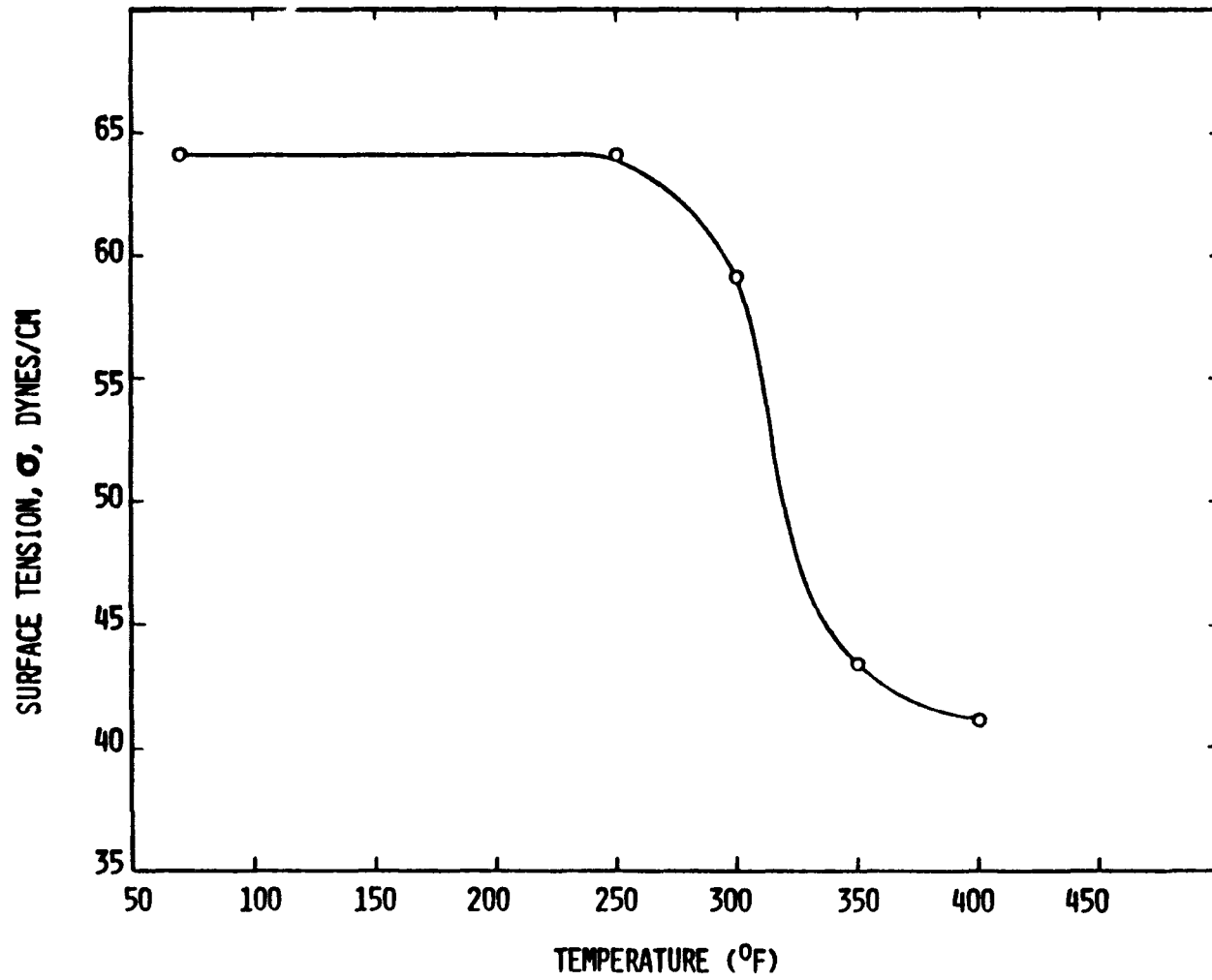


Fig. 3. Surface Tension vs Temperature for Effluent Water with Viton Sleeve.

Through several months of experimentation at the pore pressure for which the calibration was made, it was determined that the viscosity of the water was not changed by flow through the core.

Once the flow exits from the air bath, it is cooled in a counterflow heat exchanger to room temperature or below.

Absolute permeability is measured with one phase in the porous medium. At the elevated temperatures, it is necessary to keep the water from flashing to steam. This is accomplished by maintaining a pore pressure greater than the vapor pressure at the maximum temperature. The minimum pressure used in these experiments is 200 psi. Several methods have been used by previous authors to maintain this backpressure for various flow rates. The earliest was simply a needle valve. When a pulsation pump with an accumulator was used, the needle valve and the pump setting were continuously adjusted until a stable flow rate with the desired backpressure was realized. With the switching of the cylinders of the Ruska pump, the needle valve would allow complete depressurization of the system. This was unacceptable. Initially a simple pressure relief valve was used in this experiment. Unfortunately, with time it bled water during the switching of the pump cylinders so that the pressure got low enough to allow steam formation at the elevated temperatures. A more sophisticated system was sought to allow easy adjustment of the backpressure up to the maximum pressure rating of the Ruska pump without the bleeding problem.

A spring-loaded backpressure regulator was installed. Initially its performance was excellent. However, with time it too developed a bleeding problem. The solution was to place another backpressure regulator having better shut-off capabilities downstream of the adjustable spring-loaded one. A dome-loaded nitrogen backpressure regulator was installed immediately

downstream of the spring-loaded one. It is pressurized with N_2 to 220 psi and works very well.

From the second backpressure regulator, the water flows into a graduated cylinder where the effluent is measured in cubic centimeters and recorded in pore volumes.

All of the valves in the system from the pump to the backpressure regulators are "regulating and shut-off" valves rated at 6000 psi. All tubing, fittings, valves, etc., are made of 316 stainless steel. It has been found that other steels may cause difficulties in these types of experiments at elevated temperatures⁴⁶. The pump is 404 stainless steel. If it were changed to 316 stainless steel, the working pressure would be halved to 2000 psi and this would have been unacceptable for this study.

4.2 CONFINING PRESSURE SYSTEM

Figure 4 shows schematically the confining pressure portion of the apparatus added to the fluid flow system. The maximum confining pressure used in this study is 10,000 psi. All valves in this part of the system are rated at 45,000 psi.

So that leaks of the confining fluid into the core could be detected quickly, a commercial white oil No. 15 is used as the confining fluid.

The hand pump is used to pressurize the system initially. The lowest confining pressure used in this study is 1000 psi. Two pressure gauges are used to cover the entire range of confining pressures. The low pressure gauge is used to get accurate readings up to 5000 psi while the high pressure gauge is used up to 10,000 psi.

During heating and cooling cycles of the experiment, the oil in the core holder (about 100 cc) expands and contracts significantly changing the

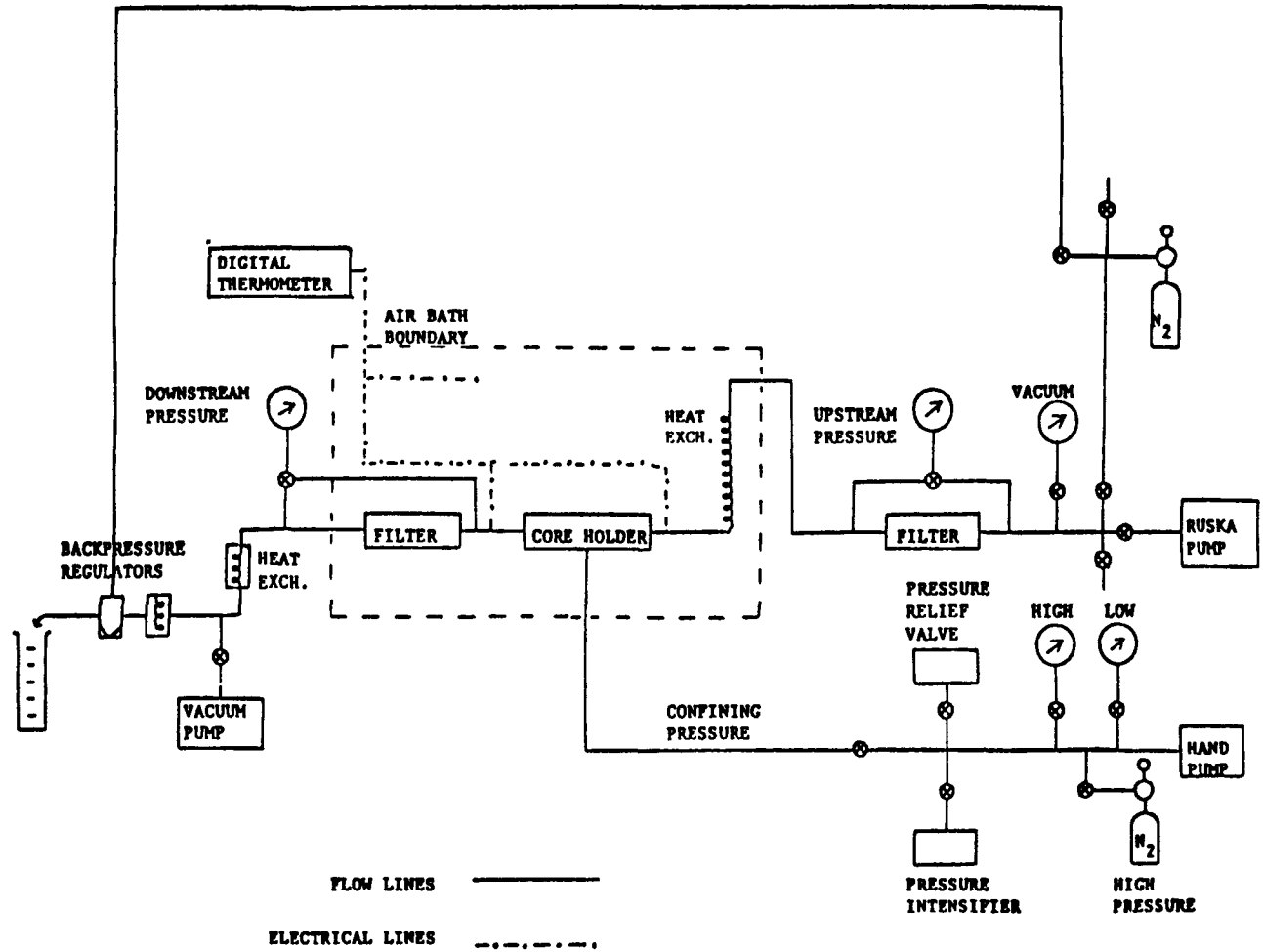


Fig. 4. Schematic Diagram of the Fluid Flow and Confining Pressure Systems.

confining pressure. A high pressure nitrogen cylinder with a self-relieving regulator is used to compensate for these changes. This cylinder and regulator keep the confining pressure constant up to a level of 6000 psi throughout the experiment. Other pieces of equipment in this system include a pressure relief valve and a pressure intensifier. Their use will be discussed in the Procedure section.

4.3 DIFFERENTIAL PRESSURE MEASUREMENT

Appendix D shows how the errors in the measured value of permeability are estimated. From this study it can be seen that the measurement of the pressure differential across the core is important in the accuracy of the permeability value calculated. This value is dependent upon using the appropriate pressure transducer diaphragm to measure the pressure differential. The pressure differential should be close to full scale but not exceed it. This is difficult with one pressure transducer when measurements are made over a range of flow rates and temperatures. To solve this problem, several differential pressure transducers are connected in parallel across the core holder (Fig. 5). With this design, the most appropriate transducer can be used.

Incorporated with each pressure transducer is a "short-circuit" loop. By using a three-way valve, the pressure can be equalized on both sides of the transducer or alternatively the differential pressure can be measured. This loop allows reading of the zero value of the transducer at any time at line pressure. This zero value is a function of line pressure and can shift due to pulsations in the system causing a transient overpressurization of the transducer. Although there is often a shift in the zero of the transducer, the calibration still holds. This loop also allows evacuation,

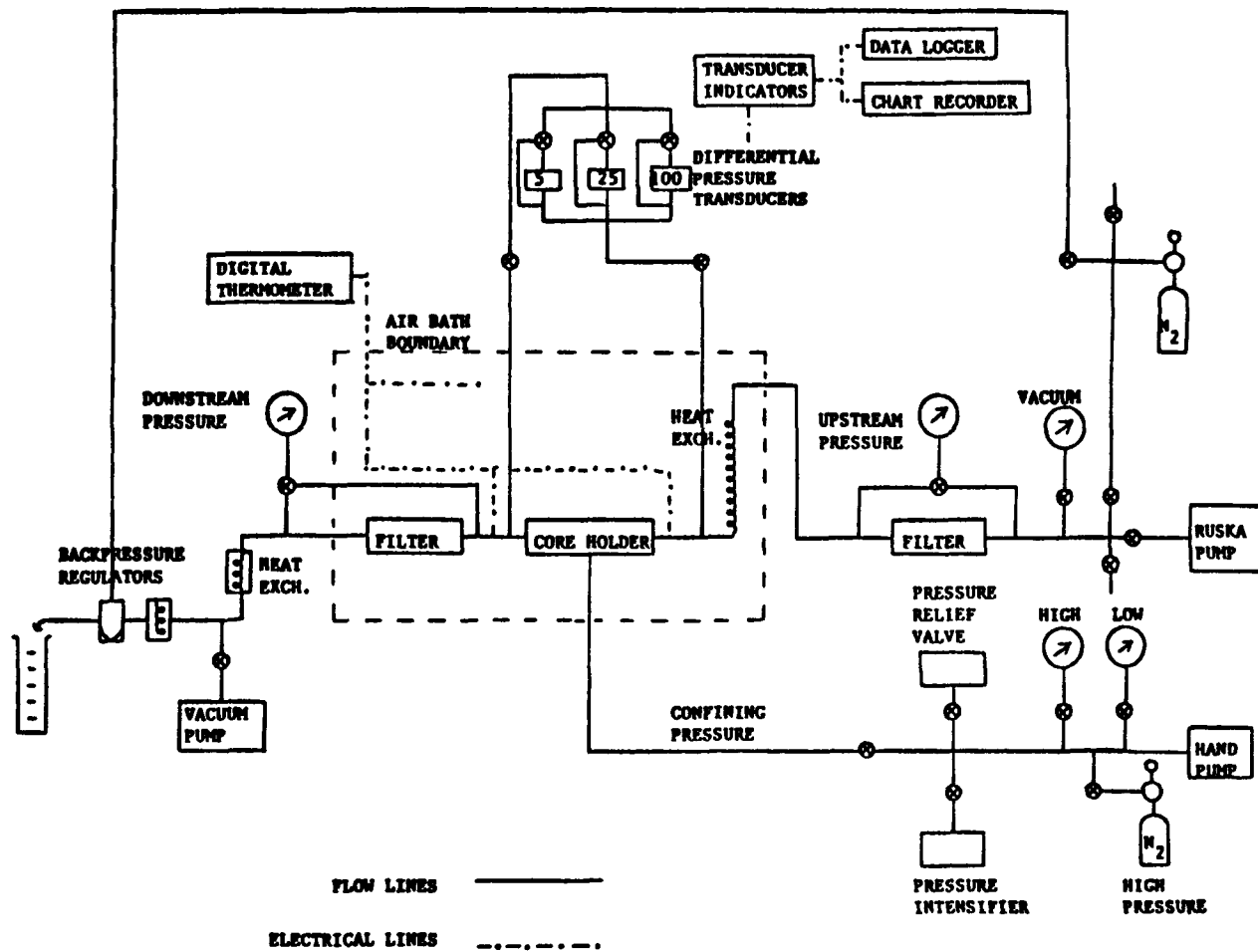


Fig. 5. Schematic Diagram of the Fluid Flow, Confining Pressure and Differential Pressure Measurement Systems.

pressurization and de-pressurization of the system without damage to the transducer. Because of the high pore pressures, the pressure transducers are high pressure models rated to 5000 psi line pressure.

Each transducer has a separate transducer indicator. The output from the indicators (0 to 10 v) is connected to a data logger which is connected to a computer. The signal is also read on a digital multimeter and recorded continuously on a two channel chart recorder. A continuous record of the pressure differential is kept throughout the experiment with the temperatures and pore volumes of throughput manually noted on the chart paper. To prevent electrical interference, the transducer indicators and the chart recorder are connected to a voltage regulator.

4.4 PRESSURE TRANSDUCER CALIBRATION

Immediately prior to each experiment, the differential pressure transducers are calibrated in situ. Figure 6 shows the complete schematic diagram of the apparatus including the calibration components.

The nitrogen cylinder supplies gas pressure to the dome-loaded regulator and the two line regulators. These are used to reduce the pressure for the 15 and 100 psi calibration pressure gauges (Heise gauges). Either regulator-gauge system may be used to calibrate a transducer.

To calibrate a differential pressure transducer, the full scale pressure is placed on the upstream side of the transducer. The short-circuit loop is used to equalize the pressures across the transducers and the indicator is adjusted to read zero voltage. This reading is taken with the multimeter. At the same time, the chart recorder is adjusted to read zero. The loop is then set to read differential pressure and the indicator calibrated to read full scale, 10 v. This process is repeated several times until the calibration remains unchanged.

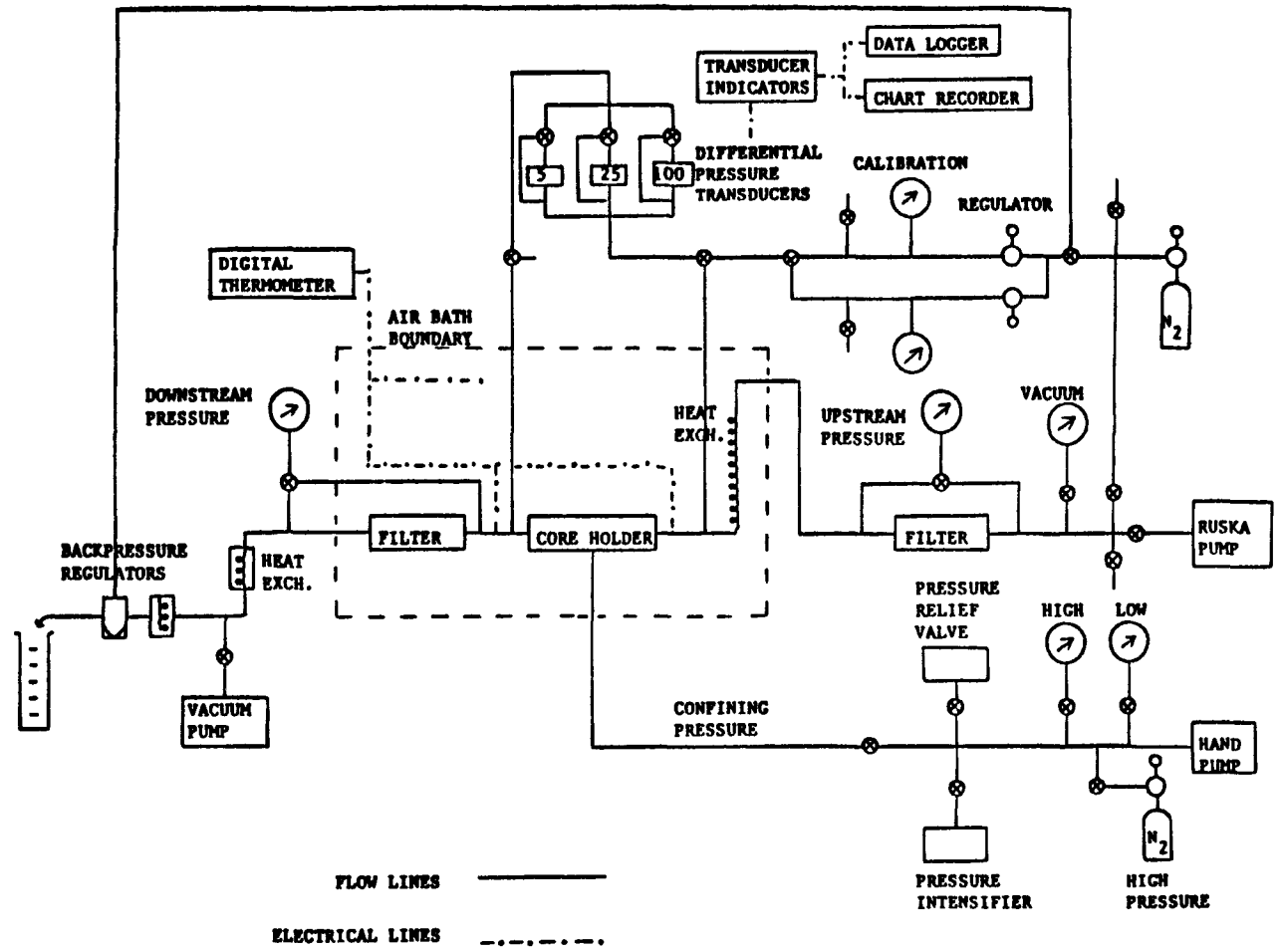


Fig. 6. Schematic Diagram of the Entire Experimental Apparatus.

5. EXPERIMENTAL PROCEDURE

The versatility of the experimental apparatus allows variables to be investigated independently during an experiment. Therefore, the procedure is basically the same whether the variable of interest is temperature or pore pressure or confining pressure.

Preparation for the experiment begins with the packing of the core. At the beginning of each experiment, the screens at each endplug (270 mesh) are replaced as are the O-rings on the two endplugs. The Viton tubing, 1 in. inside diameter, is first cut to the appropriate length (on the order of 9 in.). For the experiments on consolidated cores, a core of about 18.2 centimeters length is inserted into the tubing. The tubing is then mounted on the upstream endplug and the two hose clamps tightened around the upstream endplug. The hose clamps are used to prevent the confining oil from entering the core. The perforated aluminum sleeve is then slid over the Viton. The downstream endplug is inserted and the two downstream hose clamps tightened. Any excess Viton tubing is cut off. The entire assembly is placed in the core holder and bolted together.

For experiments on unconsolidated porous media, the Viton sleeve is first mounted on the upstream endplug and the hose clamps tightened. The perforated aluminum sleeve is placed over the Viton. After the two endplugs (with screens), four hose clamps, Viton tubing and aluminum sleeve have all been weighed, the sand, usually a two-to-one mixture of 120-200 and 100-120 mesh Ottawa sand, is poured in and tamped down in 20 gm increments. The level of the sand at completion is slightly above the aluminum sleeve so that the lower hose clamp straddles the sand and the downstream endplug. The

endplug is inserted and the two downstream hose clamps tightened. This assembly is weighed again and the length measured. Typical unconsolidated cores are 18.8 cm long with 38% porosity and 37 cc pore volume. The excess Viton tubing is cut off, the assembly placed in the core holder and the bolts tightened.

The core holder is then placed in the air bath and all lines connected. The hand pump is used to pressurize the core holder to the desired pressure level. This pressure, when first applied, will decrease with time due to compaction of the core, but after being reestablished, it will usually maintain the desired value. If it does not after repeated increases, this is a sign of an oil leak into the core.

The entire fluid flow and transducer system is evacuated with the mechanical vacuum pump overnight. If the core is consolidated, it is evacuated for another day and night. In the morning, the pressure transducers are calibrated in situ and the entire system subjected to vacuum for two hours. During this period the air bath is heated to 100°F (the lowest controllable temperature).

Water is allowed into the system, the Ruska pump started and the experiment begun. Permeability is measured at four different flow rates for each set of conditions. The first three flow rates are maintained for ten pore volumes each and the permeability for each flow rate is taken as the average of the values after first five and then ten incremental pore volumes. The fourth flow rate is a low one and lasts for only one pore volume. The purpose of this procedure is to insure that there is no flowrate dependence in permeability. The values of permeability from the first three flow rates are averaged to determine the permeability at a set of conditions. Appendix E gives the calculator program used to calculate permeability and an example

of the calculation procedure.

Water flow continues during heating and cooling cycles of the experiments and when the confining pressure or pore pressure is changed. When the confining pressure is less than 6000 psi, the high pressure nitrogen cylinder and self-relieving regulator are used to keep the confining pressure constant during the heating and cooling cycles. During heating cycles when the confining pressure is greater than 6000 psi, the pressure relief valve may be used to keep the confining pressure constant (it is adjustable from 4000 to 10,000 psi). During cooling cycles when the confining pressure is greater than 6000 psi, the pressure must be manually maintained with either the hand pump or the pressure intensifier. Because of its ease of operation, the pressure intensifier is used.

When the pressure differential is read, the reading is taken from the chart recorder. At this time the transducer is then "short-circuited" so that a reading for the zero may also be taken. The zero value is very small so it is read from the digital multimeter.

At the conclusion of the experiment the confining pressure must be released. To do so, the valve to the nitrogen cylinder is closed and the pressure between the valve and the cylinder is released through the regulator. Then the pressure in the system is bled off by allowing flow back into the hand pump. The regulating valve on the pump allows this to be done in a slow, controlled manner.

6. RESULTS

Unconsolidated Ottawa sand packs and Berea sandstone cores have several differences which might lead to somewhat different responses to temperature and pressure variations. Because of these differences and the explanations for the responses of the two porous media to the conditions of these experiments, the results and discussions will be presented separately.

6.1 UNCONSOLIDATED OTTAWA SAND

Unconsolidated Ottawa sand is one of the simplest porous media that can be used. The grain size distribution may be established and the effects of clays and consolidating material found in consolidated porous media are removed. Therefore, the results on unconsolidated sand packs will be discussed first. As previously stated, the grain size used was usually a two-to-one mixture of 120-200 and 100-120 mesh sands. The grain size for each experiment is shown on each figure from that experiment. Experiments are denoted by the date they began. For example, run 3-20-81 was the experiment begun on March 20, 1981. The detailed data taken for all the experiments can be found in the laboratory notebook kept for this study.

Early results showed permeability reductions with temperature increase^{47,48}. Later these results were found to be in error^{44,49,50}. They were due to experimental oversights. In view of these past oversights, it appeared prudent to prove that no other phenomena were occurring that could be producing or masking a change in permeability under the various conditions of interest in this study.

Two possible causes of incorrect calculation of permeability are a volumetric throughput dependence and a flowrate dependence. These are shown in the first set of figures. Figures 7 and 8 show permeability versus throughput for two different experiments. Figure 7 shows a reduction in permeability of about 200 millidarcies (from 2900 to 2700) with 600 pore volumes of throughput. Figure 8 shows a constant permeability versus throughput relationship for a higher permeability sand pack with larger sand grains. The differences between the two experiments are that the first (Fig. 7) was run before the endplugs were modified to allow flow to diverge at the endplug face. The second (Fig. 8) was packed after a long break in experimentation yielding an excessively high permeability. Error bars are shown for several points in Fig. 7 and all the points in Fig. 8. Appendix D discusses the error analysis and Appendix E discusses the calculation of permeability giving an example and the hand calculator program used to determine permeability and the error of each measurement. The variation of error in Fig. 8 occurs because of different flow rates yielding different pressure differentials that can be measured with different accuracies. In brief, both experiments show a minor effect of throughput on permeability.

Figures 9 and 10 show permeability versus flow rate for an unconsolidated sand pack at 100 and 300^oF for one experiment. These graphs show that there is little scatter and no systematic change in the measured values of permeability at various flow rates despite the rather large error bars. These large error bars are caused by measuring the pressure differential with a transducer plate that has too large a pressure range. This shows that the response of the transducers is close to being linear even in the low ranges of differential pressure.

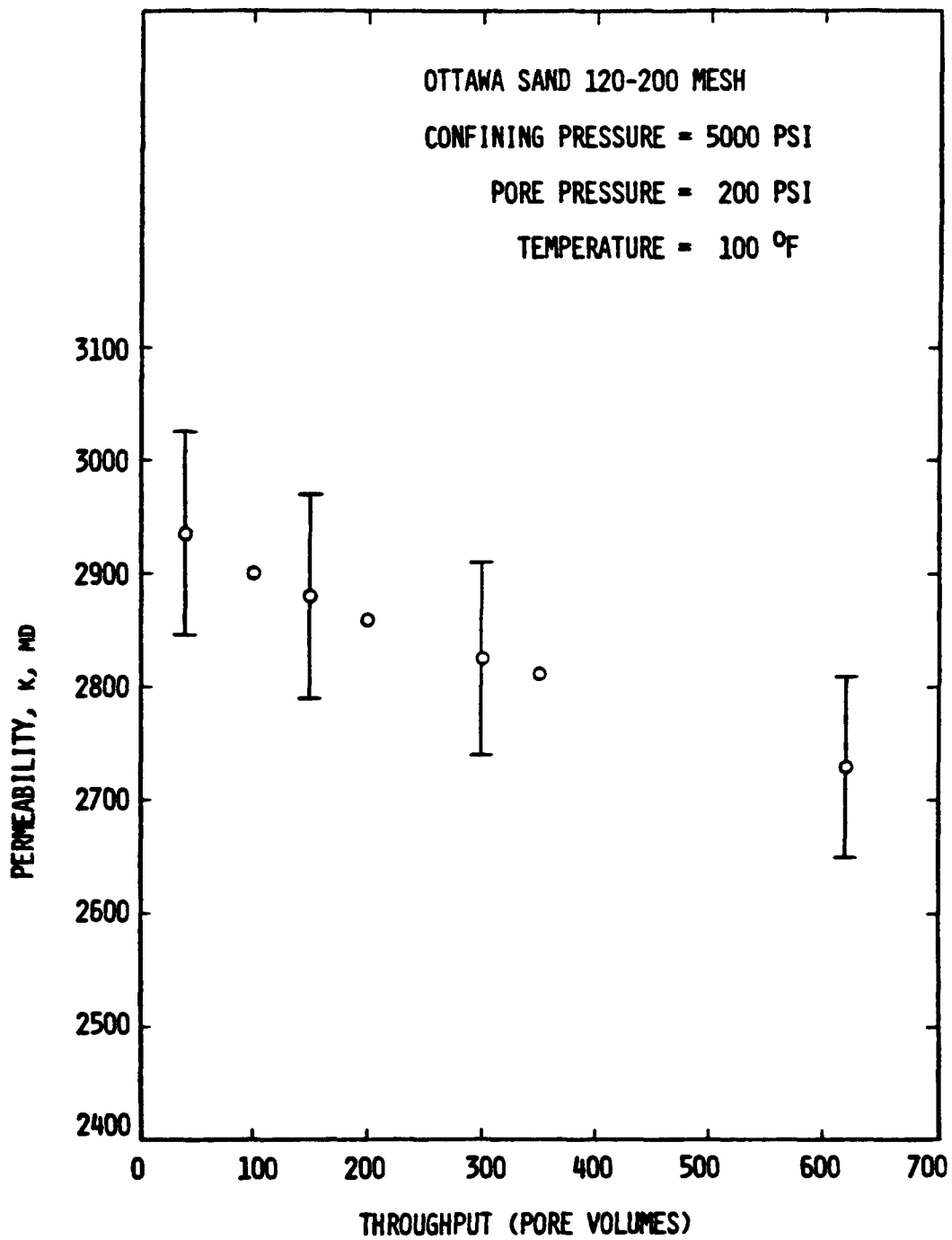


Fig. 7. Permeability vs Throughput for Run 11-22-80.

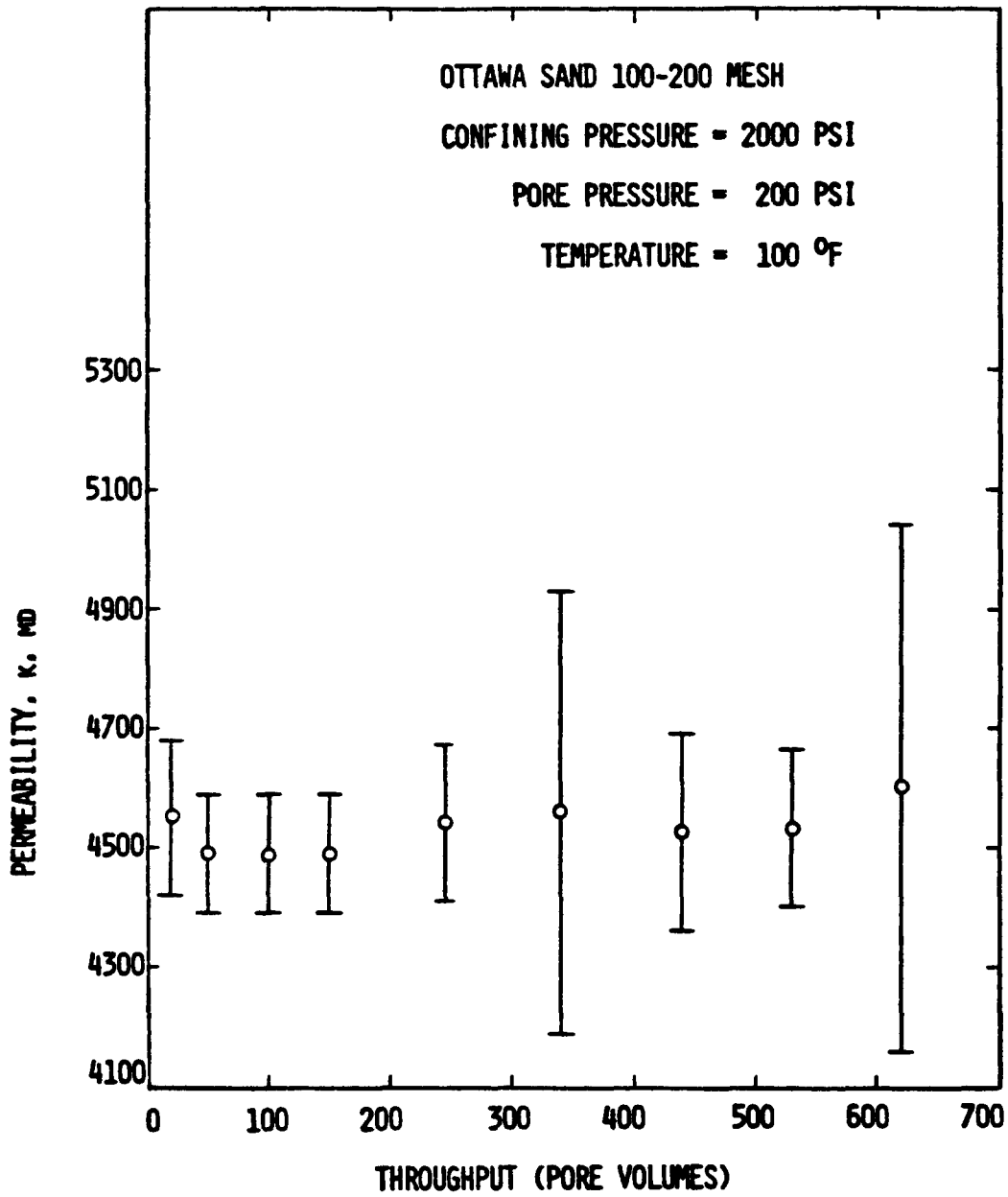


Fig. 8. Permeability vs Throughput for Run 4-10-81.

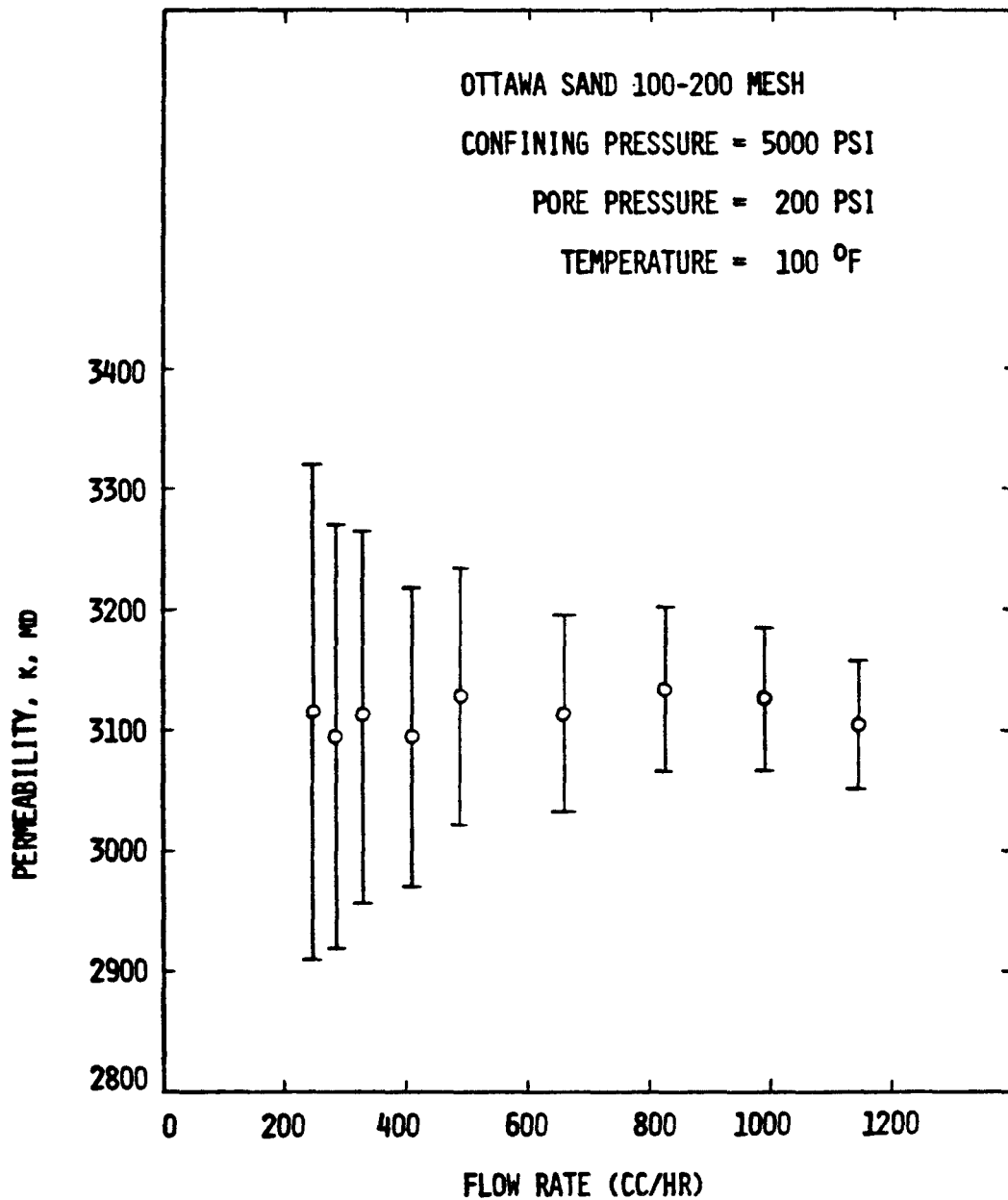


Fig. 9. Permeability vs Flow Rate for Run 2-5-81.

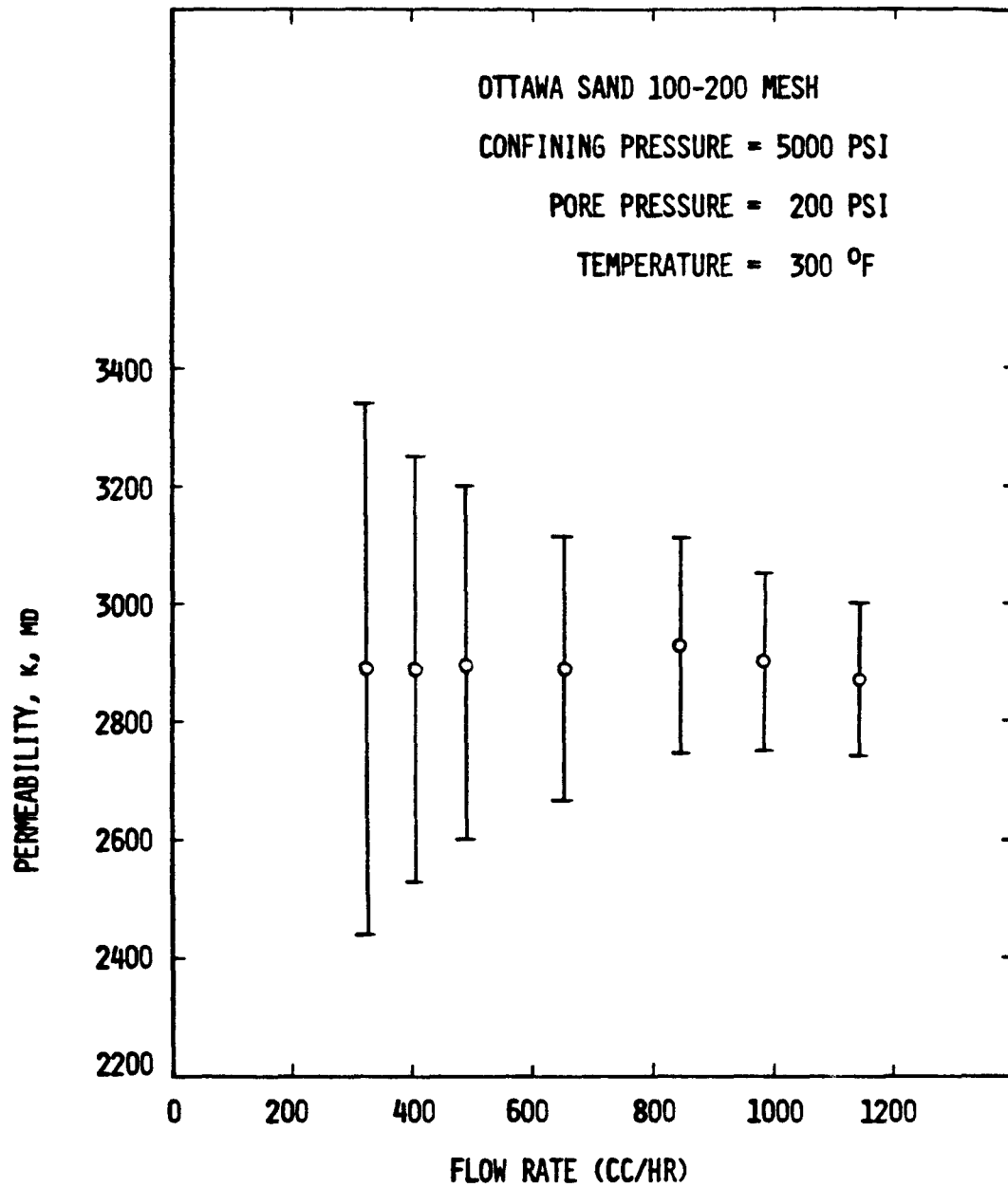


Fig. 10. Permeability vs Flow Rate for Run 2-5-81.

Once the dependence of permeability on throughput and independence of permeability on flow rate have been determined, permeability can be measured as a function of the three variables of interest—temperature, confining pressure and pore pressure. Temperature was the first variable investigated. Figures 11 and 12 show permeability graphed versus temperature at fixed confining and pore pressures with error bars indicated on some representative measurements. Figure 11 shows an increase in permeability with temperature to 250°F and then a reduction at 300°F followed by a continued decrease during the cooling cycle. From the error bars shown, it is clear that the scatter of points is within experimental error. There is possibly some overall reduction in permeability from the first data point to the last, but this is likely to be a throughput effect as seen in Fig. 7. Figure 12 has a sharp drop in permeability at 200°F caused by extended flow overnight at this temperature. While there appears to be some reduction in permeability, it is quite likely merely a throughput effect like that found in Fig. 7.

Figure 13 shows permeability graphed versus temperature at four different confining pressures with the pore pressure held constant throughout the experiment. Error bars are not indicated on the figure, but they are about ± 150 millidarcies. It can generally be said that the errors are in the range of 3 to 5% of permeability for this study. In this figure, permeability is effectively constant with temperature when the effect of settling caused by throughput is considered. So, all of these experiments show that there is probably no reduction in permeability with temperature increase for these unconsolidated Ottawa sand packs beyond the experimental error or the reduction that can be expected due to throughput. This is a significant finding in that it is in contradiction with previous investigations at Stanford University.

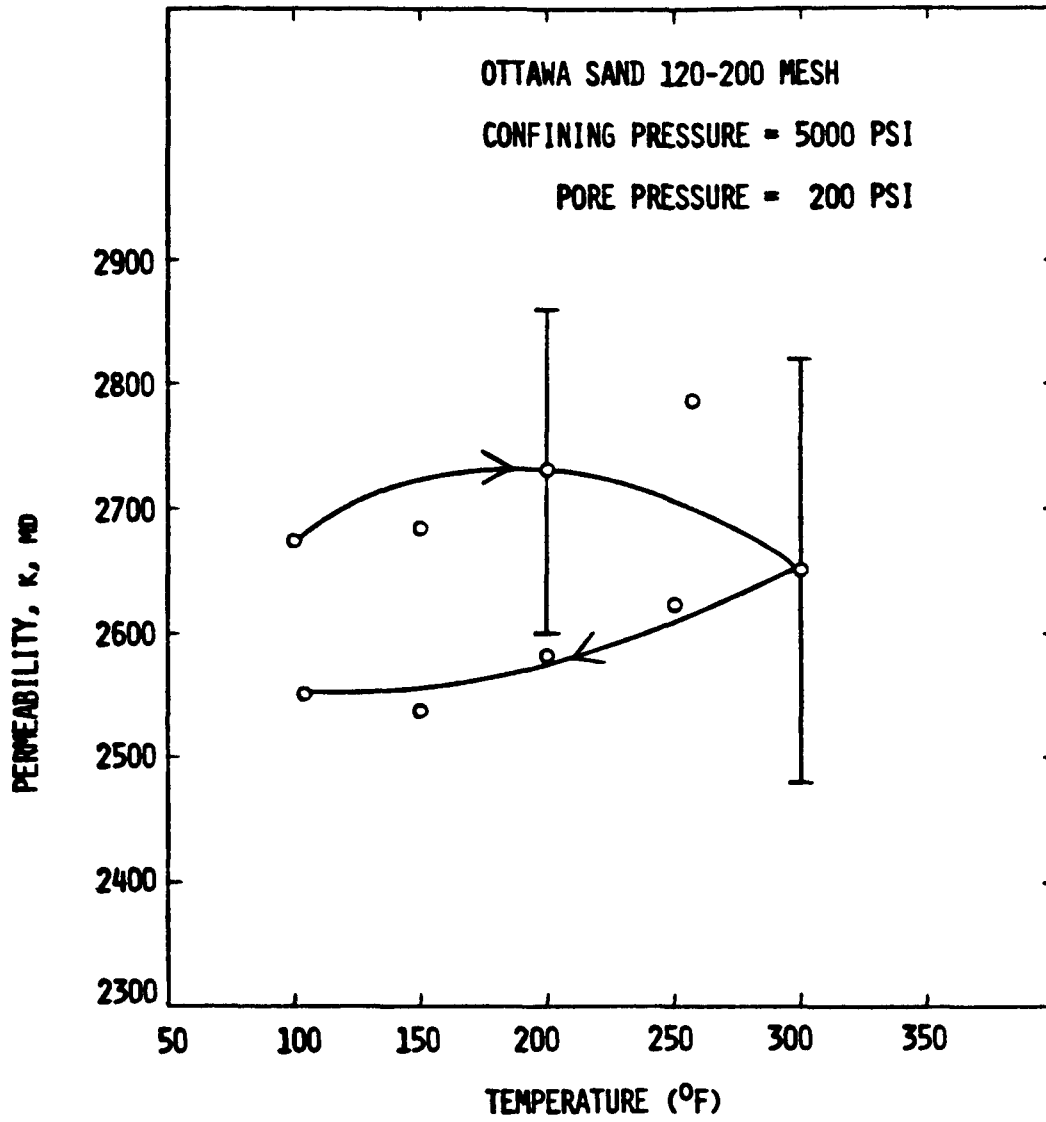


Fig. 11. Permeability vs Temperature for Run 11-22-80.

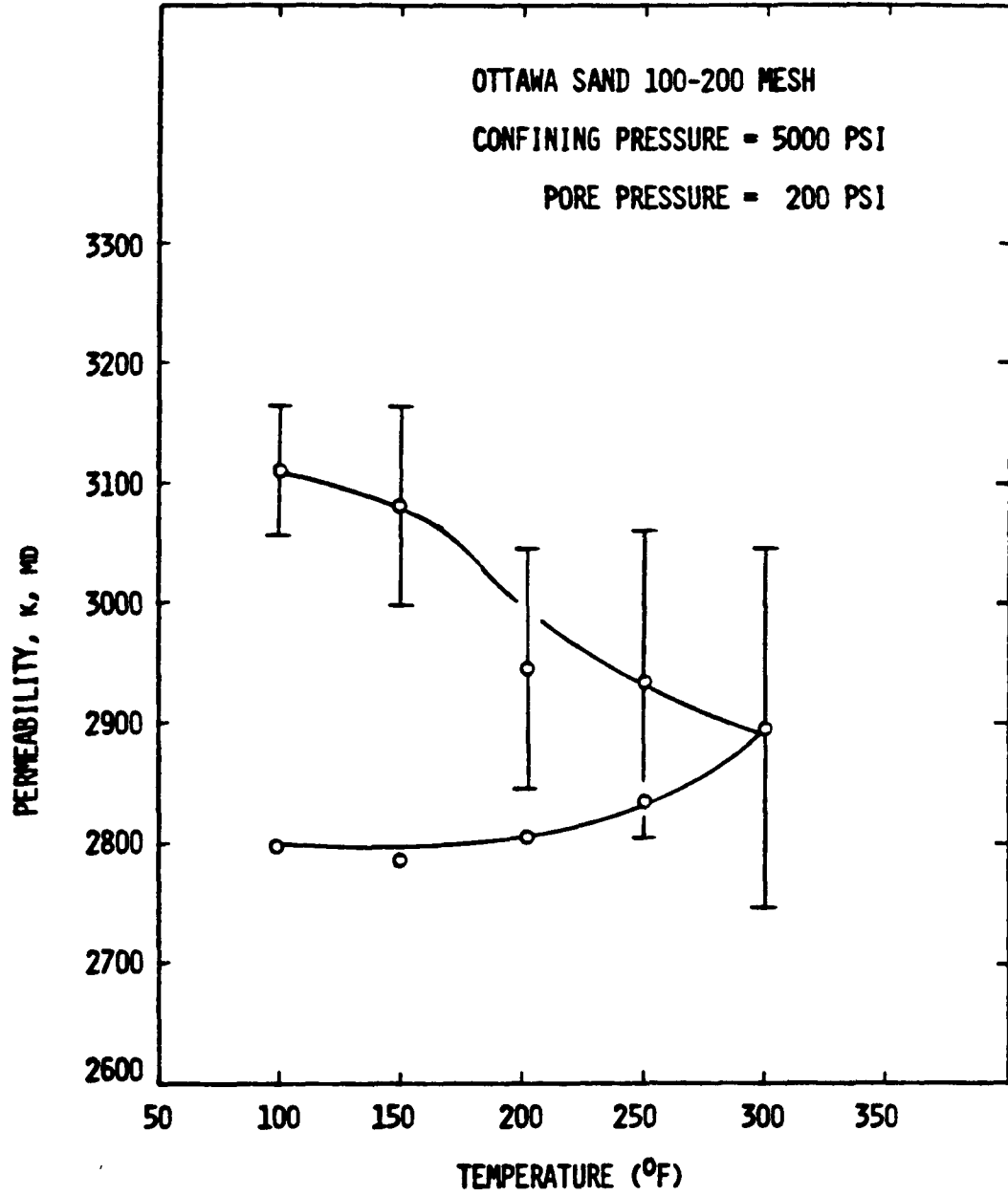


Fig. 12. Permeability vs Temperature for Run 2-5-81.

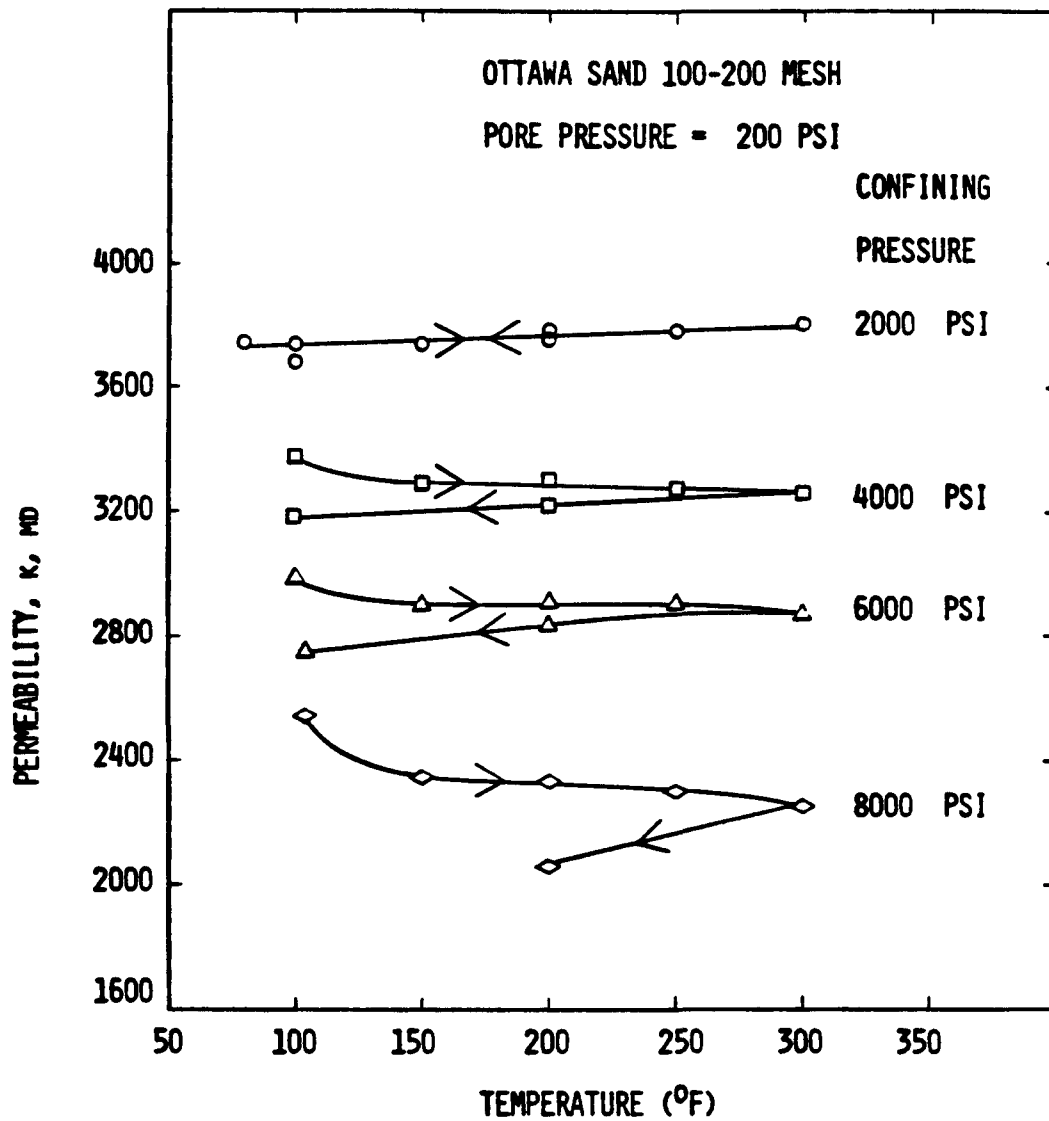


Fig. 13. Permeability vs Temperature for Run 10-10-80.

The next topic of investigation was the effect on permeability of increasing the confining pressure. Figure 14 shows the results of an experiment run at fixed temperature and pore pressure with only the confining pressure varied. There is a clear linear trend in that part of the data when the confining pressure is increasing. This will be useful later when attempts are made at correlating results under different conditions. Error bars are shown for two representative measurements. The first decrease and the second increase of confining pressure follow the same path although it is different from the first increase of confining pressure. This hysteresis after the first pressurization is noteworthy and will be discussed later.

Variation of permeability with changes in pore pressure was studied in two experiments depicted in Figs. 15, 16 and 17. Figures 15 and 16 show the effect of increasing pore pressure on permeability from the same experiment. The results shown in Fig. 15 were determined before the heat-cool cycle of Fig. 12. The measurements shown in Fig. 16 were taken after the heat-cool cycle. The lower point at 200 psi pore pressure in Fig. 15 was taken after the pore pressure had been increased and then released. There is no effective change in permeability after the pore pressure cycle. Error bars are shown for two points in Figs. 15 and 16. Figure 17 shows the effect of a complete increase-decrease pore pressure cycle. The results show that permeability measurements made at a constant temperature and confining pressure with only the pore pressure varied are linear over most of the pore pressure range. Also, in contrast with confining pressure changes, there is no hysteresis with pore pressure changes. This will be discussed in the next section of this work.

Once the effect of each variable was determined independently, the combined effects were studied. In the first case, the confining pressure to

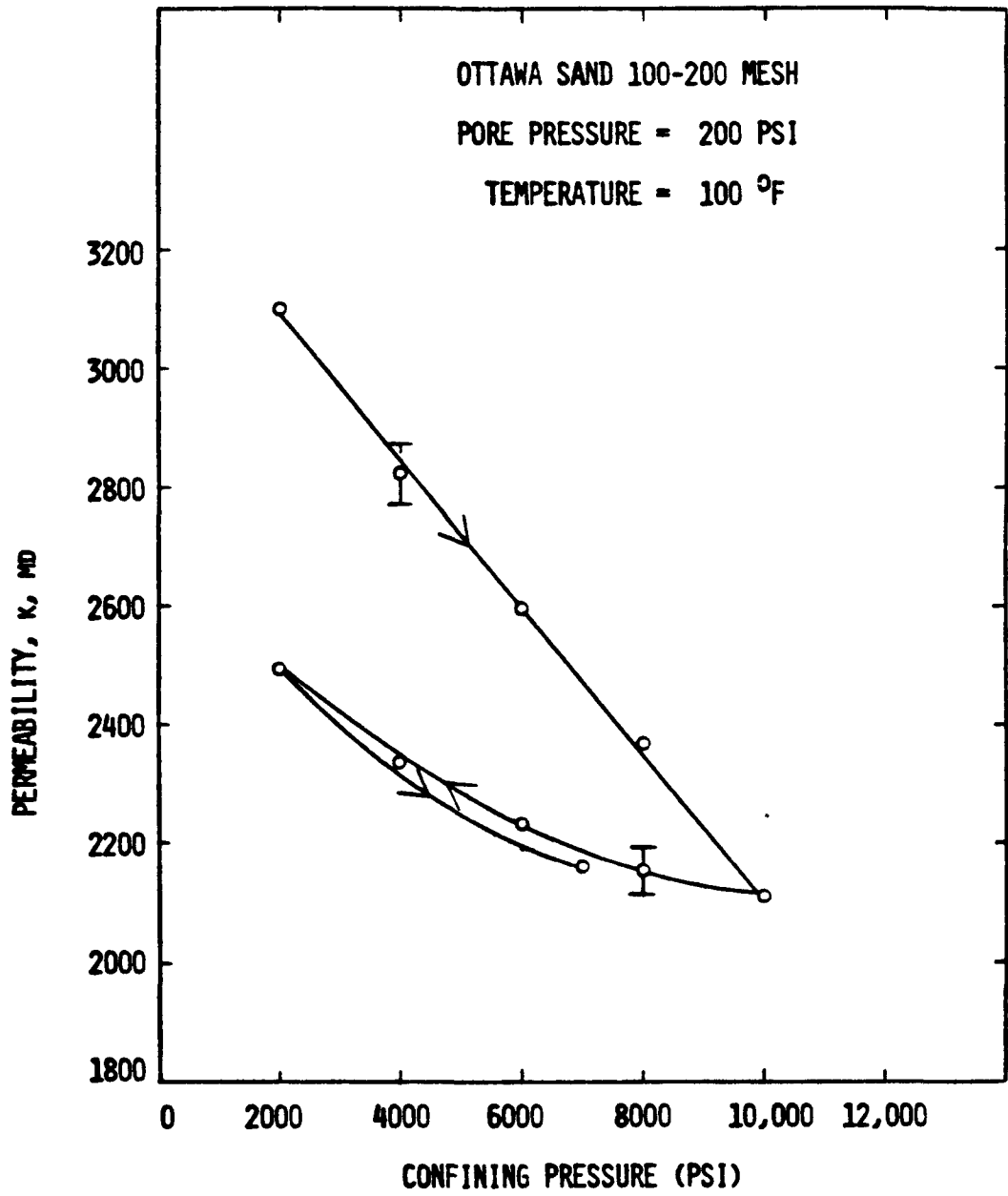


Fig. 14. Permeability vs Confining Pressure for Run 4-8-81.

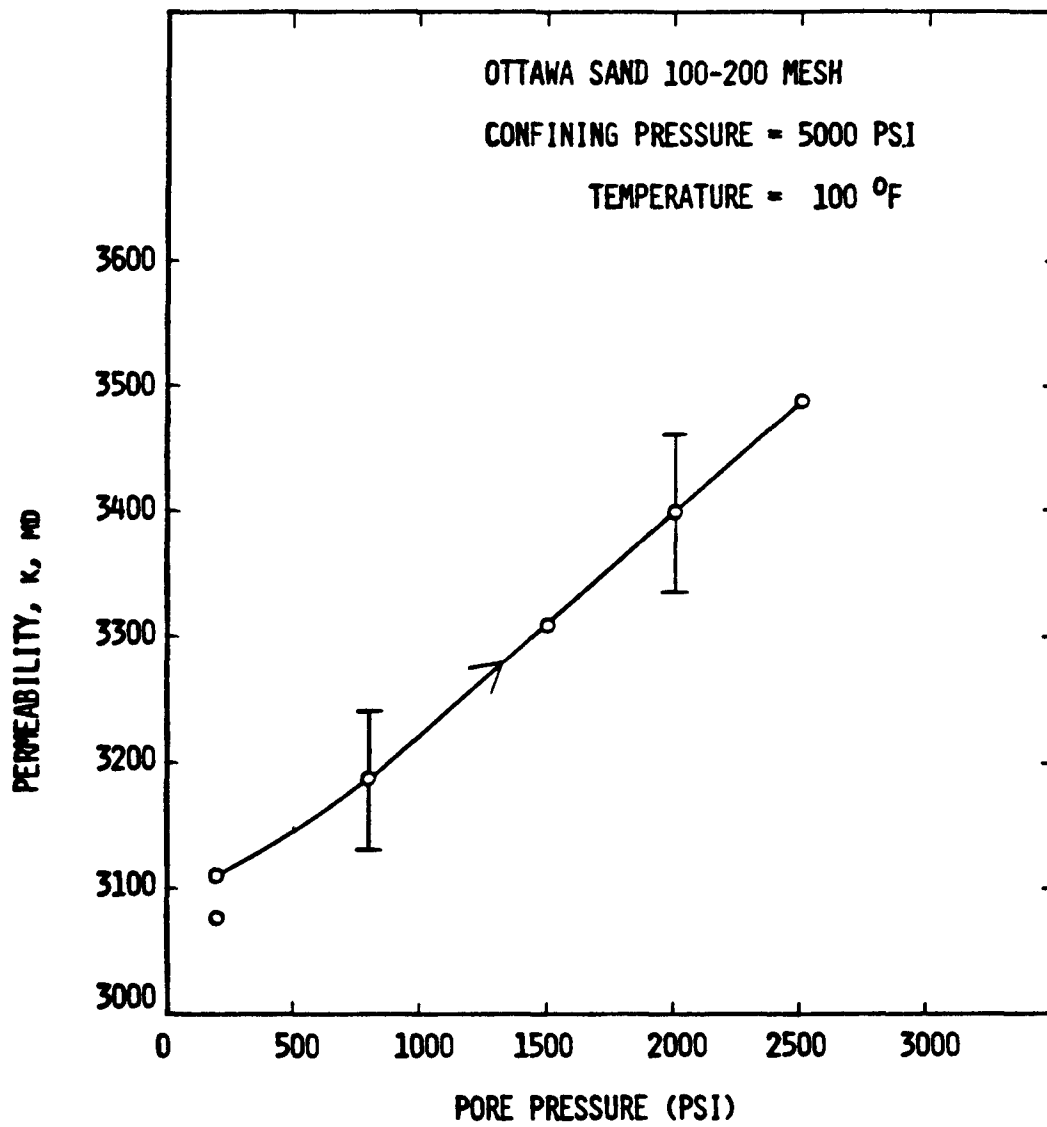


Fig. 15. Permeability vs Pore Pressure for Run 2-5-81.

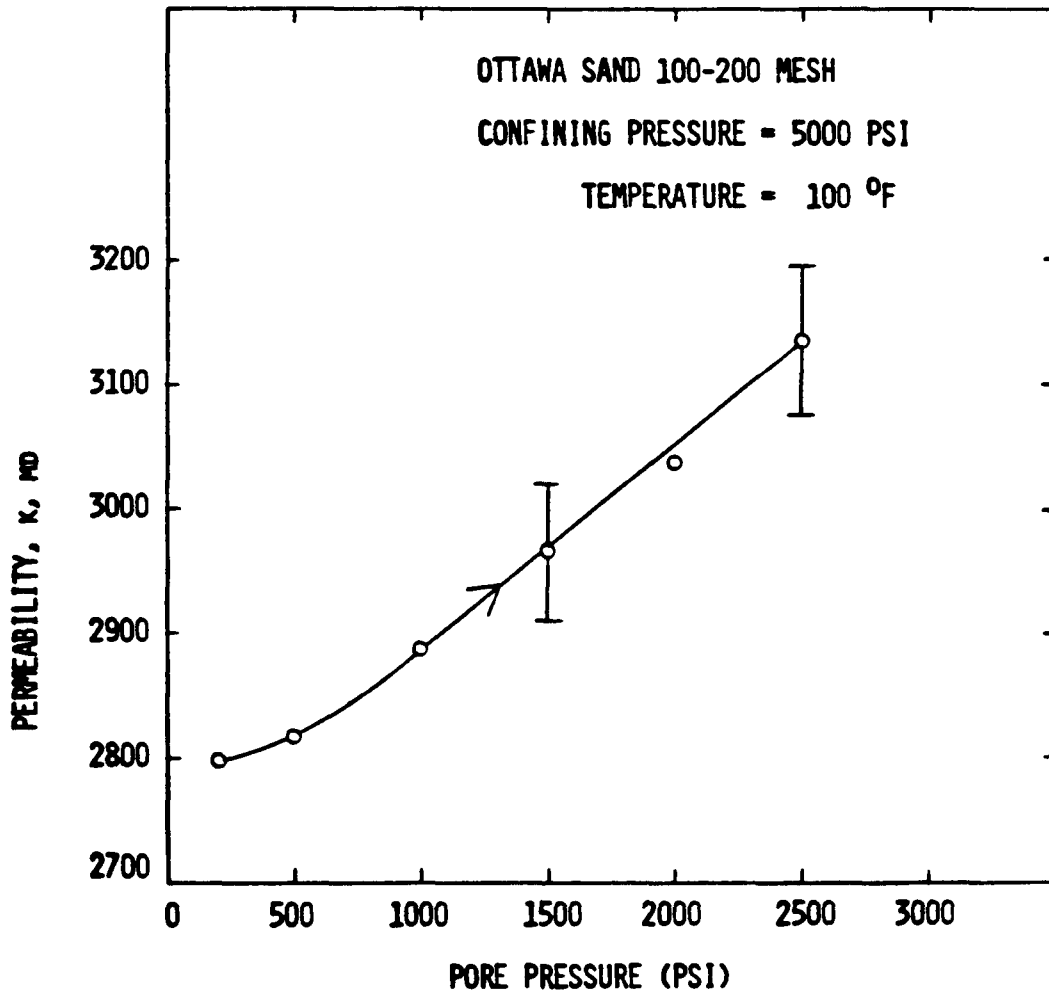


Fig. 16. Permeability vs Pore Pressure for Run 2-5-81.

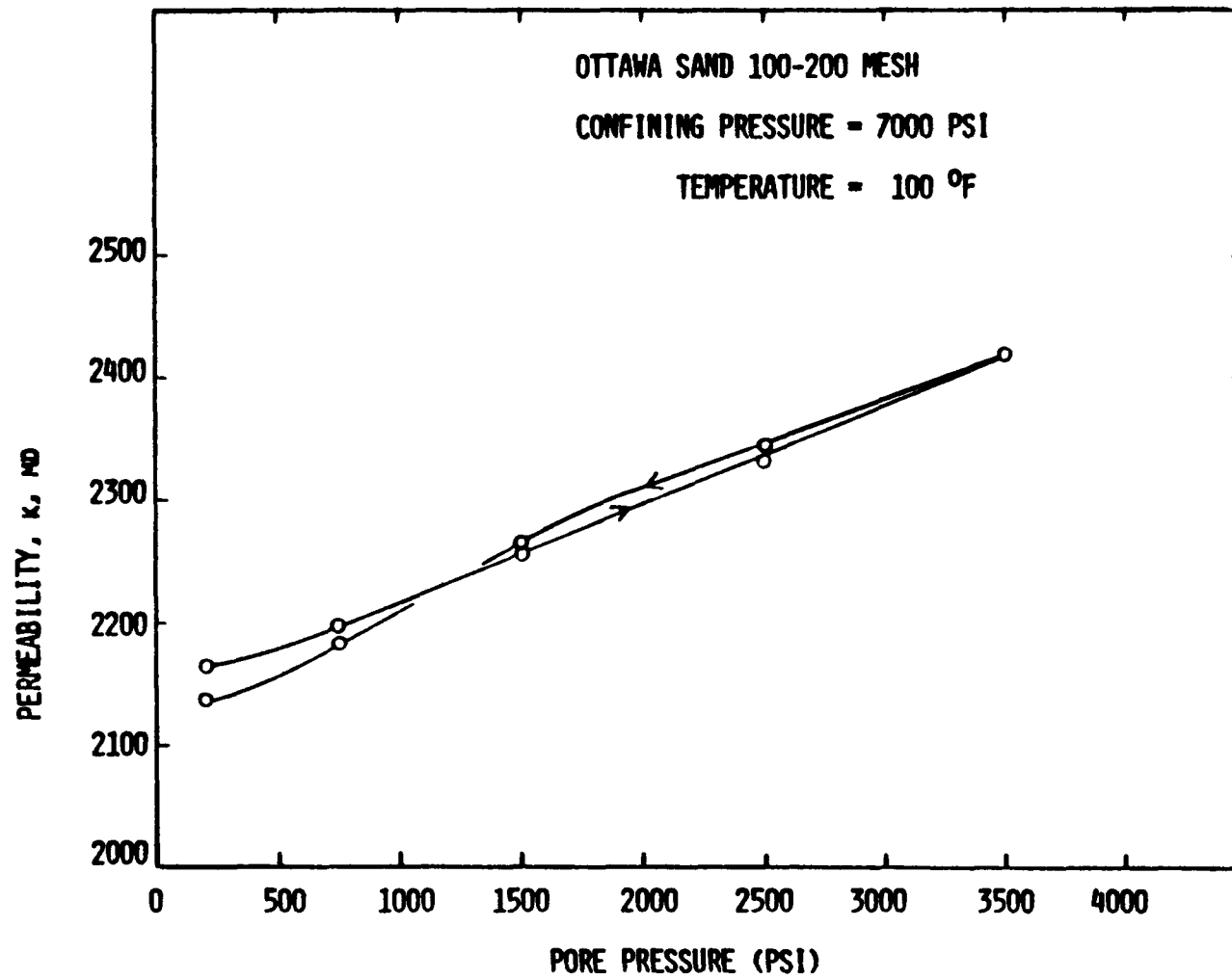


Fig. 17. Permeability vs Pore Pressure for Run 4-8-81.

pore pressure ratio was fixed at 0.40 . This is a reasonable approximation to what occurs in reservoirs (overburden pressure is on the order of 1 psi/ft of depth and fluid pressure is about 0.4 psi/ft of depth). Figures 18 and 19 show the same data graphed in two ways. Figure 18 shows permeability graphed versus confining pressure while Fig. 19 shows permeability graphed versus the difference between the confining pressure and the pore pressure. Both these figures have the same trends. This is expected for this experiment since the pressure differences are proportional to the confining pressures. These figures also have the same basic shape as Fig. 14 where the confining pressure alone was varied. Error bars are shown for two points in Figs. 18 and 19.

To find some relationship between the effective stress on the core and the confining and pore pressures, an experiment was run at a constant differential (confining minus pore) pressure. The results of this experiment are shown in Fig. 20. Here, within the accuracy of the data (error bars shown on all points), there is a constant permeability at the various confining pressures when the difference between the confining pressure and pore pressure is 3000 psi. Although the confining pressure minus the pore pressure is kept constant, due to the geometry of the endplug the axial force on the core is proportional to 0.75 times the confining pressure minus the pore pressure. So, while the difference is kept constant, the axial force is actually decreasing. It may be this decrease which causes the slight upward trend of the data with increasing confining pressure. Since the increase is so slight it is not clear whether this is a true increase or whether it is merely experimental error. It is hypothesized that, if the core were hydrostatically loaded, this upward trend would not occur. In either case, the trend is slight, and it can be concluded that the permeability depends only on the difference between the confining and pore pressures and not on the pressure level.

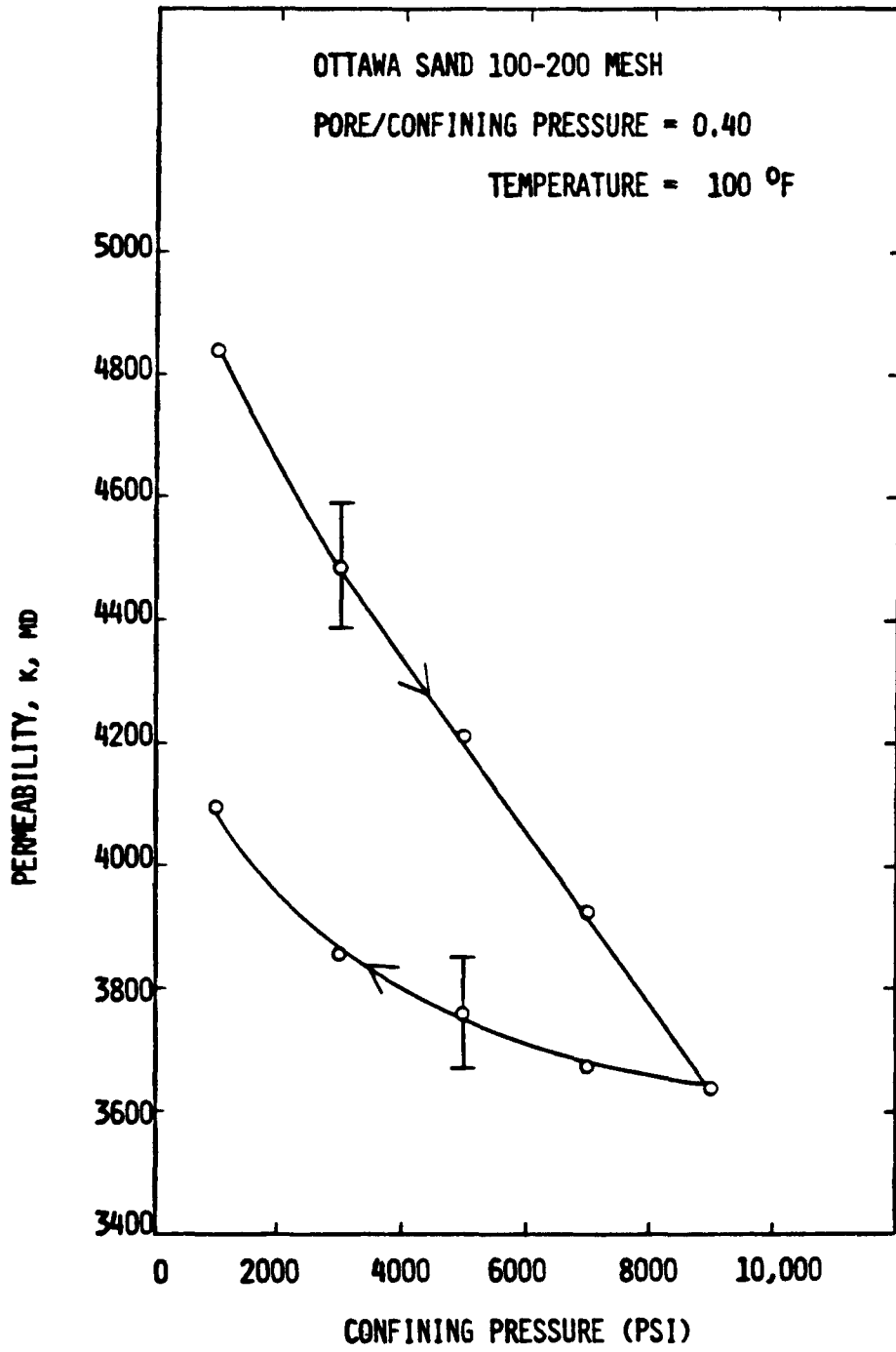


Fig. 18. Permeability vs Confining Pressure for Run 4-10-81.

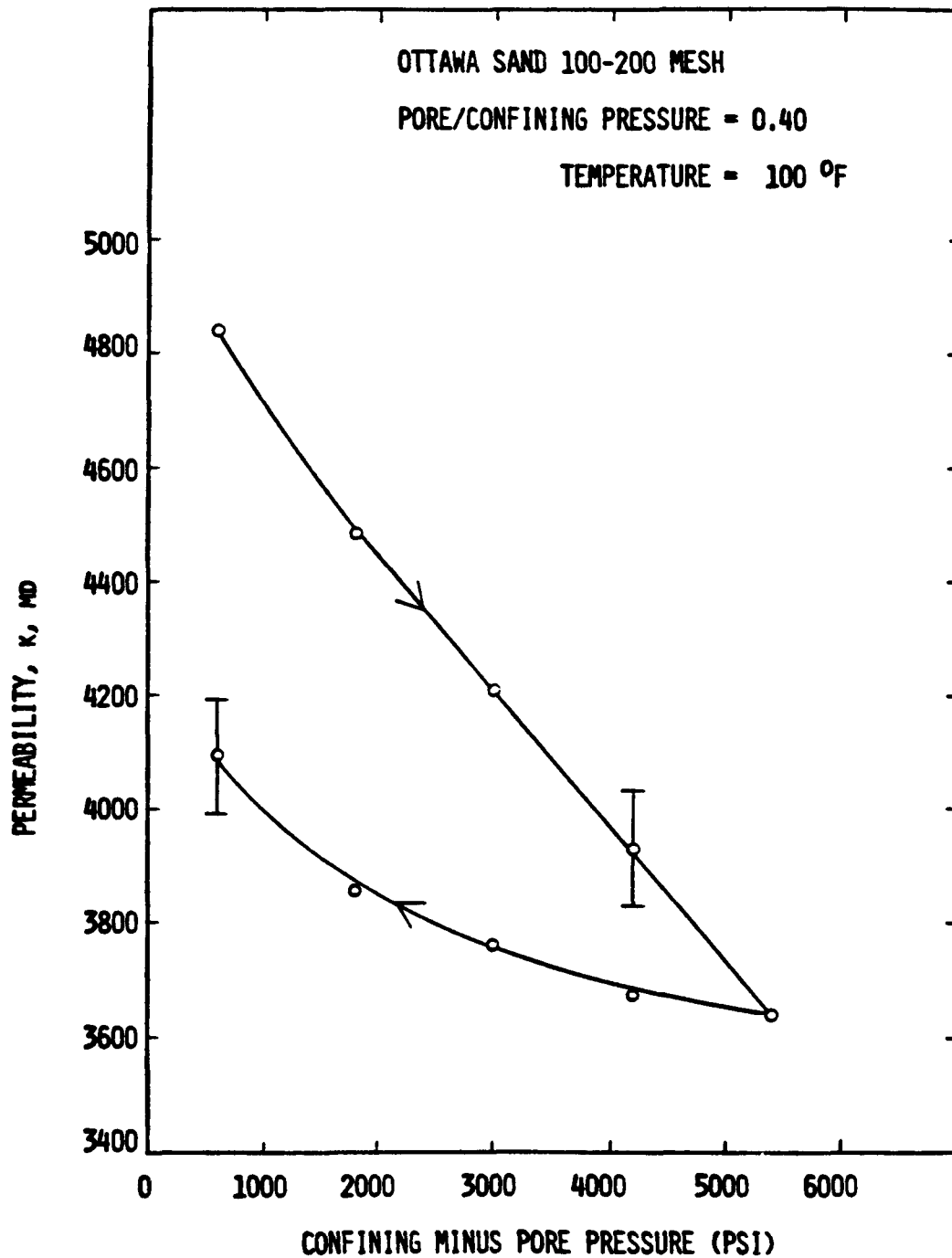


Fig. 19. Permeability vs Confining Minus Pore Pressure for Run 4-10-81.

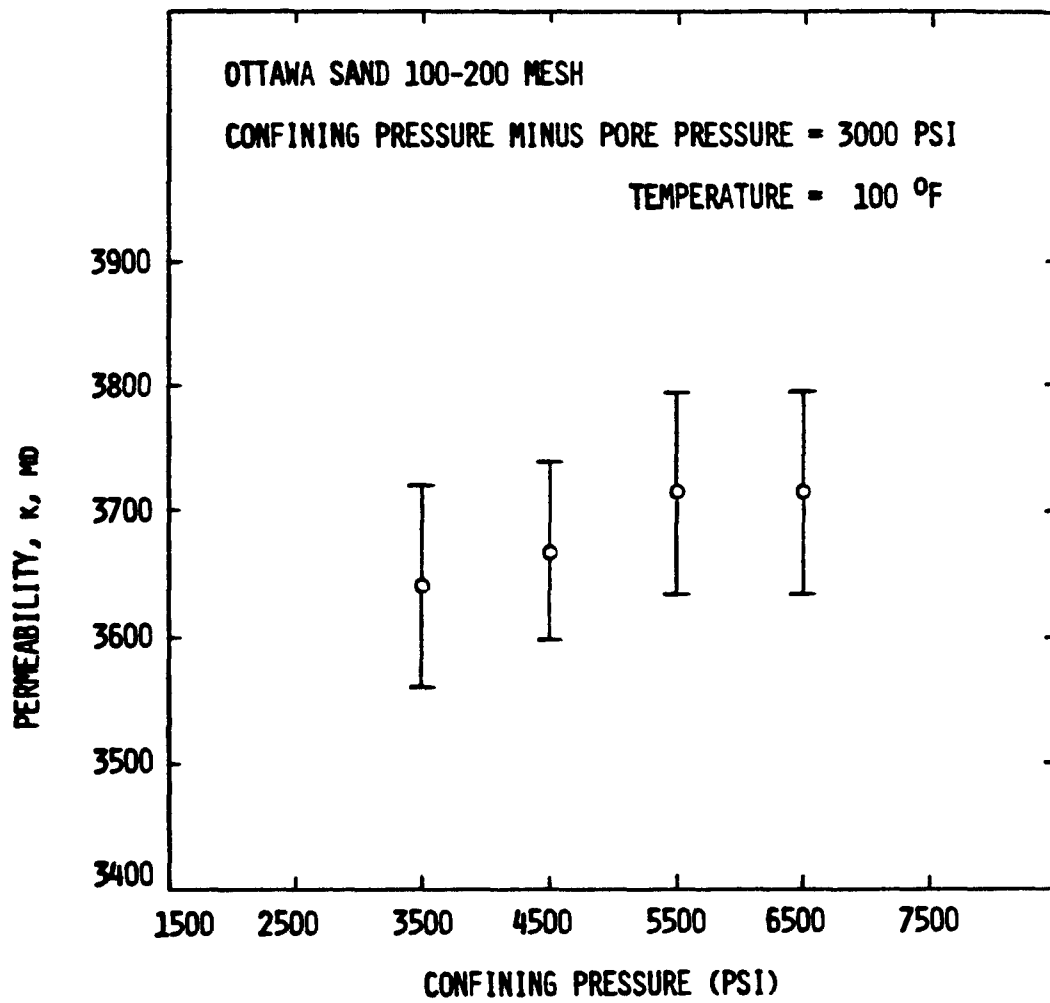


Fig. 20. Permeability vs Confining Pressure for Run 4-10-81.

6.2 CONSOLIDATED SANDSTONE

When working with consolidated sandstone, it is again necessary to determine if there is a throughput or flowrate dependence while the measurements are being made. Figure 21 shows permeability graphed versus throughput for a fired Berea sandstone core. Firing and its results will be discussed later, but it should be noted that simple dry firing of this core (without a fluxing agent present) at 500°C for six hours apparently did not deactivate mobile clay particles. Figures 22 and 23 show permeability graphed versus flow rate. As with the unconsolidated sand packs, there is little variation in the values of permeability calculated over the range of flow rates used in this experiment, even at the elevated temperatures where the differential pressure is lower and the errors higher. Within the accuracy of the data, the permeability is not flow rate dependent.

The effect of temperature on the absolute permeability to water of an unfired Berea sandstone core is shown in Fig. 24. The squares represent the measurements made during the heating cycle and the circles show the results when cooling. The error bars for two representative points (at the same value) are shown. From this it can be stated that there is no permeability dependence on temperature for this unfired Berea sandstone. The small variations in permeability are within the error bars shown in the figure.

Figure 25 shows permeability as a function of the confining pressure on the fired Berea core. The results are quite similar to those obtained for an unconsolidated sand pack. A linear decrease in permeability with the initial pressurization is observed followed by a repeatable non-linear change when the pressure is released.

Permeability is graphed versus pore pressure at a fixed confining pressure for a fired Berea sandstone in Fig. 26. A linear increase in

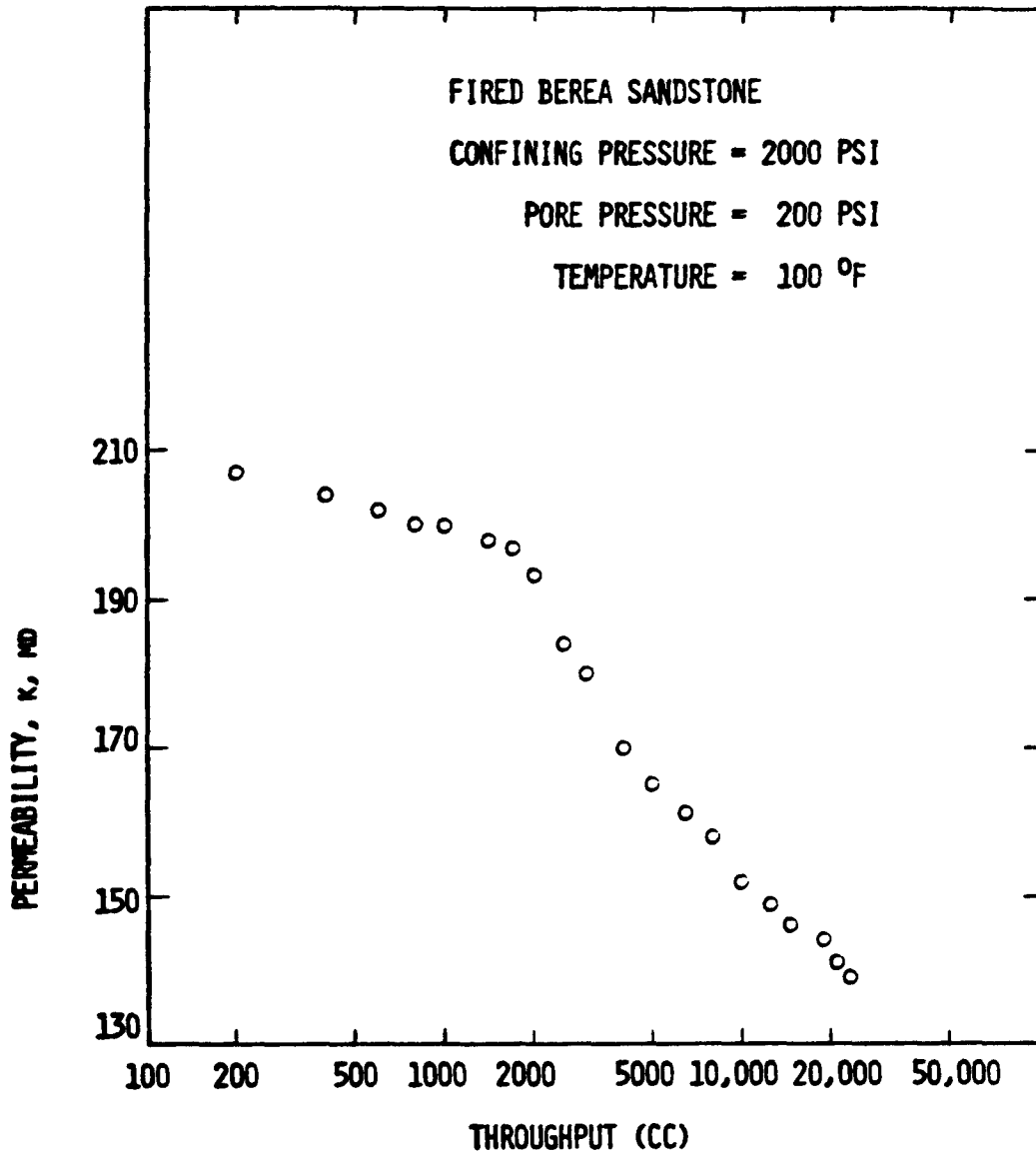


Fig. 21. Permeability vs Throughput for Run 4-16-81.

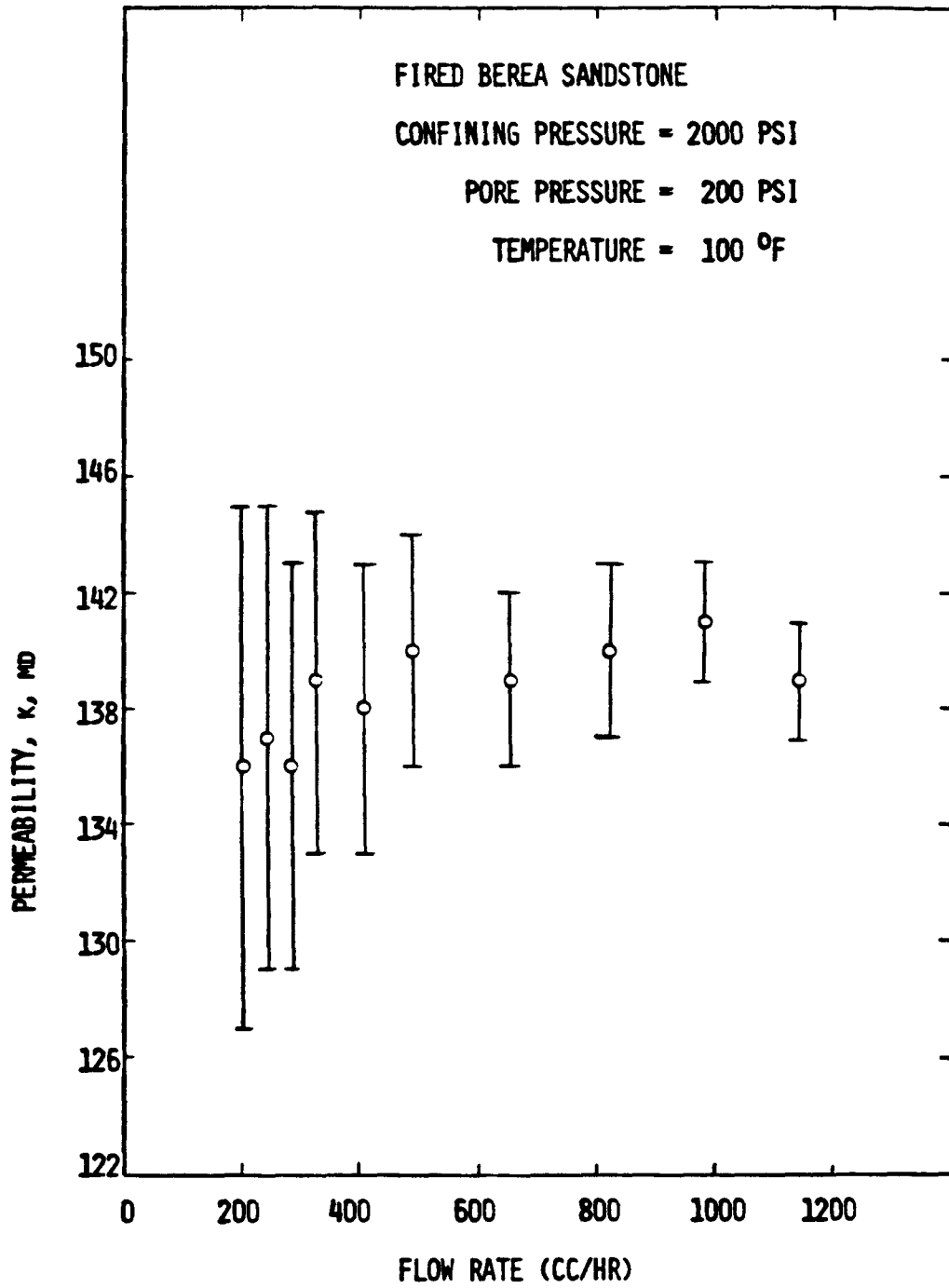


Fig. 22. Permeability vs Flow Rate for Run 4-16-81.

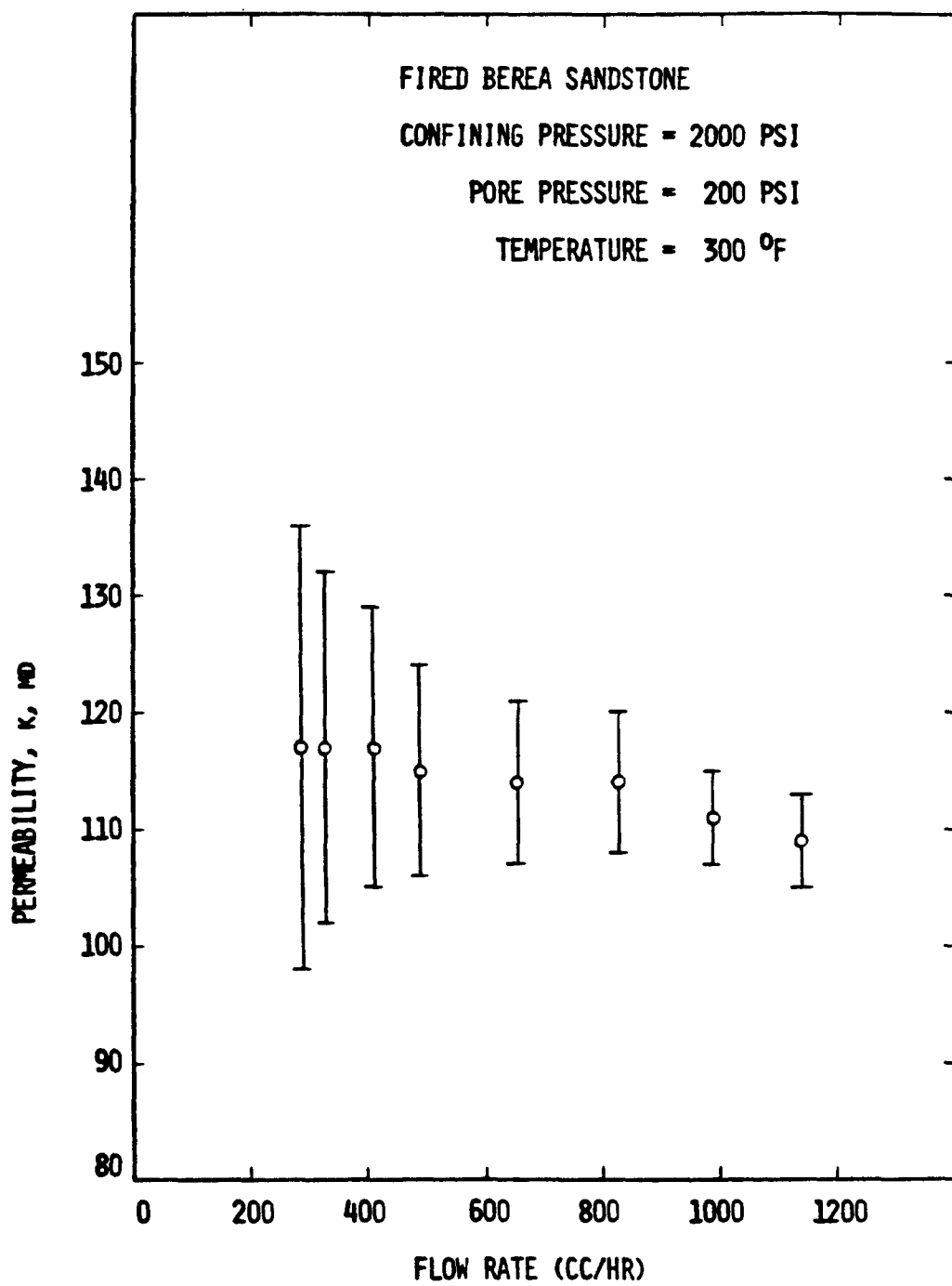


Fig. 23. Permeability vs Flow Rate for Run 4-16-81.

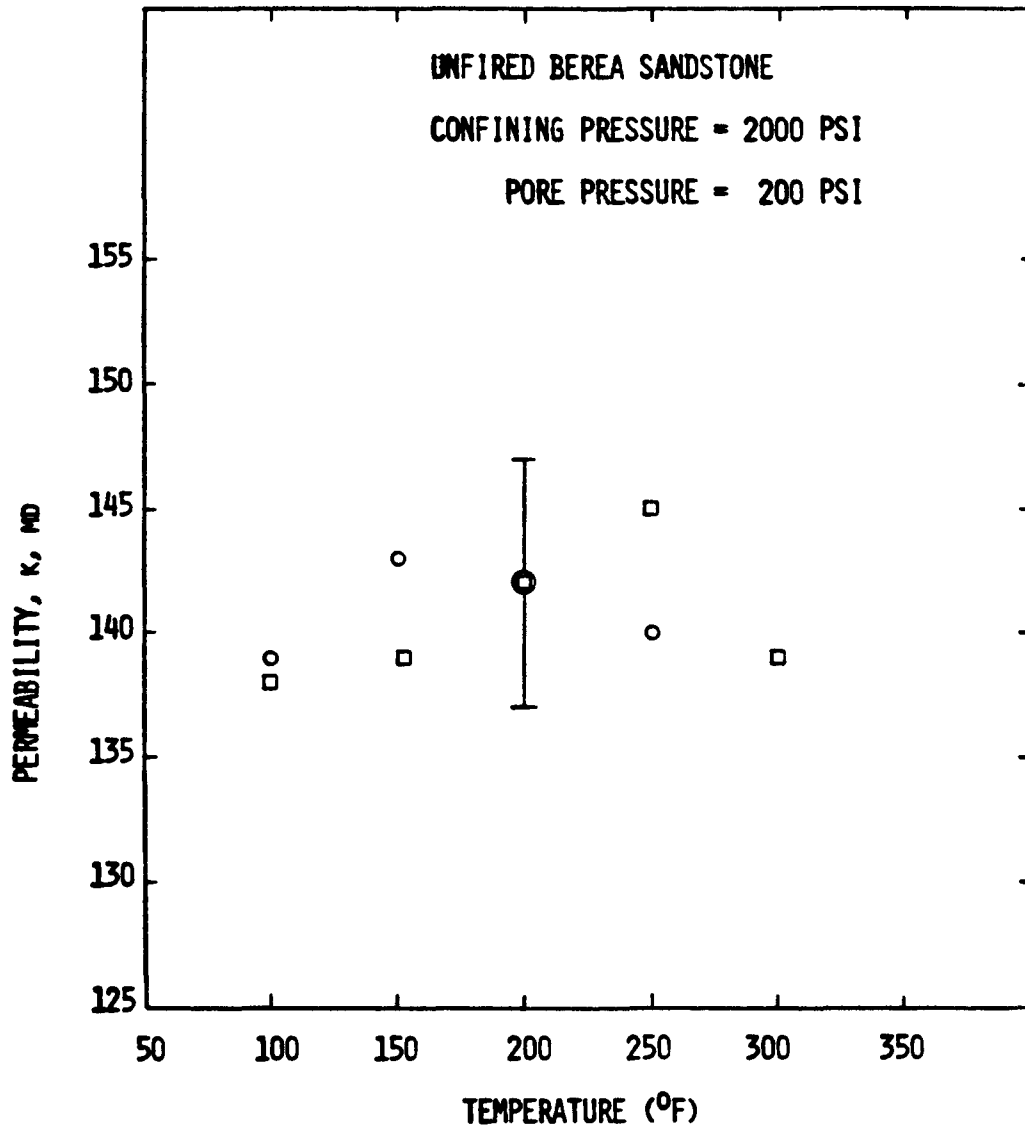


Fig. 24. Permeability vs Temperature for Run 12-24-80.

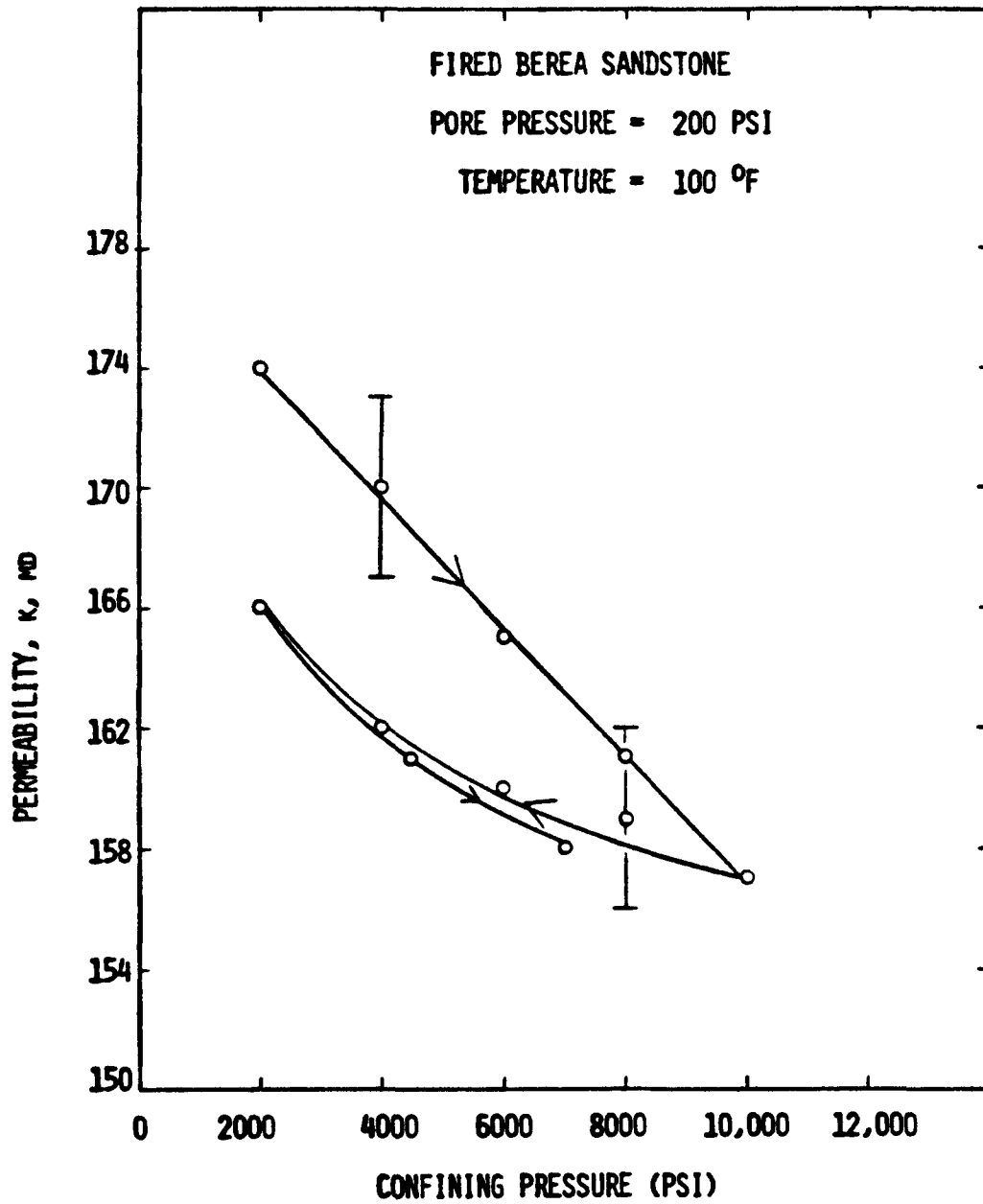


Fig. 25. Permeability vs Confining Pressure for Run 4-16-81.

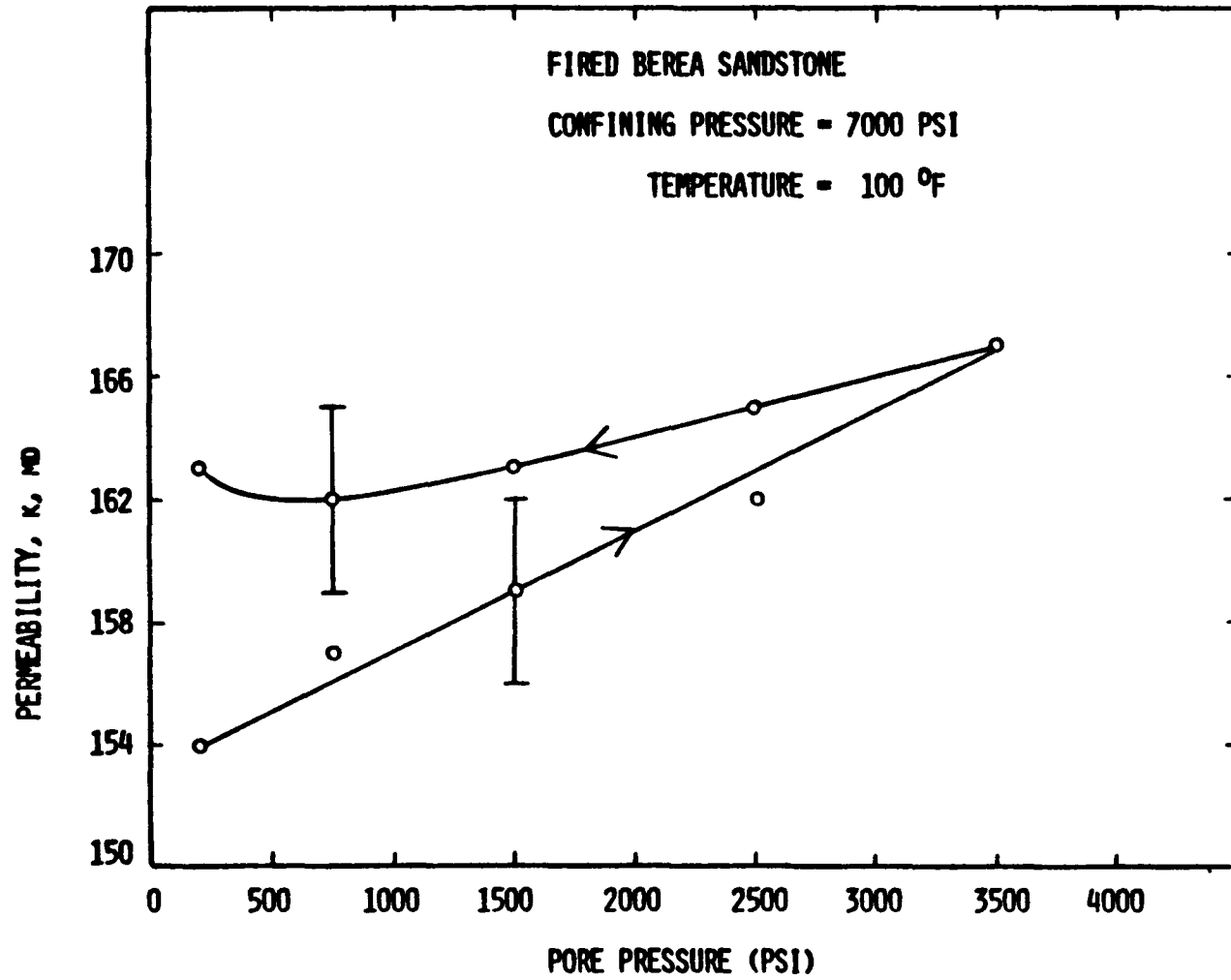


Fig. 26. Permeability vs Pore Pressure for Run 4-16-81.

permeability with increased pore pressure is found. This corresponds with the increase found with unconsolidated sand. However, unlike unconsolidated sand, this fired sandstone did not return to its initial permeability when the pore pressure was reduced. In fact, the permeability when measurements were completed was higher than the initial permeability. After these measurements were completed, the confining pressure was reduced to 2000 psi and the core left with water flowing overnight. When the confining pressure was reduced to 2000 psi the permeability increased to 170 millidarcies. While water flowed overnight, the permeability of the core decreased from 170 to 154 millidarcies. This is a value nearly equal to the permeability at the start of the pore pressure experiment. The observed pore pressure results can be explained as fines migrating through pore throats at the high pore pressures and not plugging again until later, thus giving a temporary increase in permeability when the pore pressure was reduced.

An experiment was performed with the difference between the confining pressure and pore pressure held constant at 2000 psi over a range of increasing confining pressures. The results of this experiment are shown in Fig. 27. The results compare well with those for unconsolidated sand (Fig. 20). A constant permeability (within the accuracy of the measurements $\pm 2\%$) is observed as long as the confining pressure minus the pore pressure is constant. This type of result is useful for laboratory measurements where high pressure may be unattainable but large pressure differences may be more easily attained.

The purposes of this study have been to investigate the effects of temperature, confining pressure and pore pressure on the absolute permeability of sand and sandstone porous media. Unconsolidated porous media were studied because of their simplicity. Consolidated porous media were investigated

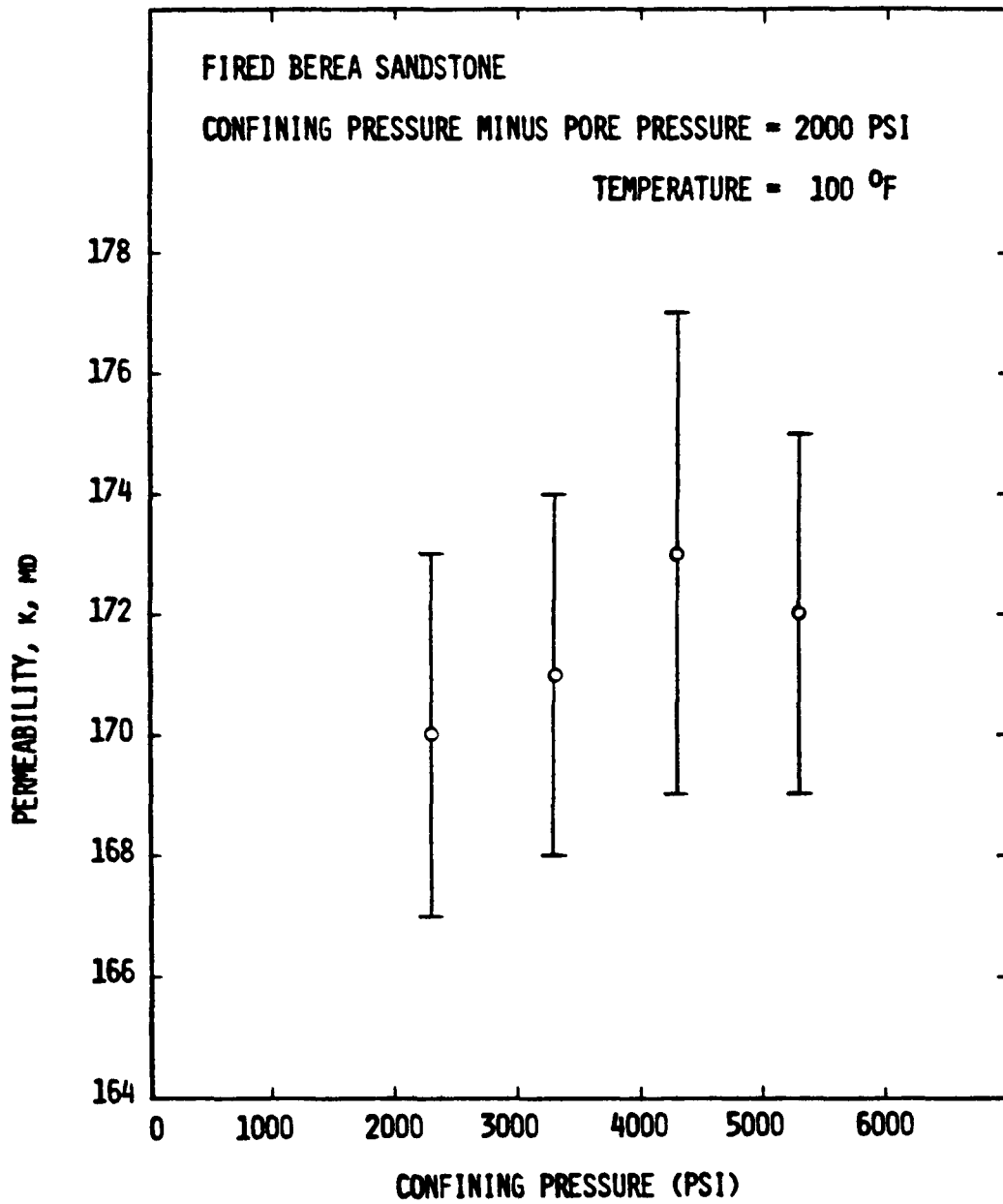


Fig. 27. Permeability vs Confining Pressure for Run 4-16-81.

because they offered a much lower permeability system with which to work.

Firing has been investigated to some extent in an attempt to understand the results of certain previous investigators. A complete understanding of the effects of firing on sandstone would require an exhaustive study that would be beyond the scope of the present study.

One Berea sandstone core was fired dry at 500°C for six hours. The effect of throughput was presented in Fig. 21. The effect of temperature on the permeability of this fired core is presented in Fig. 28. This can be compared with the permeability-temperature graph for an unfired Berea shown in Fig. 24. Several items should be pointed out when comparing the results of these two experiments. First, both of these cores came from the same 4 in. diameter Berea core. Second, although there were interruptions in the flow of the core used in the data on Fig. 24 (thus explaining why there was no throughput graph from that experiment), about 23 liters of throughput were necessary to stabilize the unfired core. This is close to the volume needed to stabilize the fired core. Their permeabilities at the start of the heat-cool cycle were almost the same. Firing apparently did little to keep clays from swelling or migrating, but did lead to a strange permeability versus temperature curve (Fig. 28). The causes for this strange behavior are unknown. One major purpose for firing a consolidated core is to stabilize it and assure that reproducible results can be seen. Clearly this did not occur when the Berea was fired at 500°C. The only conclusion is that firing at 500°C for six hours is not of value when attempting reproducible experiments.

An attempt was made to study throughput and temperature effects on permeability of a core from the same 4 in. Berea fired at 1000°C for 24 hours. Unfortunately the core broke during loading thus no data are available for a core fired at a higher temperature.

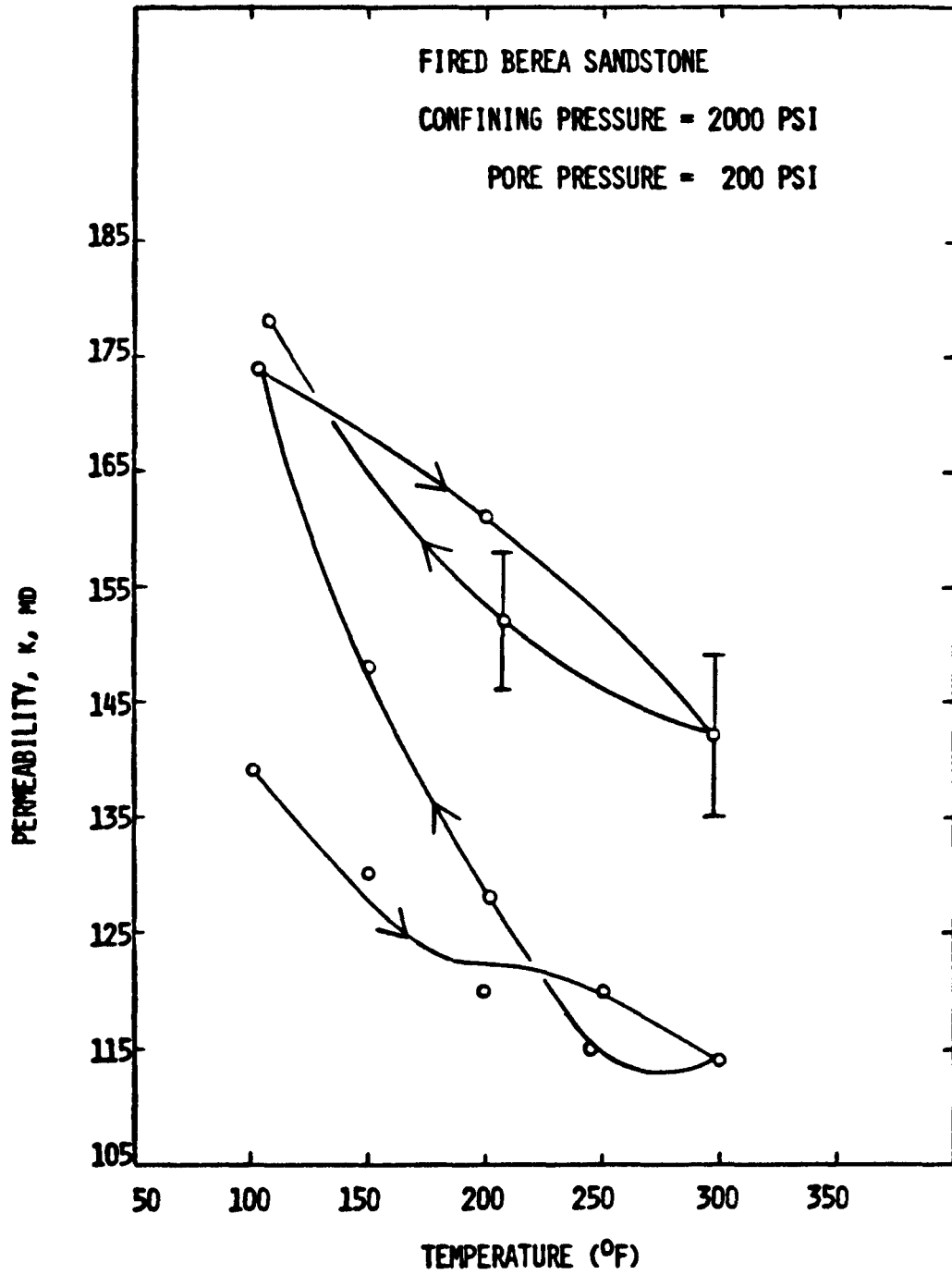


Fig. 28. Permeability vs Temperature for Run 4-16-81.

7. DISCUSSION

In this section the results presented in the previous section will be compared with those of other researchers, similarities will be examined and differences noted. Then all will be integrated into a comprehensive model.

7.1 UNCONSOLIDATED OTTAWA SAND

This discussion begins with results on unconsolidated sand packs. The most striking result is that there is no permeability change with temperature increase. This is different from the results of Aruna²⁸, who found significant reductions in absolute permeability due to temperature increase when flowing water through Ottawa sand packs. His results can be explained in a number of ways. By using a pressure transducer with too large a range, the measurement errors were often larger than the reduction in permeability that he was calculating. Other possible problems that he may have had but did not consider are a throughput dependence and a flowrate dependence that could have led to misinterpretation of results.

None of the authors discussed in the Literature Review section of this study investigated the effects of confining pressure or pore pressure exclusively on the absolute permeability of unconsolidated sand packs. This leaves nothing with which to compare these results. However, a physical model can be envisioned to explain the observed results. It is clear that confining pressure and pore pressure act differently from each other. This is seen in the hysteresis of the permeability versus confining pressure curve. It appears that an increase in confining pressure at a constant pore pressure causes the sand grains to pack more tightly. However, when

the confining pressure is released, there is no force to re-open the pores fully and the permeability-confining pressure relationship follows a path similar to the lower curves in Fig. 14. Therefore, the permeability is permanently reduced after the first pressurization of the core. Thereafter, during the first de-pressurization and subsequent pressurization cycles, the same non-linear permeability-confining pressure path is followed (the lower curves in Fig. 14).

The behavior is different when pore pressure is increased at a constant confining pressure. During this type of experiment, the pores are forced open and then allowed to close again under the effect of the confining pressure. Thus, in this case, the confining pressure is strong enough to counteract the changes caused by the pore pressure variations, and the changes seen in permeability are reversible.

While the confining pressure and pore pressure act differently on the unconsolidated sand packs, their combined effects are interesting and useful. It is interesting to note the shapes of Fig. 14 and 18. They are almost identical. It seems as though the effect of changing both confining pressure and pore pressure together is the sum of the effects of changing each one alone. This becomes useful when Fig. 20 is considered. Laboratory estimates of field permeabilities can be made at various pressure levels as long as the effective stress, defined as the confining pressure minus the pore pressure, is constant. In other words, absolute permeability of unconsolidated sand packs is only a function of effective stress and not confining pressure or pore pressure independently.

7.2 CONSOLIDATED SANDSTONE

When discussing consolidated porous media studied in the laboratory, the history of the core is important—specifically, whether it was fired. Most of the work at Stanford University was done with fired cores. In this study, one core was fired and the results of that firing will be discussed later.

In an unfired Berea sandstone core no temperature effect on permeability was found. This is in clear contrast with the results of Casse²⁵, who found significant reductions in permeability with temperature increase at various confining pressure levels. Perhaps in his work throughput dependence was mistaken for a temperature dependence. Before any measurements were made on the effect of temperature on permeability in this study, water was flowed through the cores until the permeability stabilized. This involved on the order of 20 liters of throughput during which time, the permeability was constantly decreasing. The direction of flow was reversed during one experiment. The permeability of the core increased after the initial switching and decreased with continued flow. This indicates that part of the reduction in permeability is caused by migration of fine particles.

The effect of pressure on the absolute permeability of consolidated sandstone has been studied extensively by others as Table 1 indicates. Most of these studies have involved investigation of the effect of confining pressure while little seems to have been done with pore pressure as the variable of interest. In this study, a linear decrease in permeability with increased confining pressure was observed during the initial pressurization of the core. When the confining pressure was released, there was a non-linear return to a lower permeability value. The second pressurization follows the curve defined by the de-pressurization. This is similar to the

results of this study with unconsolidated sand. However, these findings are different from the results of others. Figure 29 shows the results of Fatt⁸. The stabilized permeability-confining pressure relationship of this study matches his results very well. As with unconsolidated sand, this initial hysteresis is explained as an initial repacking of the grains into a tighter structure that changes elastically thereafter.

The effects of increasing and decreasing pore pressure on the absolute permeability of consolidated sandstones are somewhat similar to those with unconsolidated sand. There is a linear increase in permeability with pore pressure increase which is the same in both cases. However, the change in permeability with pore pressure decrease is different for consolidated sandstone than unconsolidated sand. With the consolidated sandstone (Fig. 26), the permeability was higher after the pore pressure cycle. However, as was discussed in the previous section, the permeability decreased significantly during fluid flow overnight. This indicates that fines might be migrating during the higher pore pressure portions of the cycle and then plugging later (after measurements were completed).

As with unconsolidated sand, the permeability of Berea sandstone seems to be constant at various confining pressures as long as the difference between the confining pressure and pore pressure is kept constant. This is useful for laboratory simulation of reservoir conditions.

Firing of cores is a questionable practice. Experimenters fire cores in hopes of stabilizing the clays. They hope to form a glass that will not react with distilled water and will not migrate. The only reservoir process that firing represents is in situ combustion and reservoir engineers are usually not interested in relative permeabilities, residual saturations, etc., as a function of temperature and pressure after a combustion front has passed.

The results of firing in this study are inconclusive at best. All that can be said is that there was no real change in the permeability of the Berea sandstone or in the stability of the clays or fines due to firing at 500°C for six hours. The results on the effect of temperature on a fired Berea sandstone are left unexplained.

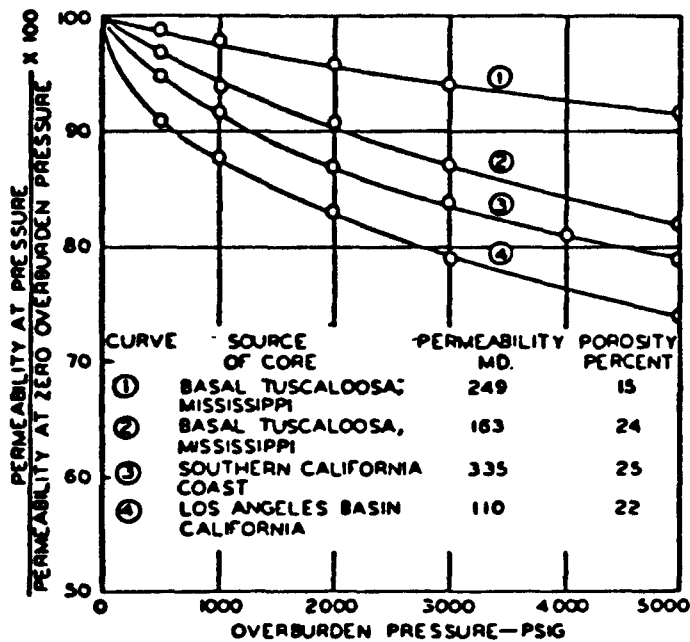


Fig. 29. Permeability vs Overburden Pressure from Fatt⁸.

8. CONCLUSIONS

1. The first result of the absolute permeability study of unconsolidated sand is that there is no effect of temperature on the absolute permeability to water. As long as the Viton sleeve is not degrading (as indicated by changes in the effluent water surface tension) and the water is flowing isothermally through the core, no temperature dependence was found.

2. The pressure effects on absolute permeability are both interesting and useful. The linear trend in the pore pressure experiments suggests that measurement made in the laboratory at the confining pressure of interest at a lower pore pressure may be extrapolated linearly to the pore pressure of interest for these unconsolidated sands. Also, since there is no hysteresis in pore pressure cycles, the pore pressure may be increased and decreased at will without changing the permeability-pore pressure relationship initially defined.

3. The effect of confining pressure changes at a constant pore pressure is an initial linear decrease in permeability with confining pressure increase. When the confining pressure is released and during subsequent pressurization cycles, the response was repeatable but non-linear.

4. Two more relationships that can be used to extrapolate laboratory measurements to field conditions are the linear trends of permeability with effective stress (defined as confining pressure minus pore pressure) and the constant value of permeability with a constant effective stress. While the relationship for permeability versus effective stress shows the same characteristics as that for confining pressure, i.e., linear on the first application of the pressure and then non-linear when the pressure is

released, the results showing a constant permeability at various confining pressures with a constant effective stress can be useful.

5. Many similar trends can be noted for the absolute permeability of Berea sandstone cores. For unfired cores, there is no dependence of permeability on temperature. Firing the cores at 500°C seems to produce a temperature effect that has not been explained.

6. The absolute permeability of Berea sandstone is reduced linearly during the first application of confining pressure and returns only partially when the pressure is released. The curve determined by the decrease of confining pressure seems to apply to subsequent pressure cycles.

7. The effect of pore pressure on the absolute permeability of Berea cores seems different than that on unconsolidated sand cores. While both are linear during the initial increase in pore pressure, the unconsolidated sand returns to its initial permeability while the Berea returns to a higher value when the pore pressure is reduced. One explanation for this involves migration of fines.

8. Lastly, the permeability of Berea sandstone cores can be expressed as a function of the difference between the confining pressure and pore pressure. This allows measurements made at one differential pressure at one set of conditions to be extrapolated to conditions of higher stress but the same differential pressure.

9. SUGGESTED ADDITIONAL WORK

While this study answers some questions concerning the effect of temperature on the absolute permeability of sand systems to distilled water, other questions still need to be answered. The most important is the effect of temperature on oil/water relative permeability.

Other investigations on the effect of temperature on absolute permeability that could be made with the present apparatus include water flow through limestone and stainless steel cores, brine flow through various porous media and oil flow through various porous media.

The results with the fired Beres core suggest a study on the effect of firing on cores to determine quantitatively the change in permeability (both initial and stabilized) and the amount of throughput necessary to stabilize a core as a function of firing temperature, duration and kind of fluxing agent.

The versatility and high pressure design of the apparatus allows more complex studies to be undertaken. An interesting one would be the effect on permeability of production from tight geopressured reservoirs. Many groups are interested in the changes in permeability caused by production from such systems and the results would be directly applicable to the energy industry.

NOMENCLATURE

A	Area of the core (cm ²)
B	Parameter in viscometer calibration
C	Parameter in viscometer calibration
d	Coiled capillary tube internal diameter (same as D)
D	Coiled capillary tube coil diameter (same as d)
De	Dean number
dk	Error in permeability (md)
f	Friction factor
k	Permeability (md)
L	Length of core (cm)
p	Pressure (psi)
q	Mass flow rate (gm/sec)
Re	Reynolds number
T	Temperature (°F)
v	Velocity
Δ	Difference or differential
μ	Viscosity (cp)
ρ	Density (gm/cc)
σ	Surface tension (dynes/cm)

Subscripts

c	Core
max	Maximum (plate size)
sc	Standard conditions
v	Viscometer

REFERENCES

1. Darcy, H.: "Les fontaines publiques de la ville de Dyon," Victor Dalmont, 1856.
2. Craft, B. C. and Hawkins, M. F.: Applied Petroleum Reservoir Engineering, Prentice Hall, Inc., New Jersey, 1959, 259.
3. Muskat, M.: The Flow of Homogeneous Fluids Through Porous Media, McGraw-Hill Book Company, New York, 1937, 71-72.
4. Muskat, M.: Physical Principles of Oil Production, McGraw-Hill Book Company, New York, 1949, 123-124.
5. Grunberg, L. and Nissan, A. H.: "The Permeability of Porous Solids to Gases and Liquids," J. Inst. Pet. Tech., 29, No. 236, 193-225.
6. Calhoun, J. C. and Yuster, S. T.: "A Study of the Flow of Homogeneous Fluids Through Ideal Porous Media," Drill. and Prod. Prac., API (1946), 335-355.
7. Fatt, I. and Davis, D. H.: "Reduction in Permeability with Overburden Pressure," Trans., AIME (1952), 195, 329.
8. Fatt, I.: "The Effect of Overburden Pressure on Relative Permeability," Trans., AIME (1953), 198, 325-326.
9. Wyble, D. O.: "Effect of Applied Pressure on the Conductivity, Porosity and Permeability of Sandstones," Trans., AIME (1958), 213, 430-432.
10. McLatchie, A. S., Hemstock, R. A. and Young, J. W.: "The Effective Compressibility of Reservoir Rock and It's Effects on Permeability," Trans., AIME (1958), 213, 386-388.
11. Waldorf, D. M.: "Effect of Steam on Permeabilities of Water-Sensitive Formations," J. Pet. Tech., (Oct., 1965), 1219-1222.
12. Knutson, C. F. and Bohor, B. F.: "Reservoir Rock Behavior Under Moderate Confining Pressure," Proc.: Fifth Symposium on Rock Mechanics, 1962, 627-659.
13. Dobrynin, V. M.: "Effect of Overburden Pressure on Some Properties of Sandstones," Soc. Pet. Eng. J., (Dec., 1962), 360-366.
14. Gray, D. H., Fatt, I. and Bergamini, G.: "The Effect of Stress on Permeability of Sandstone Cores," Soc. Pet. Eng. J., (June, 1963), 95-100.
15. Somerton, W. H. and Selim, M. A.: "Additional Thermal Data for Porous Rocks," Soc. Pet. Eng. J., (Dec., 1961), 249-253.

16. Somerton, W. H. and Gupta, V. S.: "Role of Fluxing Agents in Thermal Alteration of Sandstones," J. Pet. Tech., (May, 1965), 585-588.
17. Somerton, W. H., Mehta, M. M. and Dean, G. W.: "Thermal Alteration of Sandstones," J. Pet. Tech., (May, 1965), 589-593.
18. Paaswell, R. E.: "Thermal Influence on Flow From a Compressible Porous Medium," Water Resources Research, (1967), 3, No. 1, 271-278.
19. Wilhelmi, B. and Somerton, W. H.: "Simultaneous Measurement of Pore and Elastic Properties of Rocks Under Triaxial Stress Conditions," Soc. Pet. Eng. J., (Sept., 1967), 283-294.
20. Greenberg, D. B., Gresap, R. S. and Malone, T. A.: "Intrinsic Permeability of Hydrological Porous Mediums: Variations with Temperature," Water Resources Research, (Aug., 1968), 791-800.
21. Brace, W. F., Walsh, J. B. and Francos, W. T.: "Permeabilities of Granite Under High Pressure," J. Geoph. Res., (1968), 73, No. 6, 2225-2236.
22. Vairogs, J., Hearn, C. N., Dareing, D. W. and Rhoades, V. W.: "Effect of Rock Stress on Gas Production from Low-Permeability Reservoirs," J. Pet. Tech., (Sept., 1971), 1161-1167.
23. Afinogenov, Y. A.: "How The Liquid Permeability of Rocks Is Affected by Pressure and Temperature," SNIIGIMS (1969), 6, 34-42.
24. Weinbrandt, R. M.: "The Effect of Temperature on Relative Permeability," Ph.D. Dissertation, Stanford University, 1972.
25. Casse, F. J.: "The Effect of Temperature and Confining Pressure on Fluid Flow Properties of Consolidated Rocks," Ph.D. Dissertation, Stanford University, 1974.
26. Weinbrandt, R. M., Ramey, H. J., Jr. and Casse, F. J.: "The Effect of Temperature on Relative and Absolute Permeability of Sandstones," Soc. Pet. Eng. J., (Oct., 1975), 376-384.
27. Casse, F. J. and Ramey, H. J., Jr.: "The Effect of Temperature and Confining Pressure on Single-Phase Flow in Consolidated Rocks," J. Pet. Tech., (Aug., 1979), 1051-1059.
28. Aruna, M.: "The Effects of Temperature and Pressure on Absolute Permeability of Sandstones," Ph.D. Dissertation, Stanford University, 1976.
29. Aruna, M., Arihara, N. and Ramey, H. J., Jr.: "The Effect of Temperature and Stress on the Absolute Permeability of Sandstones and Limestones," Presented at the American Nuclear Society Topical Meeting, April, 1977.

30. Danesh, A., Ehlig-Economides, C. and Ramey, H. J., Jr.: "The Effect of Temperature Level on Absolute Permeability of Unconsolidated Silica and Stainless Steel," Trans., Geothermal Resources Council, (July, 1978), 137-139.
31. Aktan, T. and Farouq Ali, S. M.: "Effect of Cyclic and In-Situ Heating on the Absolute Permeabilities, Elastic Constants, and Electrical Resistivities of Rocks," SPE 5633 presented at the 50th Annual Fall Meeting of the SPE of AIME, Dallas, Texas, Sept.-Oct., 1975.
32. Zoback, M. D. and Byerlee, J. D.: "Permeability and Effective Stress," Am. Assoc. Pet. Geo. Bull., (1975), 59, 1, 154-158.
33. Sanyal, S. K., Marsden, S. S., Jr. and Ramey, H. J., Jr.: "Effect of Temperature on Petrophysical Properties of Reservoir Rocks," SPE 4898 presented at the 49th Annual Fall Meeting of the SPE of AIME, Houston, Texas, Oct., 1974.
34. Sinnokrot, A. A.: "The Effect of Temperature on Capillary Pressure Curves of Limestones and Sandstones," Ph.D. Dissertation, Stanford University, 1969.
35. Sanyal, S. K., Marsden, S. S., Jr. and Ramey, H. J., Jr.: "The Effect of Temperature on Electrical Resistivity of Porous Media," Trans. Thirteenth Annual Logging Symp. of Soc. Prof. Well Log Analysts, Tulsa, OK, May, 1973.
36. Sydansk, R. D.: "Discussion of the Effect of Temperature and Confining Pressure on Single-Phase Flow in Consolidated Rocks," J. Pet. Tech., (Aug., 1980), 1329-1330.
37. Davidson, D. H.: "Invasion and Impairment of Formations by Particulates," SPE 8210, Presented at the 54th Annual Fall Meeting of the SPE of AIME, Las Vegas, Nevada, Sept., 1979.
38. Gruenbeck, C. and Collins, R. E.: "Entrapment and Deposition of Fine Particles in Porous Media," SPE 8430, Presented at the 54th Annual Fall Meeting of the SPE of AIME, Las Vegas, Nevada, Sept., 1979.
39. Lippincott, E. R., Stromberg, R. R., Grant, W. H. and Cessac, G. L.: "Polywater," Science, (June 27, 1969), 1482-1487.
40. Derjaguin, B. V.: "Superdense Water," Scientific American, 233, No. 5, 52-71.
41. Derjaguin, B. V. and Churaev, N. V.: "Nature of 'Anomalous Water'," Nature, (Aug. 17, 1973), 430-431.
42. Sekita, Y. and Hayashi, N.: "Production, Thermal Stability and Mass-Spectrometry of Capillary-Grown Anomalous Water," Jap. J. App. Phys., (June, 1976), 955-962.

43. Olivei, A.: "Leaching Process of Impurities from Pyrex and Quartz in a High Yield Method of Anomalous Water," Jap. J. App. Phys., (Oct., 1973), 1534-1549.
44. Gobran, B. D. and Brigham, W.E.: "Initial Studies of Absolute Permeability," SUPRI Technical Report under preparation.
45. Schroer, T., E. I. du Pont de Nemours & Co. (Inc.), personal communication, (Oct., 1980), (800) 441-9475.
46. Potter, J. M., Nur, A. and Dibble, W. E., Jr.: "Effect of Temperature and Solution Composition on the Permeability of St. Peters Sandstone: Role of Iron (III)," Proceedings, 6th Workshop on Geothermal Reservoir Engineering, Dec. 16-18, 1980, Stanford University, 316-321.
47. Gobran, B. D., Sufi, A. H., Sanyal, S. K. and Brigham, W. E.: "Effects of Temperature and Pressure on Permeability," Proceedings, 1980 Annual Heavy Oil/EOR Contractor Presentations, U.S. Department of Energy, July 22-24, 1980, 111-123.
48. Gobran, B. D., Brigham, W. E. and Sanyal, S. K.: "The Temperature Dependence of Permeability," Trans., Geothermal Resources Council, (Sept., 1980), 397-400.
49. Sageev, A.: "The Design and Construction of an Absolute Permeameter to Measure the Effect of Elevated Temperature on the Absolute Permeability to Distilled Water of Unconsolidated Sand Cores," M.S. Report, Stanford University, 1980.
50. Sageev, A., Gobran, B. D., Brigham, W. E. and Ramey, H. J., Jr.: "The Effect of Temperature on the Absolute Permeability to Distilled Water of Unconsolidated Sand Cores," Proceedings, 6th Workshop on Geothermal Reservoir Engineering, Dec. 16-18, 1980, Stanford University, 297-302.
51. Muskat, M.: Physical Principles of Oil Production, McGraw-Hill Book Company, New York, 1949, 204.
52. Hirasuna, A. R., Sedwick, R. A. and Stephans, C. A.: "High Temperature Geothermal Elastomer Compound Development," Presented at the American Chemical Society Rubber Division meeting, Las Vegas, Nevada, May, 1980.
53. Sufi, A. H., personal communication, December, 1980.
54. Amyx, J. W., Bass, D. M., Jr. and Whiting, R. L.: Petroleum Reservoir Engineering, McGraw Hill Book Company, New York, 1960, 64.
55. Haywood, R. W.: "Sixth International Conference on the Properties of Steam—Supplement on Transport Properties," J. Eng. Power, Trans., ASME, (Jan., 1966), 63-66.
56. ASME Steam Tables, American Society of Mechanical Engineers, New York, Fourth Edition, (1979).

57. Guereca, R. A., Richardson, H. P. and Walker, L. M.: "Steady-State Laminar Flow Boundary Conditions for a Stainless Steel Coiled-Capillary Viscosimeter," USBM 6995, (Aug., 1967).
58. Dean, W. R.: "Note on the Motion of Fluid in a Curved Pipe," Phil. Mag., Vol. 4, No. 7, 1927, 208-223.
59. Dean, W. R.: "The Streamline Motion of Fluid in a Curved Pipe," Phil. Mag., Vol. 5, No. 30, 1928, 673-695.
60. Sherwood, T. K. and Reed, C. E.: Applied Mathematics in Chemical Engineering, McGraw Hill, New York, Chapter IX.
61. Rowe, A. M., Jr. and Chou, J. C. S.: "Pressure-Volume-Temperature-Concentration Relation of Aqueous NaCl Solutions," J. Chem. Eng. Data, Vol. 15, No. 1, 61-66.

APPENDIX A

CONVERGENT FLOW

The previously used core holder and the present model in the early stages of its use basically had a point inlet and point outlet. This implies that the flow was hemispherical at both ends and linear in the center. Calculations of permeability assumed linear flow throughout the core. The effect of the diverging-converging flow will be studied in this appendix.

The equation for hemispherical flow in Darcy units is:

$$q = \frac{2 \pi k (p_e - p_w)}{\mu \left[\frac{1}{r_w} - \frac{1}{r_e} \right]} \quad (A-1)$$

This equation defines the flow from the inlet to the outlet. The equation for linear flow in the bulk of the core is,

$$q = \frac{\pi r_e^2 k (p_1 - p_2)}{\mu l} \quad (A-2)$$

The length of linear flow can be approximated by assuming the sum of the hemispherical and linear flow volumes is equal to the core volume. From this concept it can be determined that the effective linear flow length is given by:

$$l = L - \frac{4r_e}{3} \quad (A-3)$$

where r_e is the core radius and L is the core length.

For a system with hemispherical flow at both ends and linear flow in the center, the flow equation is a summation of the effects in Eqs. A-1 and A-2, the result is:

$$q = \frac{\pi k r_e^2 \Delta p}{\mu L \left[1 - \frac{7}{3} \frac{r_e}{L} + \frac{r_e^2}{L r_w} \right]} \quad (A-4)$$

The deviation from linear flow is $r_e^2/Lr_w - (7/3)(r_e/L)$. This derivation is only approximate, so the constant 7/3 is not exact. However, this term is small compared to r_e^2/Lr_w , therefore r_w can be calculated reasonably accurately from the flow behavior and this result can be compared to the geometry of the endplugs. The inlet and outlet radii were approximately 0.16 cm. They can be treated as cylindrical disk sources which Muskat⁵¹ showed have effective radii equal to one-half the true radii. Thus, from the geometry of the system, the effective radii is expected to be 0.08 cm.

The data below are taken from the old core holder and the new one before the holes were drilled to disperse the flow.

L = 6.6 cm	L = 18.8 cm
q = 0.182 cc/sec	q = 0.182 cc/sec
μ = 0.92 cp	μ = 0.92 cp
Δp = 0.184 atm	Δp = 0.228 atm

Assuming the permeability of these sand packs was 3.8 Darcies as measured in the later design, using the above data and Eq. A-4, the effective r_w values could be calculated from these experiments. They were 0.09 cm for the 6.6 cm core and 0.13 cm for the 18.8 cm core. This shows that the degree of spherical flow is different for these two core holders and also that the

effective radii were larger than predicted. This difference is due to the grooves in the endplug faces. The second core holder had deeper grooves and thus had a larger effective radius. These calculations show that spherical flow was occurring in the previous core holder design and that the grooves were only partially effective in lessening this effect.

APPENDIX B

HASSLER SLEEVE MATERIALS

The degradation of the Viton tubing indicated by a reduction in the surface tension of the effluent water (Table 3, Fig. 3) led to a search for other Hassler sleeve materials. The desired qualities for a possible replacement for the Viton were temperature stability to 450 or 500°F, ability to transmit the confining pressure radially to the core and negligible permeability at the temperatures and pressures of interest.

The first compound tested was a sample of EPDM (ethylene-propylene-difunctional monomer) supplied by L'Garde, Inc.⁵² This was their Y267-LX-2 formulation. The sample was cut into strips and placed in a high pressure vessel. The vessel was evacuated, distilled water introduced into the vessel and the system pressurized with nitrogen to 800 psi. The vessel was heated in an air bath and water samples removed at various temperatures. The surface tension of the samples was measured with a ring tensiometer. The results are tabulated in Table B-1 and graphed in Fig. B-1. The large drop in the surface tension between 150 and 250°F indicates that this compound is not suitable for use at elevated temperatures.

The next compound tested was Fluorel manufactured by 3M. The Fluorel was supplied in tube form after being cured (crosslinked) with a peroxide catalyst. The tubes were loaded into the core holder and packed with unconsolidated sand. The surface tension of the effluent water was measured as a function of the system temperature. The results are given in Table B-2 and shown in Fig. B-2. The large drop in surface tension between 200 and 300°F

Table B-1

WATER SURFACE TENSION IN PRESENCE OF EPDM

<u>Temperature (°F)</u>	<u>Surface Tension (dynes/cm)</u>
70	65.3
150	65.3
200	50.8
250	32.1
300	30.6
350	32.1
400	29.7
450	29.9
500	30.3

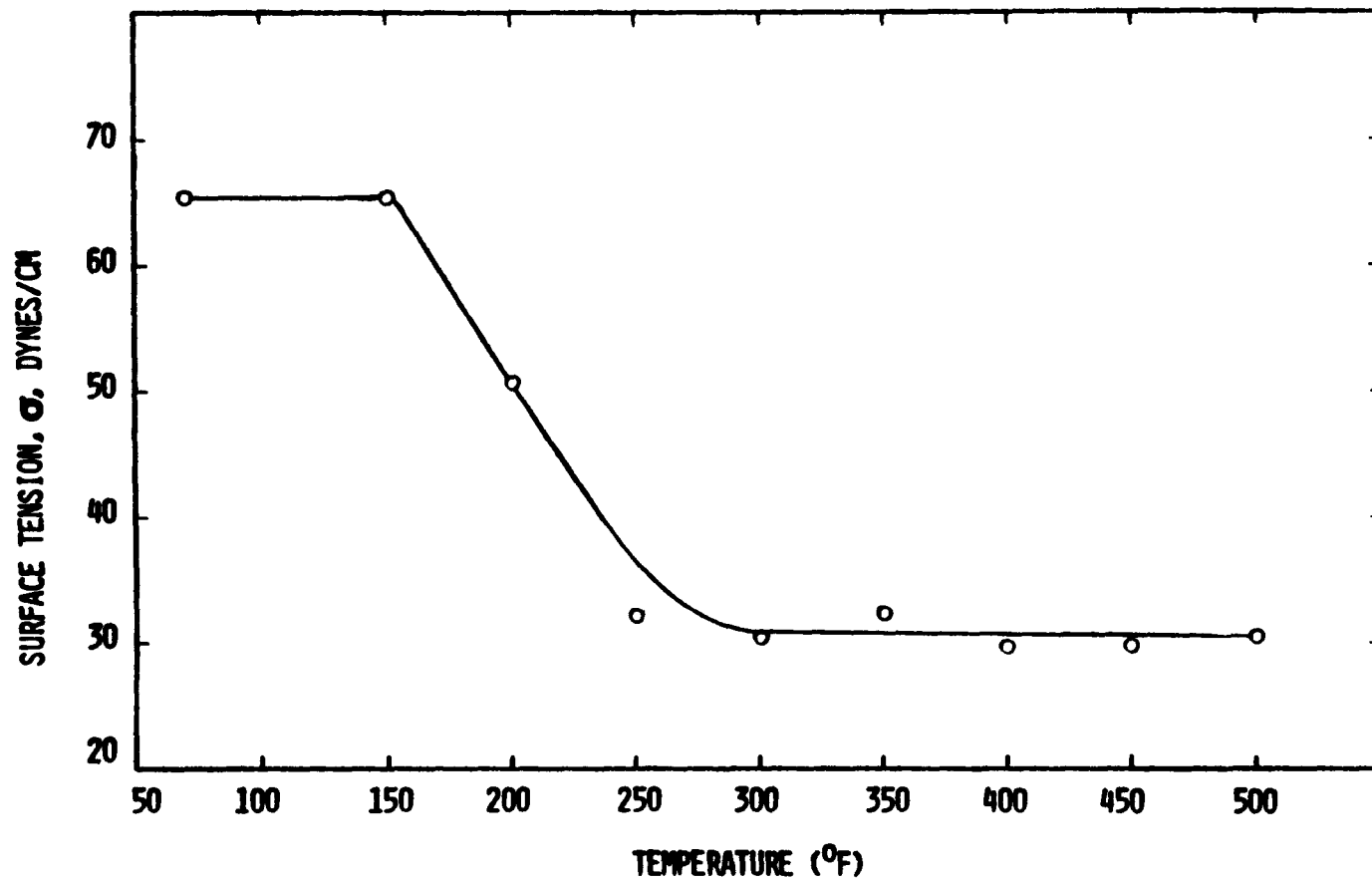


Fig. B-1. Surface Tension vs Temperature of Water in Presence of EPDM.

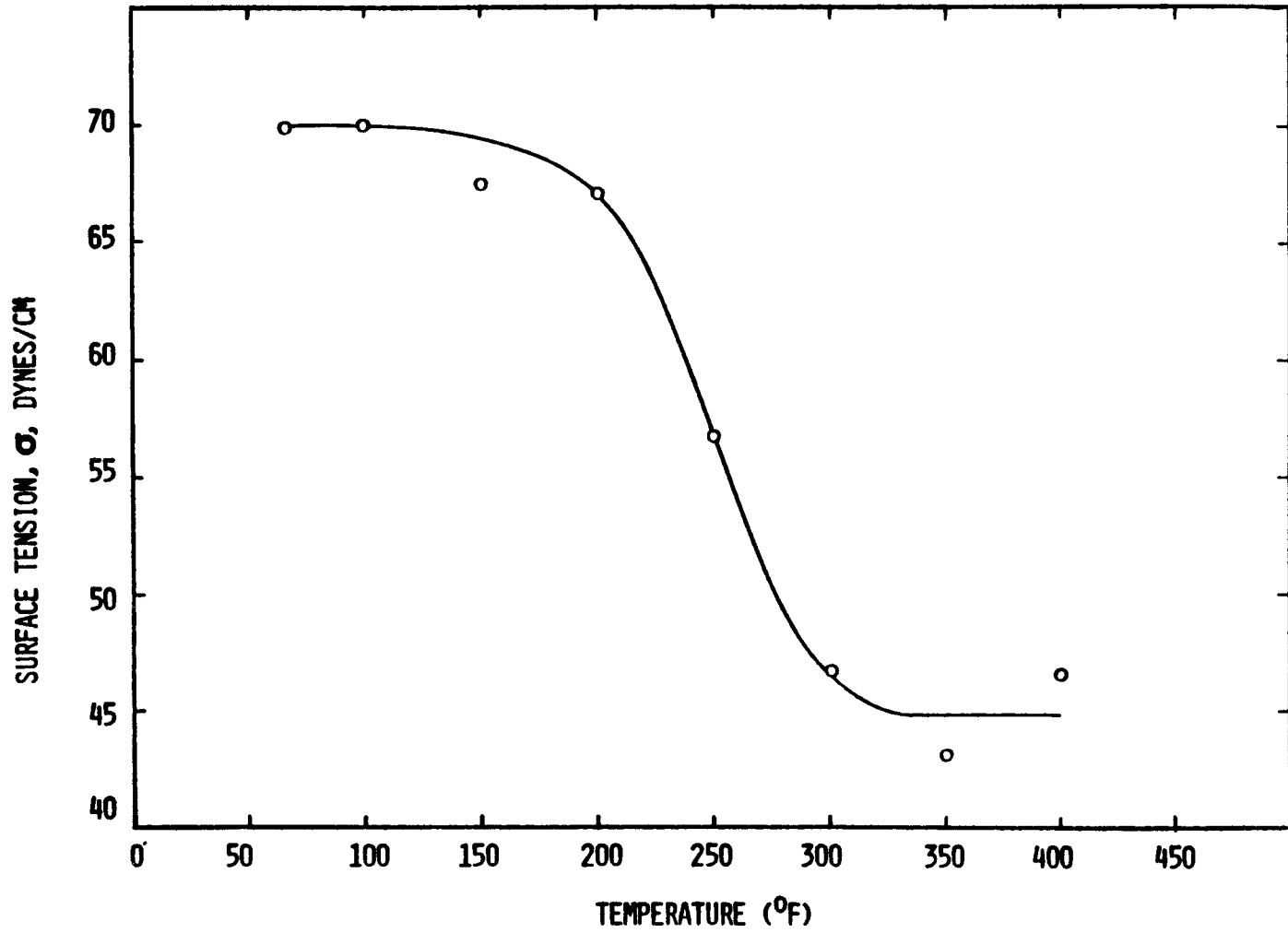


Fig. B-2. Surface Tension vs Temperature for Effluent Water with Fluorel Sleeve.

shows that Fluorel would not be a suitable replacement for Viton for these purposes.

Another compound under consideration for this study as a replacement for the Viton sleeve was Teflon FEP. This is available in heat shrinkable tube form. Unfortunately, the temperature stability limit as stated by the manufacturer was 400^oF. Therefore, it could not be used for this study and was not tested.

All of the previously mentioned compounds were elastomers that would transmit the confining pressure to the core. Since no other elastomer was found, one suggestion⁵³ was to use a steel sleeve instead of an elastomer. This would allow only axial pressure to be transmitted to the core, but the degradation problem would be eliminated. With minor modifications to the two endplugs (installing O-rings for a seal) this system could withstand temperatures up to 600^oF for short periods. This assumes the stated lifespan of Viton⁴⁵ to be correct and that there is little contact between the Viton O-rings and the flowing water. Figure B-3 shows the results of a permeability versus temperature experiment made with this system. In this case the sand was 120-200 mesh. The error bars for one measurement are shown. Within the experimental error and the effects of throughput, there is no reduction in permeability with temperature increase to 500^oF. The surface tension of the effluent water was monitored and it was reduced at the elevated temperatures (beginning at 300^oF) indicating that there was some contamination caused by the O-rings.

From the previous discussion, it can be seen that no acceptable elastomer was found that could be used to greatly increase the temperature capabilities of this study. A steel sleeve could be used to give only axial confining pressure. Another possible solution would be a thin metallic sleeve perhaps

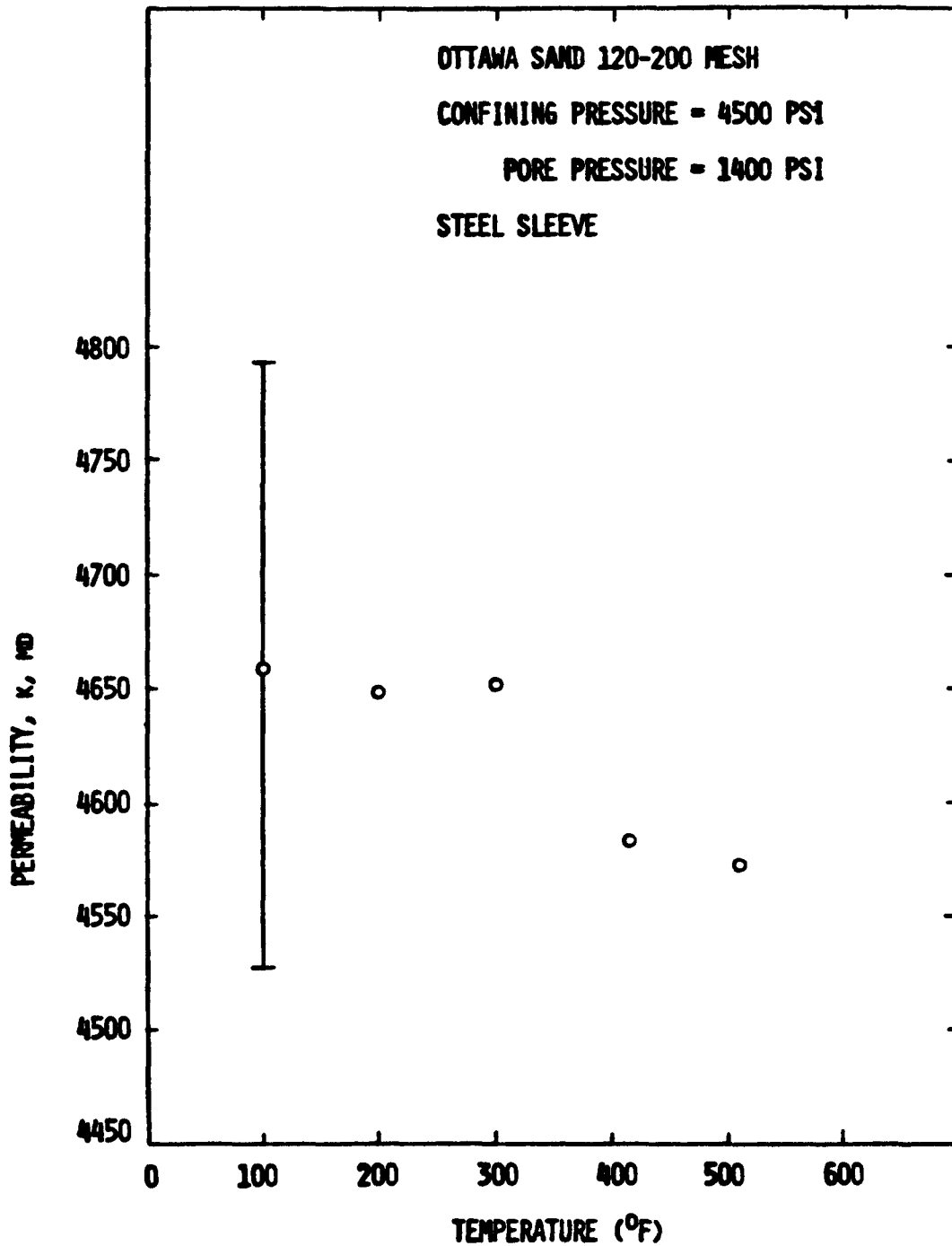


Fig. B-3. Permeability vs Temperature for Run 4-26-81 with Steel Sleeve.

made of copper. This, if thin enough, could transmit the radial confining pressure to the core and not have temperature constraints caused by the use of O-rings. This would require careful machining and was not attempted in this study.

APPENDIX C

CAPILLARY TUBE VISCOMETER

Poiseuille⁵⁴ studied the flow of a fluid through a straight capillary tube and determined that the pressure drop across a length was proportional to the flow rate. It was hoped that measurement of the pressure differential across a capillary tube in this experiment could yield a more accurate value for flow rate than by direct measurement. Also, if any phenomenon was occurring during flow through the core to change the viscosity of the water (see Theory section), the actual effluent viscosity could be measured instead of assuming values for pure water. Due to space limitations in the air bath, it was necessary to coil the capillary tube to get sufficient length to produce a measurable differential pressure at the desired flow rates. Although the flow was laminar for all flow rates at several temperatures, Poiseuille's law did not appear to hold.

By measuring the pressure differential across, and the mass flow rate through, the coiled capillary tube viscometer, a data set of the pressure differential versus volumetric flow rate-viscosity product could be constructed at each temperature at a given line pressure (200 psi). The values used for water density and viscosity as functions of temperature at 200 psi are given in Table C-1. The averaged pressure differential versus volumetric flow rate-viscosity product results at 80°F are given in Table C-2. While this data did not fit Poiseuille's law, it was found to form a straight line when graphed on log-log coordinates (Fig. C-1). This relationship held at all temperatures even when the flow was turbulent. By performing a

Table C-1

WATER PROPERTIES AT VARIOUS TEMPERATURE

<u>Temperature (°F)</u>	<u>Viscosity⁵⁵ (cp)</u>	<u>Density⁵⁶ (gm/cc)</u>
80	0.8604	0.9983
100	0.6819	0.9946
125	0.5304	0.9888
150	0.4273	0.9818
175	0.3541	0.9735
200	0.3003	0.9641
225	0.2596	0.9543
250	0.2280	0.9437
275	0.2029	0.9319
300	0.1827	0.9193
325	0.1662	0.9058
350	0.1524	0.8917

Table C-2

CAPILLARY TUBE CALIBRATION AT 80°F

<u>Δp (psi)</u>	<u>$q\mu/\rho$ (cc-cp/sec)</u>
3.9746	0.1965
2.9983	0.1568
2.1076	0.1179
1.6960	0.0977
1.3160	0.0784
1.1340	0.0685
0.9510	0.0589
0.7857	0.0490
0.6280	0.0392

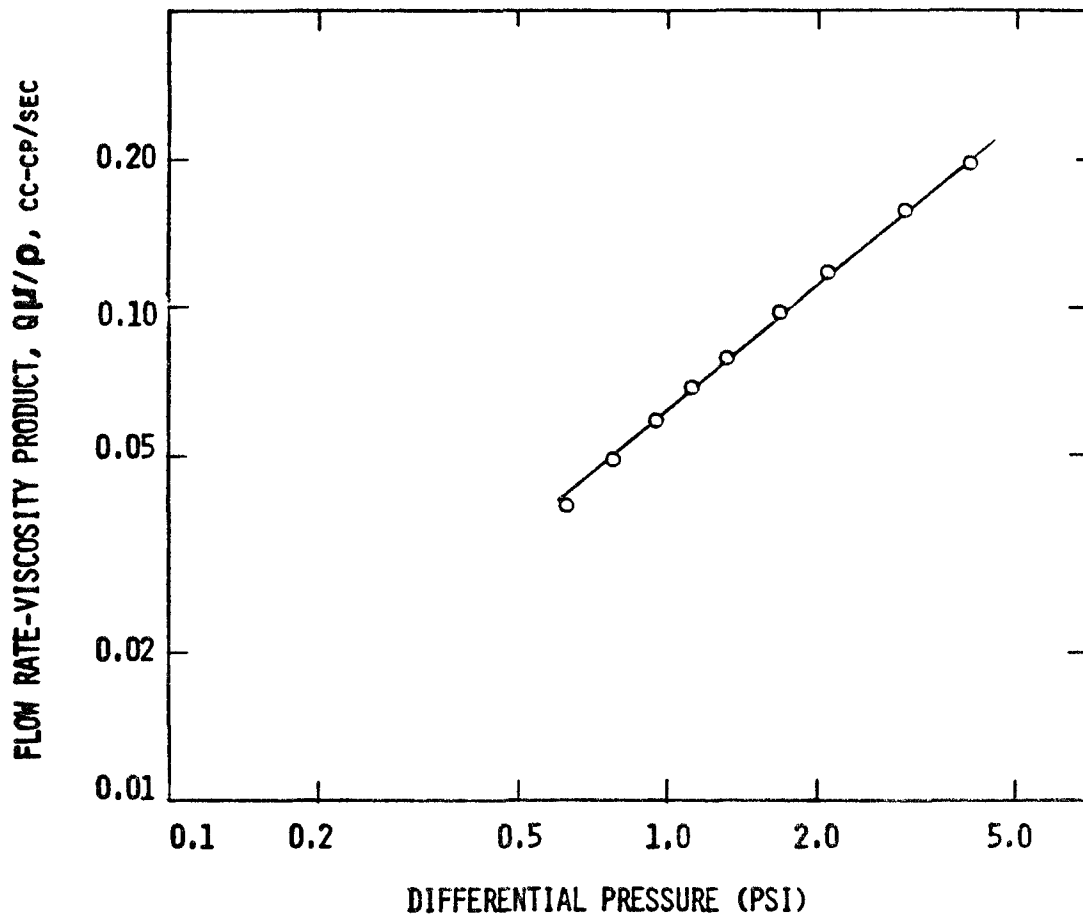


Fig. C-1. Flow Rate-Viscosity Product vs Differential Pressure for Capillary Tube at 80°F.

least-squares fit to the log-log lines and then curve-fitting the slopes and intercepts as functions of temperature, a final correlating equation was obtained:

$$\log \frac{q\mu}{\rho} = B \log \Delta p - C \quad (C-1)$$

$$B = 0.2181 (\log T)^2 - 1.2089 \log T + 2.3769$$

$$\log C = 0.0848 (\log T)^2 - 0.2225 \log T + 0.1999$$

where T is measured in °F, p in psi, q in grams per second, μ in centipoise and ρ in grams per cubic centimeter. This equation fits the data to within $\pm 2.5\%$ over the entire range of investigation (70 to 350°F, 407 to 1143 cc/hr) and within $\pm 1\%$ in most cases. This calibration was made at a downstream pressure of 200 psi.

A report by the United States Bureau of Mines⁵⁷ explained the deviation from Poiseuille's law and provided an excellent correlation with the experimental data obtained in this study. The original work in this area was by Dean^{58,59} who investigated mathematically the flow of fluid in a coil. The USBM work related the actual friction factor, f, (Eq. C-2), divided by the theoretical friction factor, 64 divided by the Reynolds number, to the Dean number, De, (Eq. C-3).

$$f = \frac{4\pi^2 r^5 \Delta p}{\rho L q^2} \quad (C-2)$$

$$De = Re \sqrt{\frac{d}{D}} \quad (C-3)$$

where r is the internal radius of the capillary tube in cm, p is the pressure in dynes/cm², L is the capillary tube length in cm, ρ is the density in gm/cm³, q is the flow rate in cm³/sec, Re is the Reynolds number, d is the internal diameter of the capillary tube and D is the diameter of the coil of the capillary tube.

To compare the results of this study with the USBM data, a value was needed for the capillary tube radius. By assuming laminar flow at the lowest flow rate (equating the friction factor to 64 divided by the Reynolds number) a radius was calculated. Using this radius and the data from Table C-2, values for the Dean number and the friction factor ratio were determined. These results are given in Table C-3 along with an example from the USBM report (nitrogen flow at 1000 psi and 300^oK). This data is graphed in Fig. C-2. There is excellent agreement between these two studies thus defining the deviation from Poiseuille's law caused by a coiled capillary tube.

Table C-3

COILED CAPILLARY TUBE DATA

<u>USBM Report</u>		<u>Capillary Calibration</u>	
<u>De</u>	<u>fRe/64</u>	<u>De</u>	<u>fRe/64</u>
4.42	1.0102	9.51	1.000
5.16	1.0096	12.00	0.994
5.90	1.0033	14.30	1.003
7.37	1.0017	16.70	1.029
8.85	1.0063	19.10	1.044
11.80	1.0032	23.80	1.078
14.75	1.0062	28.70	1.112
17.70	1.0290	38.20	1.187
20.65	1.0434	47.90	1.256
23.60	1.0630		
29.51	1.1062		
35.41	1.1481		
47.22	1.2228		
59.03	1.2914		

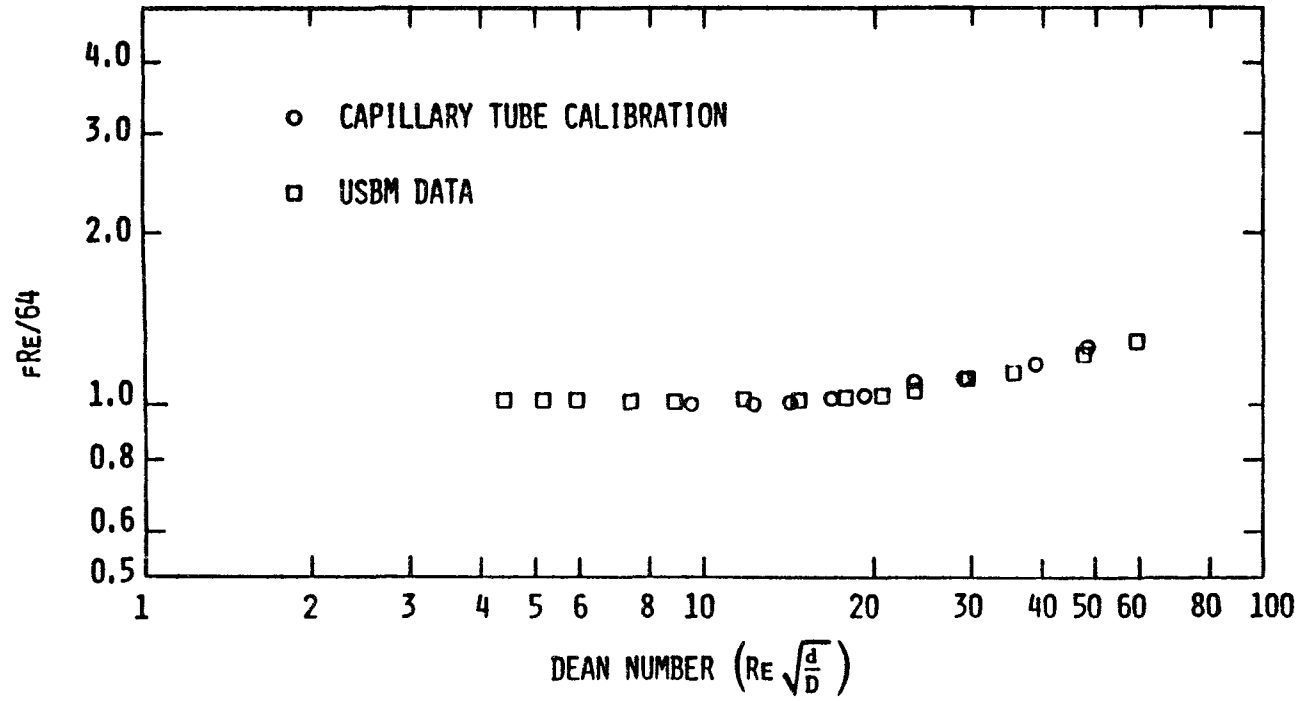


Fig. C-2. Friction Factor Ratio vs Dean Number for Coiled Capillary Tubes.

APPENDIX D

ERROR ANALYSIS

Part I: Using the Viscometer

Permeability is calculated by

$$k = \frac{14.7 \times 10^3 L}{A \Delta p_c} \frac{q\mu}{\rho} \quad (D-1)$$

where $A =$ area in cm^2

$k =$ permeability in md

$\Delta p_c =$ pressure differential across core in psi

$q =$ mass flow rate gm/sec

$\mu =$ viscosity in cp

$\rho =$ density in gm/cc

The equation for the capillary tube viscometer is

$$\log \frac{q\mu}{\rho} = B \log \Delta p_v - C \quad (D-2)$$

where B and C are functions of temperature and

$\Delta p_v =$ pressure differential across the viscometer in psi

Combining these equations yields

$$k = \frac{14.7 \times 10^3 L}{A \Delta p_c} \left[\text{antilog} (B \log \Delta p_v - C) \right] \quad (D-3)$$

To determine the error in k, we take the differential of both sides⁶⁰ of the equation and obtain:

$$dk = \frac{14.7 \times 10^3 L}{A} \left[\text{antilog} (B \log \Delta p_v - C) \right] \left[\frac{d(\Delta p_c)}{\Delta p_c^2} + \frac{B \ln 10 d(\Delta p_v)}{\Delta p_c \Delta p_v} \right] \quad (D-4)$$

or

$$dk = k \left[\frac{d(\Delta p_c)}{\Delta p_c} + \frac{B \ln 10 d(\Delta p_v)}{\Delta p_c \Delta p_v} \right] \quad (D-5)$$

This is the equation used to determine the error in the calculated value of permeability.

The error in measuring the pressure differential $d(\Delta p)$ is a combination of the error in the transducer and the error in the transducer indicator. The error in the transducer measurement is 1% of the size of the transducer plate. The error in the transducer indicator is 1% of the transducer reading. Both of these errors are independent of each other, so the combined error is given by:

$$d(\Delta p) = 0.01 \sqrt{\Delta p_{\max}^2 + \Delta p^2} \quad (D-6)$$

This equation holds for both the viscometer and the core pressure differential.

Equations D-5 and D-6 give the estimates of the error in permeability. The assumptions of this derivation were that the length and cross-sectional area of the core were constant, the temperature of the system is constant and that the constants B and C are known within the error in measuring pressure differential.

Part II: No Viscometer

When the viscometer is not used, Eq. D-1 becomes:

$$k = \frac{14.7 \times 10^3 L q_{sc} \mu \rho_{sc}}{A \Delta p_c} \quad (D-7)$$

where q_{sc} and ρ_{sc} are determined as functions of temperature and line pressure.

The equations for μ and ρ as functions of temperature and pressure are given in Appendix E, and are from references 55 and 61. Taking the differential of Eq. D-7 and assuming the only significant error is in the measurement of differential pressure yields:

$$dk = k \frac{d(\Delta p_c)}{\Delta p_c} \quad (D-8)$$

Equation D-8 is used to calculate error when the viscometer is not used. The implicit assumption that the equations for viscosity and density introduce no significant error is reasonable since the equations have an accuracy of $\pm 2\%$.

APPENDIX E

CALCULATION OF PERMEABILITY

This appendix gives the program for a Texas Instrument's TI-59 hand calculator that was used to calculate permeability and the error in permeability. An example of the calculation and measurement procedure is also given. The error analysis is based on Appendix D, Part II. The correlations for viscosity and density are given in references 55 and 61, respectively. Both are accurate to within $\pm 2\%$.

An example of the measurements made to calculate permeability is taken from Run 4-8-81. The core is unconsolidated Ottawa sand of length 18 cm. The pore pressure is 750 psi and the confining pressure is 7000 psi. Room temperature is 75°F and the air bath is at 101°F. The values tabulated below are taken directly from the laboratory notebook.

<u>Pore Volumes</u>	<u>Pump Setting</u>	<u>q</u>	<u>Δp</u>	<u>Δp_0</u>	<u>k</u>	<u>dk</u>	<u>\bar{k}</u>	<u>$\bar{\bar{k}}$</u>
460	D6	984	4.300	-.113	2192	33		
465	D6	984	4.300	-.112	2192	33	2192	
470	D4	655	2.825	-.112	2192	43		
475	D4	655	2.825	-.112	2192	43	2192	
480	D5	822	3.550	-.113	2206	37		
485	D5	822	3.550	-.112	2206	37	2206	
486	C5	204	0.800	-.112	2199	123	2199	

2197

As discussed in the Procedure section of this work, the final permeability, $\bar{\bar{k}}$, is the average of the averaged values at the three highest flow rates.

The calculator program with all the instructions for its use follow.

PROGRAM DESCRIPTION

Program calculates permeability and error in permeability from flow rate measurements.

USER INSTRUCTIONS

STEP	PROCEDURE	ENTER	PRESS	DISPLAY
1	Enter program			1,2,4
2	Enter core length (cm).	L	C'	2901.08
3	Enter pore pressure (psi)	P	B'	P (kg/cm ²)
4	Enter room temperature (°F).	T _{ROOM}	A'	t at T _{ROOM}
5	Enter experiment temperature (°F).	T	A	p at 1
6	Enter flow rate (cc/b-)	Q	B	q (cc/sec)
7	Enter pressure drop (psi)	ΔP	C	k
8	Enter plate size (psi)	ΔP _{MAX}	D	dk

USER DEFINED KEYS		DATA REGISTERS (Op 08)		LABELS (Op 08)	
A	T	1	L	40	U
B	Q	2	$34.7 \times 10^3 / A$	41	Q
C	ΔP	3	P (psi)	42	ΔP
D	ΔP _{MAX}	4	$34.7 \times 10^3 / A$	43	ΔP _{MAX}
E	T _{ROOM}	5	T _{ROOM} (°F)	44	T 10 83T 0
A	T _{ROOM}	6	T _{ROOM} (°K)	45	ΔP
B	P	7	p at room T	46	B
C	L	8	T (°F)	47	C
D		9	T (°K)	48	
E		10	p at 1	49	
FLAGS	0 1 2 3 4 5 6 7 8 9				

© 1979 Texas Instruments Incorporated

Equations

Constants Stored in Bank 4

$$k = \frac{14.7 \times 10^3 \rho \mu L \rho_{sc}}{\Delta p A \rho_1}$$

$$dk = k \frac{d(\Delta p)}{\Delta p}$$

$$n = \frac{(0.01) k \sqrt{\Delta p^2}}{\Delta p}$$

$$\rho^{-1} = A - B P - C P^2$$

$$\mu = 0.02414 \times 10^{247.8/(T - 140)}$$

P is kg/cm²

T in °R

$$A = a_1 + a_2 T + a_3 T^2 + a_4 T^{-1} + a_5 T^{-2}$$

$$B = b_1 + b_2 T + b_3 T^2 + b_4 T^{-1} + b_5 T^{-2}$$

$$C = 1.18547 \times 10^{-8} + 6.599143 \times 10^{-11} T$$

Register	Value
20	5.916365
21	-1.035794 x 10 ⁻²
22	9.270048 x 10 ⁻⁶
23	-1.127522 x 10 ³
24	1.006741 x 10 ⁵
25	5.204914 x 10 ⁻³
26	-1.0482101 x 10 ⁻⁵
27	8.328532 x 10 ⁻⁹
28	-1.1702939
29	1.022783 x 10 ²

USER DEFINED KEYS		DATA REGISTERS (R0-R7)				LABELS (Op 08)			
A		20	1						
B		21	2						
C		22	3						
D		23	4						
E		24	5						
A		25	6						
B		26	7						
C		27	8						
D		28	9						
E		29	10						
FLAGS									

PROGRAMMER _____ DATE _____

LOC	CODE	KEY	COMMENTS	LOC	CODE	KEY	COMMENTS	LOC	CODE	KEY	COMMENTS
000	76	LBL		055	47	STD		110	02	2	
001	18	C'		056	06	06		111	04	4	
002	42	STD		057	91	R/S		112	01	1	
003	00	00		058	76	LBL		113	04	4	
004	02	2		059	11	R		114	95	=	
005	09	9		060	42	STD		115	42	STD	
006	00	0		061	07	07		116	10	10	
007	01	1		062	85	Y		117	91	P/S	
008	93	.		063	04	1		118	76	LBL	
009	00	0		064	05	0		119	12	B	
010	08	8		065	05	5		120	55	-	
011	42	STD		066	95	.		121	03	3	
012	01	01		067	76	0		122	06	6	
013	91	R/S		068	07	7		123	00	0	
014	76	LBL		069	95	-		124	00	0	
015	17	B'		070	55	.		125	95	=	
016	42	STD		071	01	1		126	42	STD	
017	02	02		072	93	.		127	11	11	
018	65	X		073	08	8		128	91	R/S	
019	07	7		074	95	=		129	76	LBL	
020	93	.		075	42	STD		130	13	C	
021	00	0		076	03	03		131	42	STD	
022	03	3		077	71	SR		132	12	12	
023	00	0		078	07	SIN		133	95	1/X	
024	06	6		079	11	S/D		134	65	X	
025	09	9		080	09	09		135	43	RCL	
026	05	5		081	47	INT		136	00	10	
027	52	EE		082	17	17		137	65	Y	
028	02	2		083	76	0		138	43	FCL	
029	94	+/-		084	03	3		139	07	01	
030	95	=		085	02	2		140	60	X	
031	42	STD		086	95	.		141	43	FCL	
032	03	03		087	85	Y		142	11	11	
033	91	R/S		088	05	5		143	65	X	
034	76	LBL		089	55	.		144	43	RCL	
035	16	R'		090	09	9		145	10	10	
036	42	STD		091	35	.		146	65	X	
037	04	04		092	91	1		147	43	RCL	
038	85	+		093	31	1		148	06	06	
039	04	4		094	03	3		149	55	.	
040	05	5		095	03	3		150	43	RCL	
041	09	9		096	95	.		151	09	09	
042	93	.		097	37	1/X		152	95	=	
043	06	6		098	65	Y		153	42	STD	
044	07	7		099	07	7		154	13	13	
045	95	=		100	04	4		155	58	FIX	
046	55	.		101	07	7		156	00	00	
047	01	1		102	7	7		157	99	PRT	
048	93	.		103	05	5		158	22	INV	
049	08	8		104	95	.		159	58	FIX	
050	95	=		105	22	INV					
051	42	STD		106	20	LOG					
052	05	05		107	65	Y					
053	71	SR		108	93	.					
054	38	SIN		109	90	0					


MERGED CODES

72	73	74	75	76	77
78	79	80	81	82	83
84	85	86	87	88	89
90	91	92	93	94	95

TEXAS INSTRUMENTS
INCORPORATED

TITLE Permeability Calculation

DATE 11/11/71

Programmable
Coding Form 

PROGRAMMER _____

DATE _____

LOC	CODE	KEY	COMMENTS	LOC	CODE	KEY	COMMENTS	LOC	CODE	KEY	COMMENTS
160	91	R/S		215	43	RCL		270	95	=	
161	76	LBL		216	15	15		271	35	1/X	
162	38	SIN		217	85	+		272	22	INV	
163	42	STD		218	43	RCL		273	52	EE	
164	15	15		219	29	29		274	92	RTN	
165	43	RCL		220	55			275	76	LBL	
166	20	20		221	43	RCL		276	14	D	
167	65	+		222	15	15		277	42	STD	
168	43	RCL		223	33	X2		278	14	14	
169	21	21		224	95	-		279	33	X2	
170	65	+		225	42	STD		280	95	+	
171	43	RCL		226	17	17		281	43	RCL	
172	15	15		227	01	1		282	12	12	
173	85	+		228	90			283	33	X2	
174	43	RCL		229	01	1		284	95	=	
175	27	27		230	08	8		285	34	FX	
176	61	X		231	05	5		286	65	X	
177	43	RCL		232	04	4		287	93	.	
178	15	15		233	07	7		288	00	0	
179	37	X2		234	51	EE		289	01	1	
180	57	+		235	06	6		290	55	-	
181	43	RCL		236	94	+/-		291	43	RCL	
182	23	23		237	75			292	12	12	
183	55	-		238	0	0		293	65	X	
184	43	RCL		239	90			294	43	RCL	
185	15	15		240	07	7		295	13	13	
186	85	+		241	09	9		296	95	=	
187	43	RCL		242	09	9		297	58	FIX	
188	24	24		243	01	1		298	00	00	
189	55	-		244	04	4		299	09	PRT	
190	43	RCL		245	07	7		300	07	ADV	
191	15	15		246	01	1		301	22	INV	
192	33	X2		247	01	1		302	50	FIX	
193	95	=		248	01	1		303	91	R/S	
194	42	STD		249	07	7					
195	15	15		250	07	7					
196	43	RCL		251	07	7					
197	61	X		252	07	7					
198	81	+		253	07	7					
199	43	RCL		254	07	7					
200	26	26		255	07	7					
201	65	+		256	07	7					
202	43	RCL		257	07	7					
203	15	15		258	07	7					
204	85	+		259	07	7					
205	43	RCL									
206	27	27									
207	65	+									
208	43	RCL		262	43	RCL					
209	15	15		263	17	17					
210	33	X2		264	55	-					
211	85	+		265	43	RCL					
212	43	RCL		266	03	03					
213	28	28		267	95	=					
214	55	-		268	43	RCL					
				269	16	16					

MERGED CODES

77	78	79	80	81	82
83	84	85	86	87	88
89	90	91	92	93	94
95	96	97	98	99	00

TEXAS INSTRUMENTS
INCORPORATED

APPENDIX F
EQUIPMENT, MANUFACTURERS AND SUPPLIERS

ITEM	MODEL NUMBER	MANUFACTURER	SUPPLIER
Backpressure Regulator Spring loaded	26-1723-24-014	Tescom Corporation Minneapolis, MN	C. S. Company 22131 South Vermont Torrance, CA 90502
Nitrogen loaded	S-91XW Fig. 11506	Grove Valve & Regulator Co. 6529 Hollis Street Oakland, CA 94608	Fluid-Tech Sales 9596 Garden Grove Blvd. Suite 714 Garden Grove, CA 92644
Berea Sandstone Cores			The Cleveland Quarries Amherst, OH
Chart Recorder	1320/46/15/15	Soltec Corporation 11684 Pendelton Street Sun Valley, CA 91352	Electronic Engineering Assoc. 932 Terminal Way San Carlos, CA 94070
Cylinder Regulator (6000 psi)	3066S-677		Matheson Gas Company 6775 Central Avenue Newark, CA 94560
Digital Thermometer	2176A	Omega Electronics Inc. Stamford, CT 06907	Omega Engineering, Inc. Box 4047 Stamford, CT 06907
Filters	SS-2F-15	Nupro Company 4800 East 345 th Street Willoughby, OH 44094	Sunnyvale Valve and Fitting 929 Weddell Court Sunnyvale, CA 94086
Fittings		Crawford Fitting Co. 29500 Solon Road Solon, OH 44139	Sunnyvale Valve & Fitting 929 Weddell Court Sunnyvale, CA 94086
Gauges Line Pressure		ACCO Helicoid Gage Division 929 Connecticut Ave. Bridgeport, CT 06602	Paul Munroe Hydraulics 3701 Thomas Road Santa Clara, CA 95050
Calibration		Dresser Industries 250 East Main Street Stratford, CT 06497	Manco 2680 Bayshore Frontage Road Mountain View, CA 94043
Hand Pump	F-39	Enerpac	Paul Munroe Hydraulics 3701 Thomas Road Santa Clara, CA 95050
Line Regulator 0-25 psi 5-90	3455 3457		Matheson Gas Company 6775 Central Ave. Newark, CA 94560
Ottawa Silica	F Series		Barber Industrial and Foundary 1861 Rolling Road Burlingame, CA 94010
Pressure Intensifier	50-6-15		High Pressure Equipment Company 1701 Linden Avenue Erie, PA 16505
Pressure Relief Valve	5349T-2PF-Setting	Circle Seal Controls P.O. Box 3666 Anaheim, CA 92803	Tempresco Inc. 6291 Sierra Court Dublin, CA 94566
Pressure Transducers	F-39	Celeco Transducer Products 7800 Deering Avenue Canoga Park, CA 91304	Gado Instrument Sales 3997 East Bayshore Road Palo Alto, CA 94303
Pump	2247 WIII	Ruska Corporation 6121 Hillcroft Houston, TX 77-81	Ruska Corporation 6121 Hillcroft Houston, TX 77081
Screen	270 Mesh		Howard Wire Cloth Company 935 Howard Street San Francisco, CA
Stainless Steel			Earle Jorgensen Box 4666 Bayshore Annex Oakland, CA 94623
Stainless Steel Tubing			Kilsby Tubesupply 2077 Pike Avenue San Leandro, CA 94577
Transducer Indicators	CD-25A	Celeco Transducer Products 7800 Deering Avenue Canoga Park, CA 91304	Gado Instrument Sales 3997 East Bayshore Road Palo Alto, CA 94303

Valves		Whitey Company	Sunnyvale Valve and Fitting
Low Pressure		318 Bishop Road	929 Weddell Court
		Highland Heights, OH 44143	Sunnyvale, CA 94086
6000 Psi One-Way	SS-3NBS4	Whitey Company	Sunnyvale Valve and Fitting
		318 Bishop Road	929 Weddell Court
		Highland Heights, OH 44143	Sunnyvale, CA 94086
45,000 Psi One-Way	SS-445-FP	Sno-Trik Company	Sunnyvale Valve and Fitting
		32550 Old South Miles Road	929 Weddell Court
		Solon, OH 44139	Sunnyvale, CA 94086
6000 Psi Three-Way	7673G4Y	Hoke Inc.	Con-Val
		One Tenakill Park	412 Pendleton Way
		Cresskill, NJ 07626	Oakland, CA 95621
Viton Tubing	75F26		West American Rubber Co.
			750 North Main Street
			Orange, CA 92668
